

# **Auditory gating in the ventral striatum and auditory cortex: the role of stimulus-locking and the influence of discrimination learning**

## **Dissertation**

zur Erlangung des akademischen Grades

**doctor rerum naturalium**

**(Dr.rer.nat.)**

genehmigt durch die Fakultät für Naturwissenschaften der  
Otto-von-Guericke Universität Magdeburg



von: **Dipl.-Biol. Marie Woldeit**  
geb. am 29.08.1981 in Berlin

Gutachter: Prof. Dr. Frank Ohl  
Prof. Dr. Michael Koch

eingereicht am: 25.11.2013  
verteidigt am: 18.06.2014



Für Ingo und Alois.

## **Acknowledgements**

At the Leibniz Institute for Neurobiology I thank Dr. Andreas Schulz, Prof. Dr. Frank Ohl, Kathrin Ohl and Lydia Löw, as well as all members of the Systems Physiology of Learning group.

I am indebted to my parents and my husband for their great support.

I also like to acknowledge the MeCoSa program of the University of Magdeburg for professional support outside the LIN.

# Selbstständigkeitserklärung

Hiermit erkläre ich, dass die von mir eingereichte Dissertation zum Thema

***Auditory gating in the ventral striatum and auditory cortex:  
the role of stimulus-locking and the influence of discrimination  
learning***

selbstständig verfasst, nicht schon als Dissertation verwendet wurde, und die benutzten Hilfsmittel und Quellen vollständig angegeben wurden.

Weiterhin erkläre ich, dass ich weder diese noch eine andere Arbeit zur Erlangung des akademischen Grades doctor rerum naturalium (Dr. rer. nat.) an anderen Einrichtungen eingereicht habe.

Magdeburg, den 25.11.2013

Marie Woldeit



# Summary

## **Auditory gating in the ventral striatum and auditory cortex: the role of stimulus-locking and the influence of discrimination learning**

***Dipl.-Biol. Marie Woldeit***

Auditory gating defines an attenuation of neuronal responses to the second of two identical repetitive acoustical stimuli. The underlying mechanisms and involved brain areas in sensory gating are still not sufficiently understood. Especially, the influence of the auditory cortex and the role of stimulus-locking are under debate. Reports of behavioral task influences on auditory gating are scarce and heterogeneous, even more when it comes to animal studies.

The first objective of the present study was to analyze the dynamics of gating of local field potentials in the primary auditory cortex and the ventral striatum of awake Mongolian gerbils. To further examine decrement dynamics, responses to frequency-modulated tone trains were analyzed for characteristics of habituation or generator refractoriness. The second aim was to investigate the hypothesis that auditory gating results from phase de-synchronization of evoked potentials in response to the second auditory stimulus. Finally, the present study aimed at revealing what influences a transiently stress- and attention charged auditory discrimination task could have on auditory gating in gerbils.

Local field potentials were recorded simultaneously in the auditory cortex and ventral striatum of awake Mongolian gerbils during stimulation with trains of frequency-modulated tones. Gating was analyzed using the amplitude ratios of the auditory potentials evoked by the first two stimuli in a train; the local field potentials were also subjected to time-frequency analyses and analysis of between-area phase coupling. Additionally, response dynamics to frequency-modulated tone trains were examined for their dependence on inter-stimulus interval and tone repetition number. Estimations for the recovery times of auditory evoked potential subcomponents were made based on a two-parameter asymptotic exponential model that was fit to the data. The tested stimuli were also used as conditioned stimuli in an auditory discrimination Go/NoGo task in a shuttle-box, in which the subjects were trained to discriminate frequency modulation direction.

Notably, the strength of auditory gating in the striatum was found to exceed that in the primary auditory cortex by more than 50%. To the author's knowledge, the present study represents the first animal report using detailed time-frequency analysis in an auditory gating experiment. A key finding of the study was that while the total-signal-power between areas remained comparable, the energy in the striatum was primarily expressed in the non-phase-locked fraction. At the same time, energy in the auditory cortex remained phase-locked to the stimuli. Furthermore, during sound presentations also between-area phase unlocking was observed. Analysis beyond the second stimulus of a tone train revealed that response suppression dynamics could be best explained by the amplitude decrease between the first and second stimulus, irrespective of inter-stimulus interval. Within the auditory discrimination task, auditory gating in the striatum during stimulus registration was not altered. Long-term phase-coupling between the cortex and



the ventral striatum was also not modified by the behavioral task. Phase de-synchronization appears to be the candidate mechanism behind attenuation of responses to identical repetitive stimuli in the ventral striatum. Conclusively a direct inhibitory response suppression by the auditory cortex plays a minor role in this process. Finally, arguing from the results of the auditory discrimination task, controllable stress and attention do not alter auditory gating, supporting other findings that have characterized it as a pre-attentive mechanism.



## **Zusammenfassung**

**Die Rolle der Stimuluskopplung und der Einfluss des auditorischen Diskriminierungslernens auf das auditorische Gating im ventralen Striatum und im auditorischen Kortex**  
*Dipl.-Biol. Marie Woldeit*

Die Abschwächung neuronaler Antworten auf den zweiten zweier identischer repetitiver akustischer Reize wird als auditorisches Gating bezeichnet. Die diesem sensorischen Gating zu Grunde liegenden Mechanismen, sowie die dabei involvierten Hirnareale, sind weitgehend unbekannt. Vor allem der Einfluss des auditorischen Kortex und die Rolle der Stimulusankopplung neuronaler Antworten in diesem Prozess stehen zur Diskussion. Studien über Zustands- und Aufgabeneinflüsse aufs Gating sind rar und uneinheitlich, besonders bei Tierexperimenten.

Das erste Ziel der vorliegenden Studie war es, die Dynamik des auditorischen Gating lokaler Feldpotentiale im auditorischen Kortex und ventralen Striatum an wachen mongolischen Wüstenrennmäusen zu untersuchen. Um den Verlauf der Abschwächung evozierter Antworten auf Ton-Züge, bestehend aus repetitiven frequenz-modulierten Einzeltönen, detaillierter zu analysieren, wurden diese auf Charakteristika bezüglich neuronaler Habituation oder auf refraktäre Eigenschaften neuronaler Feldpotentialquellen getestet.

Die zweite Zielstellung der Studie basierte auf der Hypothese, dass eine Desynchronisation der Phasen der durch den zweiten

auditorischen Stimulus evozierten Potentiale dem auditorischen Gating zu Grunde liegen könnte.

In einem dritten Teilprojekt der Studie sollten mögliche Einflüsse einer vorübergehend stress-behafteten und Aufmerksamkeit erfordernder auditorischen Diskriminierungsaufgabe auf das auditorische Gating in Wüstenrennmäusen untersucht werden.

Während der Stimulation mit Tonzügen frequenzmodulierter Einzeltöne wurden lokale Feldpotentiale simultan vom auditorischen Kortex und dem ventralen Striatum wacher mongolischer Wüstenrennmäuse abgeleitet. Auditorisches Gating wurde sowohl anhand des Verhältnisses der Amplituden evozierter Potentiale auf den ersten und zweiten akustischen Reiz eines Ton-Zuges als auch mittels Zeit-Frequenz Analysen und Phasenkopplung beider Hirnareale während der Stimulation ausgewertet. Außerdem wurde das Antwortverhalten beider Hirnareale auf Ton-Züge frequenzmodulierter Einzeltöne auf ihre Abhängigkeit von Inter-Stimulus Intervall und Tonwiederholung untersucht. Schätzungen für die Regenerationszeiten der Subkomponenten auditorisch evozierter Potentiale wurden anhand einer zweiparametrischen asymptotischen Exponentialfunktion berechnet, welche auf die Daten modelliert wurde. Des Weiteren wurden die untersuchten Stimuli als konditionale Reize in einem auditorischen "Go/NoGo" Diskriminierungsparadigma in einer Shuttle-Box benutzt. Hier wurden die Tiere trainiert, die Frequenz-Modulationsrichtung der Töne zu unterscheiden.

Auditorisches Gating war im ventralen Striatum zu 50% stärker ausgeprägt als im auditorischen Kortex. Die vorliegende Studie ist nach Wissen der Autorin die erste Tierstudie, die eine detaillierte Zeit-Frequenz Analyse des auditorischen Gatings vorgenommen hat. Ein Hauptbefund der Arbeit war, dass während die Gesamtleistung in beiden Hirnarealen vergleichbar blieb, die Signalenergie im Striatum vornehmlich durch den Anteil zum Stimulus phasenentkoppelter Leistung hervorgebracht wurde. Die

Leistung im auditorischen Kortex hingegen war hauptsächlich phasen-gekoppelt an die auditorischen Reize. Weiterhin wurde beobachtet, dass die beiden Hirnareale während der Tonwiedergabe phasen-entkoppelt waren. Unabhängig vom Inter-stimulus Intervall konnte der zeitliche Verlauf der Antwortunterdrückung auf die Ton-Züge hinreichend durch die Amplitudenverminderung vom ersten auf den zweiten Ton-Reiz erklärt werden. Innerhalb des auditorischen Diskriminierungsparadigma blieb das auditorische Gating während der Stimulus Wahrnehmung durch das Training unverändert. Ebenso konnte keine Auswirkung der Verhaltensaufgabe auf die Langzeitkopplung zwischen auditorischem Kortex und Striatum festgestellt werden. Zusammenfassend gibt die Studie guten Grund zur Annahme, dass eine Antwortverminderung auf identische repetitive Tonreize im ventralen Striatum mechanistisch auf eine Desynchronisierung der Phasen zurückzuführen ist. Folglich scheint eine direkte inhibitorische Unterdrückung der Antworten im Striatum durch den auditorischen Kortex nur eine untergeordnete Rolle zu spielen. Aus den Ergebnissen des auditorischen Diskriminierungslernens wird gefolgert, dass kontrollierbarer Stress und Aufmerksamkeit auditorisches Gating nicht beeinträchtigen und somit Befunde unterstützen, die diesen Prozess als prä-attentiven Mechanismus charakterisieren.

# Contents

<b>Selbstständigkeitserklärung</b>	<b>vi</b>
<b>Contents</b>	<b>xiv</b>
<b>List of Figures</b>	<b>xviii</b>
<b>List of Tables</b>	<b>xxi</b>
<b>Nomenclature</b>	<b>xxiii</b>
<b>Introduction</b>	<b>1</b>
<b>1 Auditory gating of evoked potentials</b>	<b>3</b>
1.1 Introduction . . . . .	3
1.1.1 Auditory gating . . . . .	3
1.1.2 Auditory gating and psychotic disorders . . . . .	5
1.1.3 Putative neuronal substrates involved in auditory gating	5
1.1.4 Potential mechanisms implicated in auditory gating . . . .	7
1.2 Methods . . . . .	10
1.2.1 Subjects and procedures . . . . .	10
1.2.1.1 Animals . . . . .	10
1.2.1.2 Surgery . . . . .	10
1.2.1.3 Setup . . . . .	11
1.2.1.4 Auditory gating recordings . . . . .	11
1.2.1.5 Histology . . . . .	12
1.2.2 Data Analysis . . . . .	12
1.2.2.1 Preprocessing . . . . .	12

1.2.2.2	Peak sorting . . . . .	13
1.2.2.3	Sensory gating . . . . .	13
1.2.3	Statistical analysis . . . . .	14
1.2.3.1	Characterization of evoked potentials and sup- pression . . . . .	14
1.2.3.2	Short-term habituation . . . . .	14
1.2.3.3	Recovery time model . . . . .	15
1.3	Results . . . . .	16
1.3.1	Frequency-modulated tone-evoked potentials in the ven- tral striatum and auditory cortex . . . . .	16
1.3.2	Auditory gating of P1, N1 and P2 in striatum and auditory cortex . . . . .	18
1.3.3	Short-term habituation in the ventral striatum . . . . .	20
1.3.4	Recovery Model for Striatal N1 and P2 . . . . .	24
1.4	Discussion . . . . .	28
1.4.1	FM tone evoked potentials in the ventral striatum and auditory cortex . . . . .	28
1.4.2	Auditory gating . . . . .	29
1.4.3	Short-term habituation in the ventral striatum . . . . .	31
1.4.4	Estimated recovery times . . . . .	33
<b>2</b>	<b>Time-frequency analysis of gating</b>	<b>35</b>
2.1	Introduction . . . . .	35
2.1.1	The role of stimulus-locking in the physiology of auditory gating . . . . .	35
2.1.2	Contribution of different frequency ranges to the auditory gating phenomenon . . . . .	36
2.2	Methods . . . . .	39
2.2.1	Subjects and procedures . . . . .	39
2.2.2	Data Analysis . . . . .	39
2.2.2.1	Preprocessing . . . . .	39
2.2.2.2	Wavelet transform . . . . .	40
2.2.2.3	Induced and Evoked activity . . . . .	40

2.2.2.4	Recovery times of induced and evoked activities	43
2.2.2.5	Phase-locking	43
2.2.3	Statistical analysis	44
2.3	Results	44
2.3.1	Induced and evoked activity	44
2.3.2	Recovery time of induced and evoked activities	48
2.3.3	Between-area coherence determined by phase-locking	51
2.4	Discussion	55
2.4.1	Induced and evoked activity	55
2.4.2	Recovery times of induced and evoked activity	58
2.4.3	Coherence and phase-locking	59
<b>3</b>	<b>The impact of FM tone discrimination learning on sensory gating</b>	<b>61</b>
3.1	Introduction	61
3.1.1	State and task influences in auditory gating: Attention, memory and stress	61
3.1.2	Testing behavioral influences on auditory gating in the Mongolian gerbil	63
3.1.2.1	Auditory discrimination learning in the shuttle-box	63
3.1.2.2	Putative involvement of the auditory cortex and the ventral striatum in the Go/NoGo auditory discrimination task	64
3.2	Methods	67
3.2.1	Subjects and procedures	67
3.2.2	Behavioral Task	68
3.2.3	Data Analysis	68
3.2.4	Electrophysiological recordings	69
3.2.5	Phase-locking after the training	69
3.3	Results	70
3.3.1	Behavioral performances	70
3.3.1.1	Learning curve	70



3.3.1.2	Discrimination performance and reaction times to CS+ . . . . .	70
3.3.2	Auditory Gating during the training . . . . .	70
3.3.3	Gating and performance . . . . .	73
3.3.4	Training influence on auditory cortex – ventral striatum phase-locking . . . . .	74
3.4	Discussion . . . . .	81
3.4.1	Auditory evoked potential suppression during discrimination training . . . . .	81
3.4.2	Relation of gating scores with discrimination performances	83
3.4.3	Long-term changes in cortico-striatal phase-locking . . .	84
<b>4</b>	<b>Conclusions</b>	<b>86</b>
	<b>Appendix A</b>	<b>91</b>
	<b>Appendix B</b>	<b>95</b>
	<b>Appendix C</b>	<b>102</b>
	<b>References</b>	<b>105</b>
	<b>Lebenslauf</b>	<b>124</b>
	<b>List of Publications</b>	<b>126</b>

# List of Figures

1.1	Frequency-modulated (FM) tone evoked potentials in the auditory cortex and striatum showed different temporal dynamics.	17
1.2	Auditory gating was found for all three subcomponents of the striatal auditory evoked potential (AEP) but for none of the cortical AEPs. . . . .	19
1.3	Inter-stimulus interval (ISI) effects on grand-average evoked potentials. . . . .	22
1.4	Marginal means of amplitudes as a function of stimulus repetition (within a train) for three inter-stimulus intervals (ISIs).	23
1.5	Asymptotic exponential function used to model the recovery of auditory gating of striatal N1 and P2. . . . .	25
1.6	Auditory evoked potential recovery fits. . . . .	26
1.7	Estimated recovery times for repetitive FM tone stimulation exceeded 4 s. . . . .	27
2.1	Schematic display how averaging of local field potentials blurs information on non-phase-locked (induced) activity. . . . .	41
2.2	Trains of frequency-modulated (FM) tones stimulated primarily evoked activity in the auditory cortex but mainly induced activity in the striatum. . . . .	45
2.3	Total-signal-power was split differently between evoked and induced activity in the auditory cortex and ventral striatum. . .	46
2.4	Only evoked activity was subject to auditory gating in the striatum. . . . .	49

2.5	Gating dynamics were only seen for evoked activity in the ventral striatum in the 2-268 Hz range. . . . .	50
2.6	Estimated recovery time of striatal evoked activity for repetitive frequency modulated (FM) tone stimulation exceeded 4 s. . . .	52
2.7	Stimulation with frequency modulated tones resulted in diminished phase synchrony between auditory cortex and ventral striatum. . . . .	53
2.8	Phase-locking between the cortex and striatum was significantly decreased during tone presence in lower frequency bands. . .	56
3.1	Successful discrimination of frequency modulated (FM) tones was attained after three training sessions. . . . .	71
3.2	Discrimination performances and CS+ reaction times changed with training. . . . .	73
3.3	Better discrimination performance correlated strongly with faster reaction times to the CS+. . . . .	74
3.4	Reaction times of “Go” responses were slower during CS+ trials during the discrimination. . . . .	75
3.5	Amplitude suppression during discrimination training in the ventral striatum and auditory cortex. . . . .	76
3.6	AEP suppression did not correlate with discrimination performance. . . . .	77
3.7	Phase-locking before and after discrimination training. . . . .	78
1	Median recovery times estimated on individual subject exponential fits. . . . .	92
2	Stimulation with with FM tones and a longer interstimulus interval (ISI) resulted in diminished phase synchrony between auditory cortex and ventral striatum, as well. . . . .	99
3	Phase-locking between the cortex and striatum was significantly decreased during tone presence only in the theta band for the longer ISI stimulation. . . . .	100

4	Individual suppression scores for the CS+ and CS- during discrimination training in the ventral striatum. . . . .	103
5	Individual suppression scores for the CS+ and CS- during discrimination training in the auditory cortex. . . . .	104

# List of Tables

1.1	Latencies and amplitudes of identified AEP subcomponents were not influenced by frequency modulation direction. . . . .	18
1.2	Means and standard deviations of amplitude suppression in the auditory cortex and ventral striatum. . . . .	18
1.3	ANOVA results for short-term habituation of striatal amplitudes.	21
2.1	Repeated-measure ANOVA for FREQUENCY band and STIMULUS POSITION effects on induced and evoked activity in the auditory cortex and ventral striatum. . . . .	47
2.2	Repeated-measure ANOVA for STIMULUS PRESENCE and POSITION effects on between-area phase-locking. . . . .	54
3.1	Training effects on striatal auditory gating. . . . .	72
3.2	Training effects on baseline phase-locking. . . . .	79
3.3	Training effects on phase-locking during FM tone stimulation. . . . .	80
3.4	Training effects on phase-locking during FM tone stimulation split by frequency. . . . .	80
1	Average amplitudes split by the used test factors. . . . .	93
2	Average latencies split by the used test factors. . . . .	94
3	Summary of model parameters from the exponential fits. . . . .	96
4	Estimated recovery times of evoked and induced activities. . . . .	97
5	Repeated-measure ANOVA on between-area phase-locking during the 0.5 s ISI testing for FREQUENCY band influences, STIMULUS PRESENCE and POSITION effects. . . . .	98

6	Repeated-measure ANOVA on between-area phase-locking during the 1.2 s ISI testing for FREQUENCY band influences, STIMULUS PRESENCE and POSITION effects. . . . .	98
7	Repeated-measure ANOVA for STIMULUS PRESENCE and POSITION effects on between-area phase-locking during the 1.2 s ISI.	101

# Nomenclature

## Roman Symbols

$d'$	Discrimination performance sensitivity index
$f$	Frequency
$n$	Number of trials
$t$	Time variable, for the asymptotic exponential model, ISI
$t_0$	Time-axis origin parameter of the asymptotic exponential model
$W$	Wavelet coefficient
A1	Primary auditory cortex
N1	First negative AEP peak in the present study
N100	Human negative wave peak after 100 ms, MEG nomenclature N100m
N40	Animal negative wave potential after 40 ms, corresponding striatal N1 in the present study
P1	First positive AEP peak in the present study
P2	Second positive AEP peak in the present study
P200	Human positive wave peak after 200 ms, MEG nomenclature P200m
P50	Human positive wave peak after 50 ms, MEG nomenclature P50m
S1	Conditioning tone, first stimulus

S2 Test tone, second stimulus

T/C Test-conditioning ratio

### **Greek Symbols**

$\Delta$  Difference

$\phi$  Instantaneous phase angle

$\tau$  Scale parameter of the asymptotic exponential model

### **Other Symbols**

$\Im$  Imaginary part of the wavelet coefficient

$\Re$  Real part of the wavelet coefficient

### **Acronyms**

ACX Auditory cortex

AEP Auditory evoked potential

AMPA  $\alpha$ -Amino-3-hydroxy-5-methyl-4-isoxazolepropionic acid

ANOVA Analysis of variance

CR Conditioned response

CS Conditioned stimulus; CS+: Go CS; CS-: NoGo CS

DA Dopamine

EA Evoked activity

EEG Electroencephalogram

EP Evoked potential

FA False alarm

FM Frequency modulated



GABA  $\gamma$ -Aminobutyric acid  
H Hit  
INDA Induced activity  
IQR Inter-quartile range  
ISI Inter-stimulus interval  
MEG Magnetoencephalogram  
NA Not available  
NMDA N-Methyl-D-aspartate  
PLI Phase-locking index  
sd Standard deviation  
SE Standard error of the mean  
SR Stimulus-response  
STR Ventral striatum  
TSP Total-signal-power  
US Unconditioned stimulus

# Introduction

“If he isn’t hallucinating, his hearing is different when he’s ill. One of the first things we notice when he’s deteriorating is his heightened sense of hearing. He cannot filter out anything. He hears each and every sound around him with equal intensity. He hears the sounds from the street, in the yard, and in the house, and they are all much louder than normal.” (Anonymous, 1985)

The perception of one’s environment constitutes the basis of flexible planning and decision making that governs almost all non-reflexive behavior. While the mammalian primary sensory brain areas of the cortex are thought to build percepts pertaining to the five senses, certain subcortical structures are believed to use these percepts for calculation, analysis and categorization of the perceived events, finally allowing the organism to take action.

The primary auditory cortex is the core center for the formation of sound percepts and their integration with other sensory impressions. While to some extent population encodings for the spatial localization of sounds is known, how spectro-temporal parameters of sound are decoded is less clear (reviewed by Recanzone, 2011). Recent findings have stressed that the auditory cortex cannot simply be reduced to a sound processor, but that its function is adaptive and plastic, in a way that “responses in the auditory cortex must be understood as an interwoven tapestry of relevant multimodal contextual inputs” (Sutter & Shamma, 2011). Moreover, as strategies and learned concepts change, not only tonotopic maps and receptive fields in the cortex appear to be altered, but entire up- and downstream networks

are likely to be modified (Scheich *et al.*, 2007; Xiong *et al.*, 2009).

The striatum represents the first input structure of the subcortical basal ganglia, with strikingly high convergence of sensory and associative cortical afferents. At this brain nexus perceived events are transformed into actions. Striatal function is thought to be organized into different, but tightly interacting cortico-striatal loops (Alexander *et al.*, 1986), in which dopamine signals act to gate incentive cortical glutamatergic signals (reviewed by Horvitz, 2002). Especially the ventral division has been related to motivational and emotive coloring of goal directed behavior according to the saved associated valence, by integrating information from other limbic areas such as the amygdala and the ventral hippocampus and prefrontal cortex (Gruber & McDonald, 2012). Recently it has been shown that biologically salient events could be presented to the striatum shunning thalamo-cortical signalling (Schulz *et al.*, 2009), putting classical views on action selection into question (Redgrave *et al.*, 2008).

The present study was set out to analyze a very basic auditory sensory filter mechanism and evaluate the roles and interactions of the auditory cortex and the ventral striatum herein. Putative task influences on this paradigm were meant to be assessed in a simple operant conditioning task, as well.

# Chapter 1

## Auditory gating of evoked potentials

### 1.1 Introduction

#### 1.1.1 Auditory gating

Proper integration between the perception of the environment and internal states benefits from the organism's active processing of those signals that lie within its focus of attention or represent highly salient cues, immediately to be acted upon. Therefore the brain must provide some physiological mechanism to reduce redundant information and protect itself from sensory flooding. Auditory gating has been proposed to represent such a filter mechanism within the brain (Freedman *et al.*, 1991). Gating has been extensively examined for auditory stimuli, but can also be found in the somatosensory, but not visual domain (Adler *et al.*, 1985; Arnfred *et al.*, 2001).

In a classical auditory gating paradigm test subjects are presented with pairs of identical clicks, that are separated by 500 ms, while inter-pair intervals are typically larger than 8 s. Gating is determined by calculating the ratio of amplitudes of evoked responses to the first (S1) and second

(S2) stimulus, respectively called “conditioning” and “test” tone. Normally, the response to S2 is diminished and hence the test-conditioning (T/C) tone ratio is less than 100%. Linking auditory gating to neurophysiological filter processes within the brain emerged only by identifying deficient gating in subjects suffering from schizophrenia (Adler *et al.*, 1985), a complex psychiatric illness that comes along with deranged sensory registration like acoustical hallucinations and delusions (positive symptomatology, see Section 1.1.2).

In humans auditory gating is commonly recorded from the vertex electrode during electroencephalogram (EEG) scalp measurements of the auditory evoked P50 component. Gating of this positive auditory evoked potential (AEP) peak around 50 ms after stimulation onset, is most often reported, but later wave-peaks like the human N100 and P200, have also been shown to be liable to auditory gating. Yet, the test-retest reliability is under debate for all components (Fuerst *et al.*, 2007).

Auditory gating has also been detected in animal studies that can use more locally defined recordings directed at certain brain structures of interest (reviewed in Adler *et al.*, 1986; Cromwell *et al.*, 2008). These studies showed that auditory gating is not necessarily limited to local field potentials, but can also be observed in recordings from single neuronal cells; however, a direct correlation of the two neuronal measures is not necessarily given (Cromwell *et al.*, 2008). In a study by Boutros *et al.* (1997) it was shown that N40 gating of identical stimuli in rats was strongly independent of stimulus duration, intensity or frequency, but dishabituated once a deviant stimulus was introduced. A similar effect was reproduced in human subjects (Boutros & Belger, 1999), leading the authors to postulate that auditory gating also encompasses the ability to “gate-in” novel sensory input, allowing the brain to “modulate its sensitivity to incoming stimuli”. The bigger the physical difference between S1 and S2 the stronger was the modulation on auditory gating (Zhou *et al.*, 2008).

### **1.1.2 Auditory gating and psychotic disorders**

Schizophrenia is the most often cited psychiatric illness that has been examined for its relation to P50 gating in human studies with human subjects (reviewed by [Potter et al., 2006](#)), but dysfunctional gating is also found in other diseases, e.g. Alzheimer's disease and obsessive-compulsive disorders ([Jessen et al., 2001](#); [Rossi et al., 2005](#)). Since P50 gating is also decreased in half of the first-degree relatives of patients and subjects with schizotypal personality disorder ([Adler et al., 1998](#); [Cadenhead et al., 2000](#)), it may represent the neurophysiological marker of a genetic risk for schizophrenia. Both animal research and linkage analyses in families with schizophrenia point to a role of the cholinergic system within this psychiatric disease. In support of this, the prevalence of smoking in schizophrenic subjects is significantly higher from the normal population average and probably marks self-medication to overcome concentration deficits. High dose nicotine inputs by patients could target the low-affinity  $\alpha$ -7 receptor, that was found to be dysfunctional in schizophrenia (reviewed by [Adler et al., 1998](#)). Markedly, heavy smoking transiently attenuated the P50 gating deficit in schizophrenic subjects ([Adler et al., 1998](#)).

A complete animal model of schizophrenia does not exist, as there is no such thing as a rodent psychosis; but animal research has proved helpful in investigating pharmacological effects on the gating phenomenon. Amphetamine, a psycho-stimulant, and phencyclidine, an N-Methyl-D-aspartate (NMDA) receptor antagonist, both mimicked a psychotic state in rats, and decreased N50 gating ([Adler et al., 1986](#)). Either was reduced by anti-dopaminergic haloperidol treatment, a typical schizophrenia neuroleptic.

### **1.1.3 Putative neuronal substrates involved in auditory gating**

Due to its clinical relevance, the majority of auditory gating results are based on EEG, magnetoencephalogram (MEG) or intracranial EEG techniques in

human subjects. Human P50 generators are not unambiguously identified and possibly result as an overlap of multiple sources. Additionally, it remains an open question if the same generators that effect the P50 wave also mediate its suppression, for instance by neuronal fatigue, or if sequentially different brain circuits become active. Scalp-EEG source reconstruction reckon P50 generators to be localized within the auditory and prefrontal cortex (Weisser *et al.*, 2001). Using subdural grid electrodes Korzyukov *et al.* (2007) were able to show, that P50 originated from sources in the temporal and frontal lobe, but that gating related changes were most probably due to the frontal generator.

The accuracy of source reconstruction from EEG (and other) signals is affected by many factors. Especially for sources in deeper brain structures, the underlying mechanisms and involved brain circuits in auditory gating are still under debate. In contrast, animal experiments allow for the direct examination of gating in specific brain structures using chronic microwire implants that yield defined localizations and higher signal-to-noise ratios (Cromwell *et al.*, 2008). Here, gating has been mainly identified in areas belonging to the limbic system including amygdala, striatum, prefrontal cortex and hippocampus (Cromwell & Woodward, 2007; Cromwell *et al.*, 2005, 2007; Mears *et al.*, 2006; Moxon *et al.*, 1999). Especially the latter -due to its strong septal cholinergic innervation that would match inhibition dynamics (Luntz-Leybman *et al.*, 1992)- has been designated to be the source of gating in animals studies (Bickford-Wimer *et al.*, 1990).

Suppressive gating of acoustical stimuli has been identified in the basal ganglia in animal studies already 40 years ago (Dafny & Gilman, 1973, 1974), and robust suppression of AEPs in the central striatum has been demonstrated more recently (Cromwell *et al.*, 2007).

In the auditory cortex, a suppressive effect occurs at much shorter temporal intervals between two acoustical events and only in half of the investigated single cells (Brosch & Schreiner, 1997; Brosch *et al.*, 1999; Wehr & Zador, 2005). Several animal studies did not find any relation between the activity of the auditory cortex and the magnitude of gating in other brain areas (for instance in the hippocampus), and rather point to the reticular system of

the pons (Bickford-Wimer *et al.*, 1990; Moxon *et al.*, 1999) or the thalamic reticular nucleus (Krause *et al.*, 2003) as mediator of the auditory response suppression.

Vertex-recorded auditory gating has already been shown to be independent of stimulus parameters like frequency or intensity (see above Boutros *et al.*, 1997), yet spectro-temporally complex stimuli have not been studied in an auditory gating paradigm. Since Ohl *et al.* (1999) demonstrated that categorization and discrimination of frequency-modulated (FM) tones are primary auditory cortex-dependent, the absence of gating in the cortex at longer temporal intervals could be due to the low spectro-temporal complexity of acoustical stimuli.

The auditory cortex and the ventral striatum are both believed to play an important role in decoding the behavioral context of acoustical stimuli and in goal-directed behavior (Goto & Grace, 2008; Gruber *et al.*, 2009; Weinberger, 2007), a process possibly disturbed in schizophrenia (Grace, 2000; Shi, 2007).

Therefore, the first objective of this work was to study auditory gating in locally defined recordings in the ventral striatum and auditory cortex simultaneously in freely behaving Mongolian gerbils, using spectro-temporally complex FM tones as stimuli.

#### **1.1.4 Potential mechanisms implicated in auditory gating**

The functional significance of auditory gating would be clarified if its neurophysiological implementation could be revealed. A multitude of studies relate gating to short-term habituation experiments with the intention of illustrating its genesis. Auditory gating experiments and short-term habituation studies are methodologically overlapping: Rather than using two identical stimuli, in a short-term habituation experiment the test subjects are presented with a train of identical cues, allowing for a more detailed analysis of the dynamics of the amplitude suppression beyond the test



stimulus. Within these studies a debate has been waxing and waning if amplitude decrements upon auditory stimulus repetition would represent a neuropsychological (“top-down”) phenomenon signifying habituation, a simple form of learning, or an inherent “bottom-up” feature, based on the refractoriness of the neuronal generator pool responsible for the AEP formation (Budd *et al.*, 1998; de Bruin *et al.*, 2001; Rosburg *et al.*, 2004). While the former would be supported by findings addressing task influences on auditory gating (discussed later, cf. Chapter 3), the latter would be in support of a mechanism depending purely on inherent neuronal properties. Full recovery of the human vertex recorded P50 wave has been estimated to be as long as 8 s (Zouridakis & Boutros, 1992), while animal vertex N50 wave reaches 100% of the control value after approximately 4 s (Adler *et al.*, 1986). The image of N100 recovery is blurred by the fact that this wave might consist of different sub-components itself that possibly originate from different sources (discussed in Budd *et al.*, 1998). Monkey P1 and N1 waves have been shown to possess different recovery curves, with P1 recovering significantly faster (Javitt *et al.*, 2000).

Rosburg *et al.* (2004) have shown that human intracranially recorded P50 and N100 show similar amplitude suppression in a short-term habituation experiment, and that dishabituation through a change stimulus (cf. Thompson & Spencer, 1966, criteria for habituation) evoked smaller responses than those registered to S1. Similar results were seen for EEG/MEG recorded N100 and P200 (Rosburg *et al.*, 2010). These findings are in contrast to studies that are more in support of an active inhibition mechanism by showing a progressive amplitude decline with increasing latency from first stimulus onset (Sable *et al.*, 2004) or facilitated human N1 amplitude at inter-stimulus intervals shorter than 500 ms (Budd & Michie, 1994). However, this reversal of the N100 repetition suppression was not replicated in rats (Budd *et al.*, 2012).

A way to analyze the influence of both potential mechanisms is to evaluate the dependence of the amplitude suppression from inter-stimulus interval (ISI) and stimulus repetition number or stimulus position in the tone train (Rosburg *et al.*, 2004). A habituation-characterized mechanism would be

marked by a strong dependence of the amplitude suppression from stimulus position in the tone train, i.e. amplitudes should gradually decrease with the number of stimulus repetitions. Recovery from neuronal or receptor fatigue should mainly be determined by the factor ISI.

Therefore in the present study, the dynamics of the inhibitory effect were examined in further detail by also investigating suppression effects beyond the test stimulus for the auditory cortex and the ventral striatum. Finally, estimates for the time needed for full recovery of the auditory evoked potentials' subcomponents have been made.

In summary AEP gating in the ventral striatum and the auditory cortex was analyzed in the first section of the study under following working hypotheses:

1. As a first step, to analyze auditory information processing in the ventral striatum and auditory cortex simultaneously, a detailed description of auditory evoked potentials and their interaction would be given. The author hypothesized that auditory information reaching both brain areas might be exploited differentially by the brain and that this would be mirrored by the dynamics of the wave shape of the auditory evoked potentials evoked by single frequency-modulated tones.
2. Auditory gating has been demonstrated in many limbic brain areas including the central striatum in animal studies (Cromwell *et al.*, 2007). The role of the auditory cortex within this process is indistinct considering the results of human auditory gating studies that included source reconstructions. Nevertheless rodent experiments have not detected auditory gating in the auditory cortex. Therefore the author expected that repetitive auditory stimulation would result in amplitude suppression in the ventral striatum but most likely not in the auditory cortex. In this section, auditory gating was characterized by simultaneously recorded auditory evoked potentials from both brain areas.

3. Finally, to further illuminate the mechanism involved in auditory gating, response dynamics of both brain areas to trains of FM tones were going to be analyzed with respect to influences of ISI and repetition number. The author predicted that repetition suppression was going to be similar to results seen in rat (Budd *et al.*, 2012) rather than bearing a habituation-like character, and that there was not going to be a further response decrement after the second tone of a train. It was also suspected that the auditory gating paradigm would work in time ranges that do not effect inhibitory or habituating responses in the auditory cortex.

## **1.2 Methods**

All experiments were performed in accordance with the European Communities Council Directive of November 24, 1986 (86/609/EEC), and according to the German guidelines for the care and use of animals in laboratory research. Experiments were approved by the Ethics Committee of the state Saxony-Anhalt. All efforts were made to reduce the number of gerbils used in the experiment and their suffering.

### **1.2.1 Subjects and procedures**

#### **1.2.1.1 Animals**

All gerbils (*Meriones unguiculatus*, obtained from Tumblebrook Farms, West Brokfield, MA, USA) were single-housed under a 12h light/dark regimen (lights on at 8.00 am). They had ad libitum access to food (ssniff Spezialdiäten GmbH, Soest, Germany) and water.

#### **1.2.1.2 Surgery**

Gerbils (3-5 months old, n = 15) were anesthetized with an initial dose of Pentobarbital (5 mg/kg intraperitoneally, Sigma-Aldrich, St.Louis, MO, USA)

and mounted into a stereotaxic frame (Stoelting, Illinois, USA). Additional doses of anesthetic were supplied if necessary. After partial removal of the temporal muscle and trepanation of the skull, one custom-made surface electrode array (4 x 4 steel electrodes, 100  $\mu\text{m}$  diameter, impedance 0.2-0.6  $\text{M}\Omega$ ) was placed on the dura above the auditory cortex, using major blood vessels for spatial guidance. A depth electrode array (13 animals: 2 x 4 bundle of twisted microwires, 50  $\mu\text{m}$  diameter per single wire, impedance 0.4-0.7  $\text{M}\Omega$ , 2 animals: 2 x 4 twisted microwires, 23  $\mu\text{m}$  diameter inside a guiding steel cannula, impedance 1-2  $\text{M}\Omega$ ) was stereotaxically lowered into the ventral striatum proximal to the nucleus accumbens (antero-posterior: +0.5 mm, medio-lateral: -1.3 mm, dorso-ventral: -4.1 mm from bregma; all wires: Science Products GmbH, Hofheim, Germany). A stainless steel screw (Optotec GmbH, Rathenow, Germany) in the frontal bone served as reference electrode for both arrays. Dental resin and further anchoring screws were used to secure the wiring and fix electrical connectors (Molex, USA) to the skull. Following surgery, animals were allowed at least five days for recovery.

#### **1.2.1.3 Setup**

All electrophysiological recordings were carried out in a sound-proof chamber; during the measurement animals could move freely within a shuttle-box (38 x 19 x 22.5 cm; Hasomed GmbH, Magdeburg, Germany). The implanted electrodes were connected to the recording system (MAP, Plexon Inc., Dallas, TX, USA) via a tether. Field potentials were filtered between 0.7-300 Hz and digitized at 1 kHz. Stimuli were generated in MATLAB (Mathworks, Natick, TX, USA) and presented inside the chamber by a data acquisition card (PCI 6713, National Instruments, Austin, TX, USA) connected to a modified headphone audio amplifier and electrostatic speaker (SRM313, Stax Ltd., Japan; average free-field sound amounted to 75 dB SPL).

#### **1.2.1.4 Auditory gating recordings**

Before the recording session started, animals were habituated to the experimenter and electrophysiology setup prior to the experimental day.

During the recording session, animals were stimulated with trains of identical repetitive frequency modulated tones (rising: 1-2 kHz or falling: 2-1 kHz; both 200 ms long with 5 ms on- and offset cosine squared ramps, 6 repetitions). Inter-trial intervals were varied between 11 and 19 s. Inter-stimulus intervals within the train were varied from 0.5 to 4.3 s. The first stimulus presentation in all trains was used for the characterization of auditory evoked potentials in both brain areas. For the short-term habituation experiment three ISIs were analyzed: 0.5, 1.2 and 4.3 s (Section 1.3.3). Animals were presented with at least 360 trains in a session.

#### **1.2.1.5 Histology**

After termination of experiments, iron deposits were produced at the tip of the striatal electrodes via delivery of current pulses to determine their correct placement (stimulator: STG 1008, Multi Channels Systems, Reutlingen, Germany; four rectangular pulses, 5  $\mu$ A for 25 s each). Afterwards, animals were sacrificed and the brain removed. Brains were cut into 40  $\mu$ m histological slices, mounted on glass slides and subjected to Nissl and Prussian blue iron staining. Electrode locations of the striatal arrays were verified with a gerbil brain atlas (Loskota *et al.*, 1974).

### **1.2.2 Data Analysis**

#### **1.2.2.1 Preprocessing**

Trials showing obvious movement artifacts were discarded. To analyze evoked potentials, recorded electrophysiological data were averaged across all channels of a region (cortex and striatum), baseline-corrected (1 s at the beginning of a trial) and low-pass filtered at 40 Hz (phase-neutral 6<sup>th</sup>-order Butterworth filter). To compensate for both, possible inter-animal-differences, as well as between-area-differences in signal strengths, averaged signals were z-transformed to their own baseline (1s before stimulus presentation). Baseline segments were qualitatively controlled for stability of variances (via visual inspection).

### 1.2.2.2 Peak sorting

For each subject, time windows for AEP peaks were identified separately. For each trial a moving average that replaced a point with the average of the neighboring data points in a 250 ms span, was calculated. The baseline standard deviation was calculated as well. All identified extrema that passed the smoothing line plus/minus one baseline standard deviation were plotted and with this diagram time windows for component clusters were determined for each subject. Within these defined time windows, the global maxima and minima were taken as peaks of the evoked potentials. Three peaks of evoked potentials (P1, N1 and P2; Figure 1.1 B) could be robustly identified in the auditory cortex in all animals. Striatal AEPs normally allowed to identify at least a large negativity and a large positivity (here called N1 and P2); a smaller negative-positive deflection previous to N1 often failed to cross the threshold and was then manually identified. Latencies were measured from the stimulus onset to the determined peak- or trough-maximum. Amplitudes in the gating analyses were calculated as peak-to-peak values from preceding troughs or peaks (e.g. N1 was calculated as difference between P1 and N1). For the characterization of AEPs, measured peak amplitudes and latencies evoked by the first stimulus of presented trains of FM tones were averaged for each animal, distinguishing between rising and falling direction of modulation.

### 1.2.2.3 Sensory gating

The ratio of the second (S2) and first (S1) stimulus presentation of an FM tone train was calculated to assess the amount by which the potential evoked by S2 is suppressed compared to the S1 tone evoked potential:

$$Suppression [\%] = 100 * \left(1 - \frac{peak(S2)}{peak(S1)}\right)$$

Thus a positive suppression value indicates a decrease in the response to the second stimulus, while a negative suppression value indicates that the amplitude evoked by S2 is facilitated compared to the S1 tone evoked

response. All animals that showed absolute S2/S1 ratios  $> 3$  were excluded as outliers from the respective analysis (P1:  $n = 7$ , N1:  $n = 1$ ; Mears *et al.*, 2009; White & Yee, 1997; Yee & White, 2001). In the correlation analysis, two points were suspected outliers; removing them from the correlations produced non-significant statistics: they were therefore excluded from these particular analyses.

### **1.2.3 Statistical analysis**

Statistics were computed using R (R Foundation for Statistical Computing, Vienna, Austria) and SPSS (PASW Statistics 18, SPSS, Inc., Chicago). For all statistical computations a significance level of 0.05 was chosen.

#### **1.2.3.1 Characterization of evoked potentials and suppression**

Peaks and latencies of auditory evoked potentials as well as suppression scores were compared with paired t-tests. The interrelation of gating scores and evoked amplitudes between areas was assessed by calculating Pearson's correlation coefficients.

#### **1.2.3.2 Short-term habituation**

For the analysis of the short-term habituation data, striatal amplitudes were tested with repeated-measure analysis of variance (ANOVA) for within subject influences of three factors: FM type (levels: rising and falling), STIMULUS POSITION (or repetition number) in train (levels: positions 1-6) and ISI (levels: short (507 ms), intermediate (1217 ms) and long (4259 ms)). Greenhouse-Geisser corrections were used as appropriate. Significant effects were analyzed *post-hoc* with planned contrasts, using a polynomial contrast for the factor ISI, difference contrast for FM and repeated-measure contrasts for STIMULUS POSITION.

### 1.2.3.3 Recovery time model

To model the striatal N1 and P2 T/C ratio dependences on inter-stimulus intervals, the animals were passively presented with trains of different ISIs. One group of animals ( $n = 7$ ), was presented with shorter ISIs (507- 1216 ms, 14 ISIs) and another with longer ISIs ( $n = 8$ : 507- 4259 ms , 13 ISIs). An asymptotic exponential with two parameters ( $\tau$ : scale parameter and  $t_0$ : origin) was chosen to fit the model.

$$T/C = 1 - e^{-\frac{t-t_0}{\tau}}$$

The asymptotic value was set to one, assuming that with infinite ISIs, gating is not suppressed or facilitated and the T/C ratio will approach a constant value (Figure 1.5). This model assumption led to a rejection of a linear model. Other exponential models with more or less parameters were tried as well, but the two-parameter asymptotic model yielded the tightest fit to the data. Models were fitted using the Gauss-Newton algorithm for non-linear fits implemented in R cran (<http://www.R-project.org/>). Bootstrapping ( $k = 999$ ) with sampling and replacement of the dataset was used to determine the timepoint at which the model approached its asymptote. For this purpose a bootstrap dataset was drawn with replacement that had the same distributions of datapoints for each ISI as the original dataset. If an asymptotic exponential (see above) model could be fitted to this hypothetical dataset, its coefficients were used to calculate the ISI at which the function would have reached 90% of its asymptote value. This timepoint was taken as recovery time. The procedure was repeated 999 times to obtain mean and standard deviation.

For a qualitative comparison, asymptotic exponential fits were also obtained for each individual animal.



## 1.3 Results

### 1.3.1 Frequency-modulated tone-evoked potentials in the ventral striatum and auditory cortex

Stimulation of awake, passively listening animals with trains of FM tones evoked consistent auditory potentials in both auditory cortex and ventral striatum during the first tone presentation (Figure 1.1 A). The first tone of a train of six FM-sweeps was used to characterize these potentials. Cortical and striatal AEPs allowed for the robust identification of 3-4 middle-latency peaks, here termed P1 (24 - 28 ms), N1 (47 - 79 ms) and P2 (129 ms - 234 ms) (Figure 1.1 B; Table 1.1). AEPs showed similar shapes in both brain regions with differing latencies of subcomponents. P1 components in the cortex and striatum peaked at the same time [rising:  $t = 1.45$ ,  $p = 0.17$ ; falling:  $t = 0.85$ ,  $p = 0.41$ ], but striatal amplitudes were significantly smaller in both FM conditions compared to the cortical amplitudes [rising:  $t = 3.3$ ,  $p < 0.001$ ; falling:  $t = 3.5$ ,  $p < 0.001$ ]. After P1, the time-courses of evoked peaks differed in both areas: N1 peaked earlier in the striatum during both FM conditions [rising:  $t = 9.8$ ,  $p < 0.001$ ; falling:  $t = 9.9$ ,  $p < 0.001$ ] and with a smaller amplitude than in the cortex [rising:  $t = 4.2$ ,  $p < 0.001$ ; falling:  $t = 5.5$ ,  $p < 0.001$ ]. The P2 deflection appeared approximately 100 ms earlier in the striatum than in the cortex during falling and rising FM [rising:  $t = 9.0$ ,  $p < 0.001$ ; falling:  $t = 9.8$ ,  $p < 0.001$ ], but striatal amplitudes were significantly smaller [rising:  $t = 3.7$ ,  $p < 0.001$ ; falling:  $t = 5.5$ ,  $p < 0.001$ ]. When comparing AEPs to frequency-rising and -falling tones within both brain areas, all corresponding peaks appeared at comparable latencies [ $-1.62 < t < 1.13$ , all  $p > 0.05$ ; Table 1.1]. P1 amplitudes in the cortex, however, were larger when evoked with rising than with falling FM tones [ $t = 3.4$ ,  $p < 0.01$ ]. In the striatum, all subcomponents evoked by rising tones had significantly larger amplitudes than those evoked by falling FM tones [P1:  $t = -3.79$ ,  $p < 0.01$ ; N1:  $t = -3.76$ ,  $p < 0.01$ ; P2:  $t = -2.16$ ,  $p = 0.048$ ].

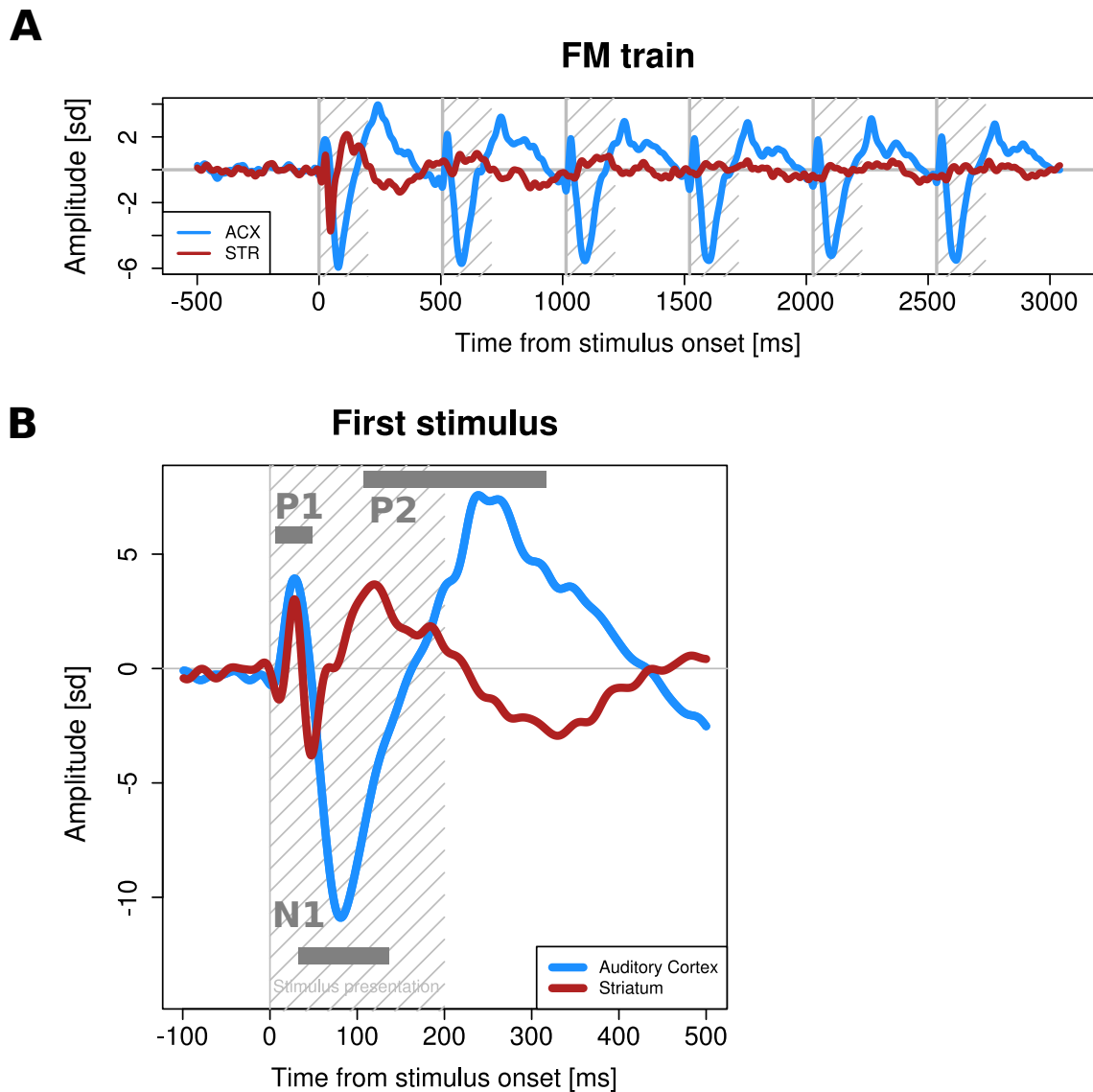


**Figure 1.1: Frequency-modulated (FM) tone evoked potentials in the auditory cortex and striatum showed different temporal dynamics. (A)** Grand-average field potential traces during the stimulation with a train of six FM tones with an onset inter-stimulus interval of 0.5 s. Strongly evoked responses in the striatum (red line) could only be found for the first tone presentation, while in the cortex (blue line) an auditory evoked potential was present at each repetition. **(B)** Exemplary grand average from one animal of evoked potentials in both brain areas demonstrates the identification of three subcomponents (P1, N1, P2) with similar shape in both brain areas but differing amplitudes and latencies after P1. N1 and P2 peaked earlier in the striatum than in the cortex. Stimulus presentation (0-200 ms) is indicated as gray shaded areas behind evoked potentials. Amplitudes were normalized to baseline standard deviation (sd). ACX: auditory cortex; STR: ventral striatum.

**Table 1.1: Latencies and amplitudes of identified AEP subcomponents were not influenced by frequency modulation direction.** Amplitudes are peak to peak values. Data are means and standard deviation.

Area	FM	Latency [ms]			Amplitude [sd]		
		P1	N1	P2	P1	N1	P2
ACX	rising	28±8	79±12	234±29	3.4±2.4	9.9±4.1	12.0±3.4
	falling	28±9	79±10	227±32	2.5±1.9	9.1±3.2	11.9±2.9
STR	rising	25±4	47±3	129±27	2.4±2.1	5.9±2.6	8.1±2.4
	falling	26±5	49±6	131±22	1.7±1.5	4.1±2.3	6.9±2.4

### 1.3.2 Auditory gating of P1, N1 and P2 in striatum and auditory cortex

Following classical gating protocols, the responses to the first and second tone of FM tone trains with an inter-stimulus interval of 0.5 s were used to calculate the amplitude suppression of P1, N1 and P2 at S2 (Figure 1.2). Gating was not different for rising and falling FM tones in both areas [ACX: P1  $t = 0.28$ , N1  $t = 0.44$ , P2  $t = 0.7$ , all  $p > 0.45$ ; STR: P1  $t = 0.11$ , N1  $t = -0.32$ , P2  $t = -0.57$ , all  $p > 0.58$ ], therefore gating values were pooled across FM directions (Table 1.2).

**Table 1.2: Means and standard deviations of amplitude suppression in the auditory cortex and ventral striatum.** Numbers in brackets give standard error of the mean.

Area	Component	Suppression [%]
ACX	P1	-1.2 ± 67.3 (13.5)
	N1	-3.1 ± 51.3 (9.5)
	P2	3.8 ± 30.2 (5.5)
STR	P1	38.5 ± 67 (12.7)
	N1	60.1 ± 46.2 (8.4)
	P2	58.1 ± 25.3 (4.6)

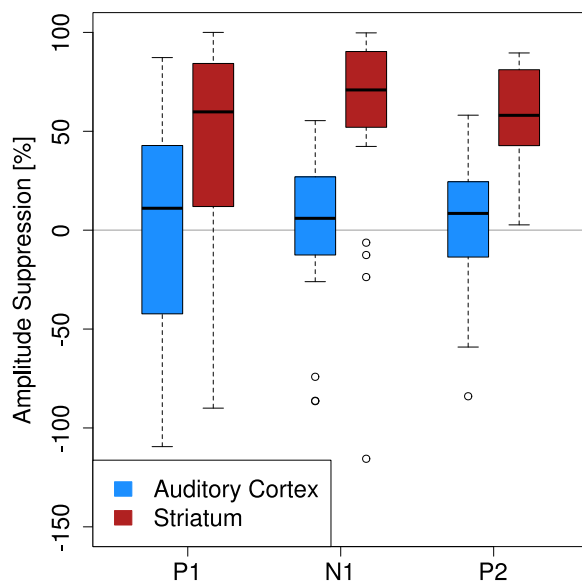


**Figure 1.2: Auditory gating was found for all three subcomponents of the striatal auditory evoked potential (AEP) but for none of the cortical AEPs.** Suppression of the peak amplitudes was calculated using the first and second stimulus. Boxes show the interquartile range (IQR) and the median of the data distribution. The whiskers display the data range. Outliers outside the 1.5\*IQR are represented by circles.

Suppression values of the three analyzed peaks were comparable within the brain areas [ACX:  $0.42 > t > -1.1$ , all  $p > 0.29$ ; STR:  $0.3 > t > -1.6$ , all  $p > 0.12$ ]. Comparisons of gating of the three peaks between both areas yielded a larger average P1 suppression in the striatum than in the auditory cortex. Due to the large variance in both areas the comparison failed to reach significance [42% vs. 2%;  $t = -2$ ,  $p = 0.054$ ]. However, suppression of the N1 and P2 peak from S1 to S2 was significantly stronger in the striatum than in the cortex: While the cortical N1 peak seemed to be weakly enhanced on average (-3% suppression), the striatal N1 peak of the S2 evoked amplitude was clearly suppressed to 61% of S1 evoked amplitude [ $t = -5$ ,  $p < 0.001$ ]. The cortical P2 wave showed a weak suppression (4%), contrary to the striatal peak which was also strongly gated (58%) [ $t = -7.5$ ,  $p < 0.001$ ]. Across animals, there were no significant correlations between striatal and cortical suppression scores, no correlations between striatal evoked amplitudes and cortical suppression values and also no significant correlations between cortical evoked amplitudes and striatal amplitude suppression [all  $R^2 < 0.14$ , all  $p > 0.05$ ].

### **1.3.3 Short-term habituation in the ventral striatum**

To evaluate if the dynamics for the suppression of amplitudes found in the ventral striatum can be classified as short-term habituation or are rather due to recovery processes of the neuronal generator pool of AEPs, the whole stimulation train of six tones was subjected to repeated-measure ANOVAs investigating three different ISI lengths: small (0.5 s), intermediate (1.2 s) and long (4.3 s), as well as the effects of STIMULUS POSITION and FM sweep direction (Figure 1.3).

N1 and P2 subcomponents of the striatal AEP were similarly influenced by ISI, STIMULUS POSITION and their interaction. These effects were also seen as statistical trends in the P1 subcomponent data (for statistics see Table 1.3; Figure 1.4).

**Table 1.3: ANOVA results for short-term habituation of striatal amplitudes.**  
Greenhouse-Geisser epsilons are cited where appropriate corrections have been made.

<b>Component</b>	<b>Effect</b>	<b>df</b>	<b>F</b>	<b>ε</b>	<b>p</b>
<b>P1</b>	FM	(1, 7)	1.82	-	0.220
	ISI	(1.1, 8.0)	5.08	0.568	0.051
	POSITION	(1.8, 11.0)	12.06	0.315	0.003
	FM x ISI	(2, 14)	1.66	-	0.225
	FM x POSITION	(5, 35)	2.33	-	0.063
	ISI x POSITION	(1.7, 11.9)	2.05	0.171	0.174
	FM x ISI x POSITION	(3.1, 21.7)	0.79	0.310	0.519
<b>N1</b>	FM	(1, 7)	2.56	-	0.154
	ISI	(1.1, 7.8)	21.47	0.560	0.002
	POSITION	(1.5, 10.6)	19.41	0.302	0.001
	FM x ISI	(2, 14)	1.61	-	0.235
	FM x POSITION	(5, 35)	0.42	-	0.832
	ISI x POSITION	(3.5, 24.3)	5.17	0.347	0.005
	FM x ISI x POSITION	(3.8, 26.7)	0.79	0.381	0.539
<b>P2</b>	FM	(1, 7)	0.03	-	0.872
	ISI	(2, 14)	17.36	-	<0.001
	POSITION	(1.4, 9.5)	12.24	0.272	0.004
	FM x ISI	(2, 14)	0.76	-	0.486
	FM x POSITION	(5, 35)	1.39	-	0.253
	ISI x POSITION	(3.4, 23.5)	5.43	0.335	0.004
	FM x ISI x POSITION	(3.5, 24.6)	0.62	0.352	0.635

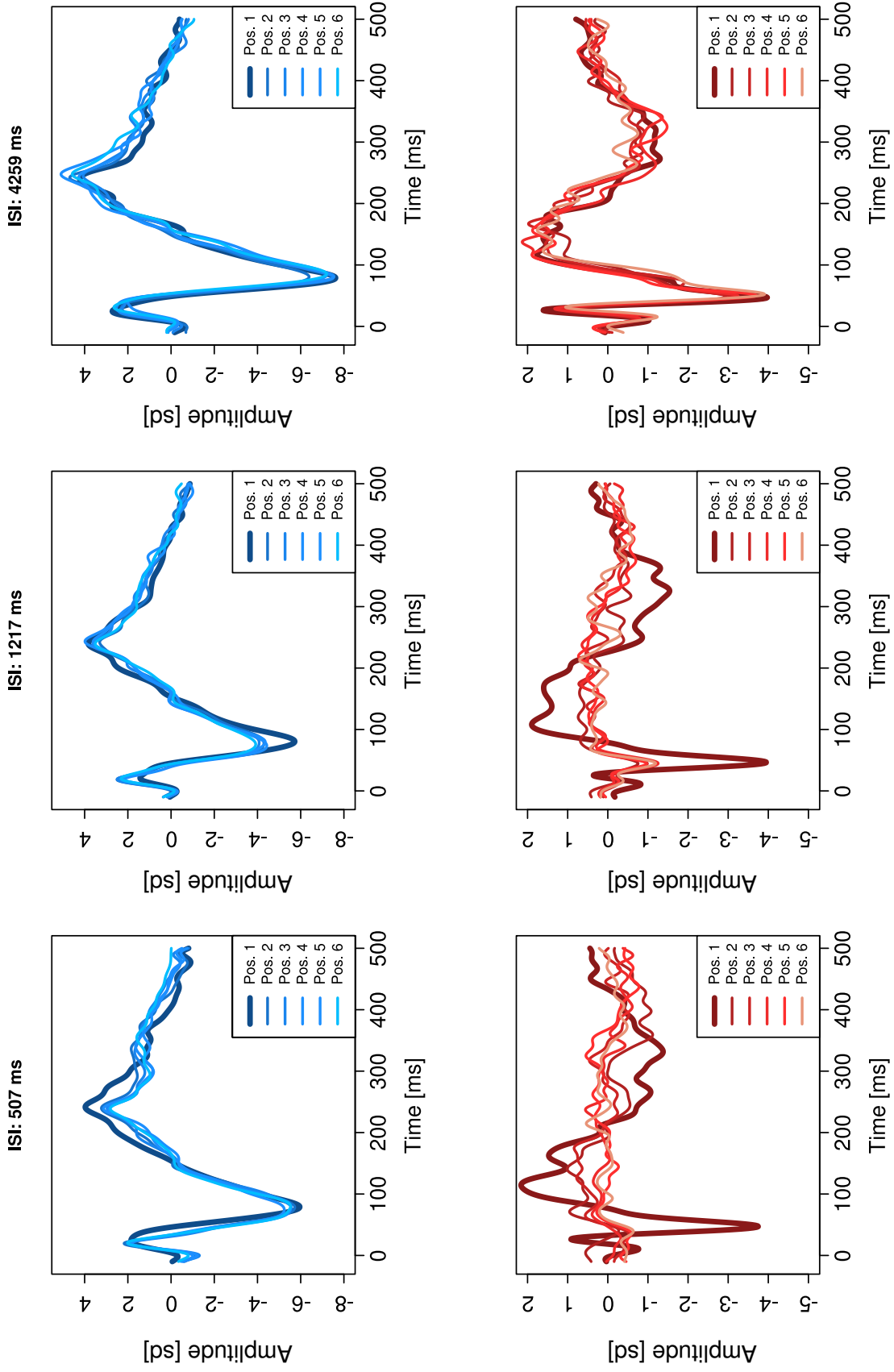


**Figure 1.3: Inter-stimulus interval effects on grand-average evoked potentials.** Time-spans of stimulus presentation are overlaid to compare auditory evoked potentials (AEPs) at every stimulus position within a train. The gradual recovery in the striatum with longer ISIs can be seen in the *bottom row*. Stimulus evoked potential deflections at different stimulus positions within a train were of comparable strength only at the longest ISI. Cortical AEPs (*top row*) correlated strongly with each stimulus repetition.

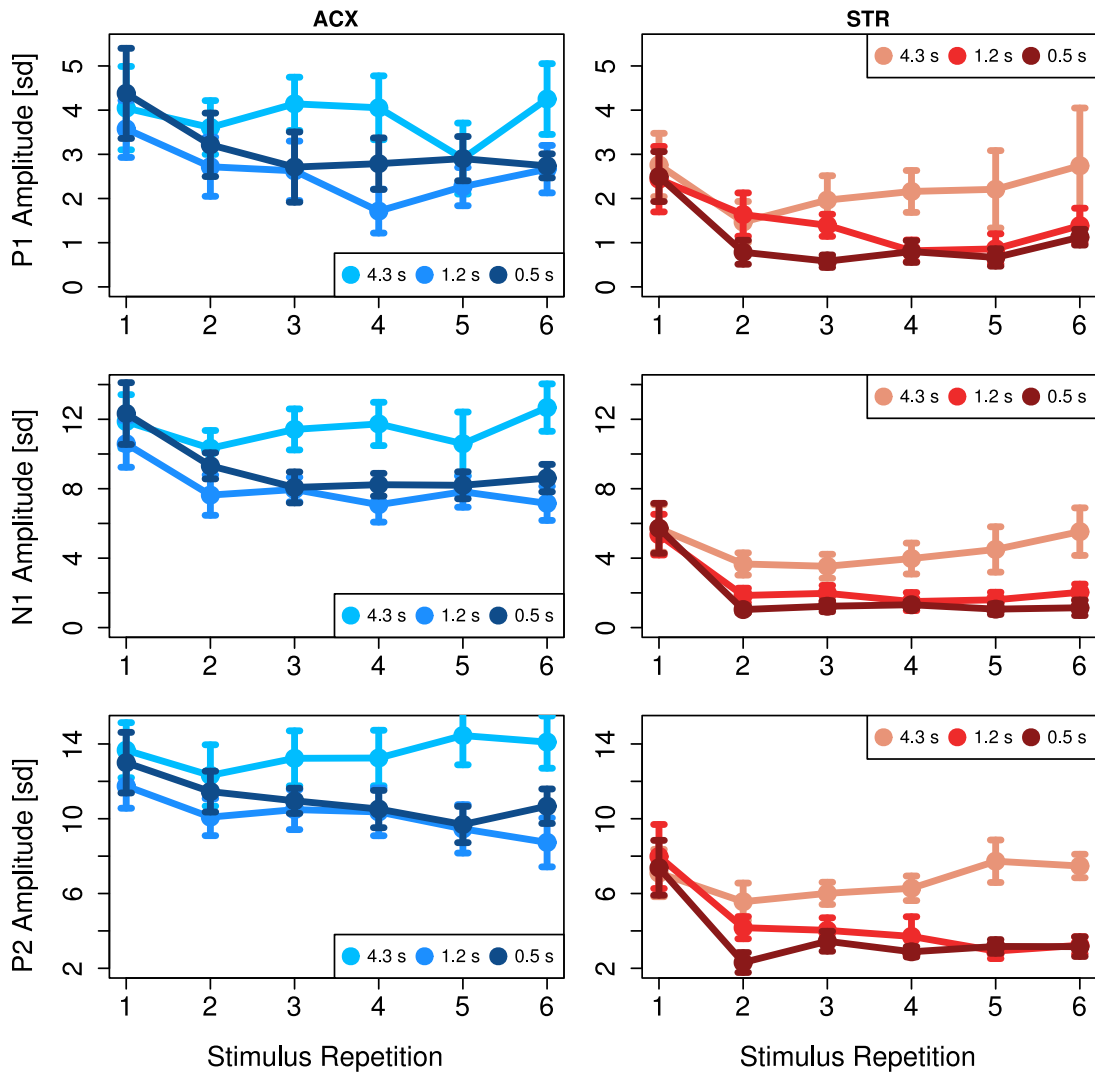


**Figure 1.4: Marginal means of amplitudes as a function of stimulus repetition (within a train) for three inter-stimulus intervals (ISIs).** The standard error of the mean is given as confidence interval. Cortical amplitudes are plotted for a qualitative comparison. ACX: auditory cortex. STR: ventral striatum.

P1 amplitudes in the striatum were influenced by the factor STIMULUS POSITION, while the ISI main effect was only marginally significant. Analysis of the planned contrasts revealed that only the comparison of the first versus



the second stimulus position yielded a significant effects for P1 [ $F(1, 7) = 24.8, p = 0.002$ ].

N1 amplitudes were influenced by ISI, STIMULUS POSITION and the interaction of the two factors. ISI effects were significant for the linear [ $F(1, 7) = 26, p = 0.001$ ] and the quadratic polynomial contrast [ $F(1, 7) = 11.5, p = 0.012$ ]. When comparing stimulus positions only the difference between the first and second stimulus was highly significant ( $F(1, 7) = 22.2, p = 0.002$ ), but not the comparisons of subsequent stimulus positions. Within the interaction effect, the linear polynomial contrast model for the difference between stimulus position one and two proved to be significant [ $F(1, 7) = 14.5, p = 0.007$ ], but not for the other differences between stimuli.

Statistics for the P2 subcomponent were much alike the N1 result: P2 amplitudes were affected by ISI, STIMULUS POSITION and their interaction. The factor ISI was significant for the linear [ $F(1, 7) = 21.2, p = 0.002$ ] and the quadratic polynomial contrast [ $F(1, 7) = 9, p = 0.02$ ]. Only the difference between the first and the second stimulus proved to be significant [ $F(1, 7) = 10.8, p = 0.013$ ] and within the interaction of ISI and STIMULUS POSITION only the linear polynomial contrast for stimulus one versus two was found significant [ $F(1, 7) = 8.1, p = 0.025$ ].

In summary, striatal N1 and P2 and marginal P1 amplitude decrements were mainly due to ISI effects, while the STIMULUS POSITION effect was concentrated on the difference between the first and the second stimulus within a FM tone train. Direction of frequency modulation did not play a role. Striatal and cortical amplitudes and corresponding latencies split by the used testing factors are summarized in the Appendix A: Tables [1](#) and [2](#).

### **1.3.4 Recovery Model for Striatal N1 and P2**

The mean T/C ratio across animals in dependence of different ISIs was used to fit an asymptotic exponential function to the data with scale parameter  $\tau$  and abscissa intercept  $t_0$  (Figure [1.5](#)).

Since there were no differences between falling and rising FM sweeps in gating (Section [1.3.2](#)), those data points were pooled. All three

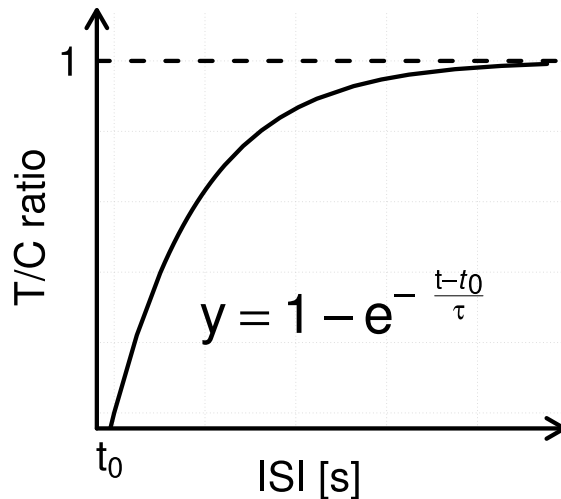


**Figure 1.5: Asymptotic exponential function used to model the recovery of auditory gating of striatal N1 and P2.** The plot shows the theoretical curve progression. The function was dependent on two parameters:  $\tau$  as a scale factor and  $t_0$  as origin. Additionally, the fit was forced to approach one as T/C ratio (stippled line).

subcomponents showed gating in the ventral striatum, but P1 test-conditioning (T/C) ratios were not robust enough to use it for the fitting procedure. Therefore fits were only derived for N1 and P2 data. There was no inhibitory gating effect within the auditory cortex at the used ISIs. Nonetheless, to have a qualitative comparison to the striatum, the model was also fitted to cortical data points (Figure 1.6, left panels).

When the model was fitted to the dataset from the auditory cortex, there was no convergence of the algorithm for data points of N1 or P2 T/C ratio. Established parameters showed that cortical data points hardly laid in the non-stationary part of the curve (Figure 1.6, left panels). When fitted to the striatal dataset, the model proved to be highly convergent for both, N1 [ $t_0 = -1.68$ ,  $t = -2.25$ ,  $p = 0.03$ ;  $\tau = 4.22$ ,  $t = 3.92$ ,  $p < 0.001$ ; residual standard error = 0.44 on 425 df] and P2 [ $t_0 = -0.63$ ,  $t = -2.33$ ,  $p = 0.02$ ;  $\tau = 2.17$ ,  $t = 6.23$ ,  $p < 0.001$ ; residual standard error = 0.35 on 432 df]. The model was used to bootstrap recovery times for both components, i.e. the ISI necessary

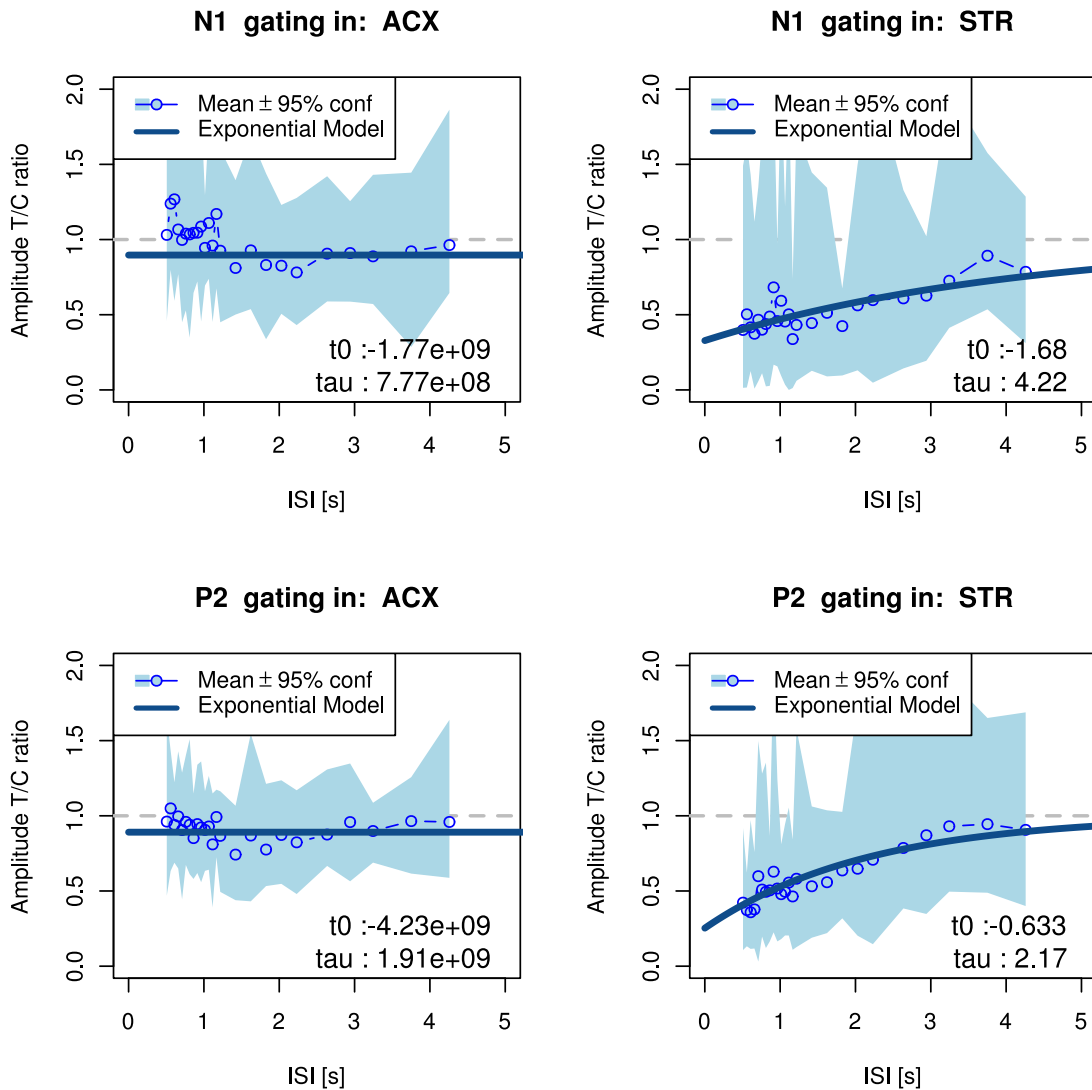


**Figure 1.6: Auditory evoked potential recovery fits.** Mean population data points (blue circles) with 95% confidence intervals (blue shaded area behind the curve). The fitted curve is displayed by the continuous blue line. Auditory cortex data (ACX: left panels) could not be fitted in a convergent manner with the same function, as most of the data lay in the stationary part of the assumed model. In the striatum (STR: right panels), the model converged for both peaks. Parameters from the exponential fits are displayed for both areas.

for a subcomponent to approach the asymptote at a 90% confidence interval (see method section). While striatal N1 attained a recovery time of 8.3 s, P2 peaks recovered in shorter time (4.4 s) (Figure 1.7).

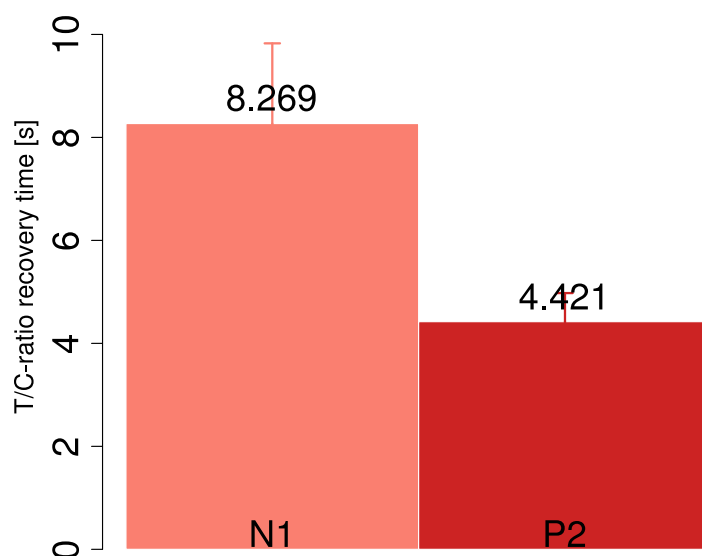


**Figure 1.7: Estimated recovery times for repetitive FM tone stimulation exceeded 4 s.** Striatal N1 and P2 peaks needed a recovery time of 8.3 and 4.4 seconds, respectively, to reach 90% of the full amplitudes. Displayed are the bootstrapped mean and standard deviation.

Since pooling population data lack inter-individual variance, the population fits were also compared to models fitted on individuals' data sets (Appendix A, Figure 1, p. 92). Derived median recovery times were comparable to the values based on population data estimates (Figure 1.7), the obtained confidence intervals were larger, however.

## 1.4 Discussion

### 1.4.1 FM tone evoked potentials in the ventral striatum and auditory cortex

Stimulating Mongolian gerbils passively with frequency-modulated tones evoked robust potential deflections in the ventral striatum and the primary auditory cortex (Figure 1.1). Rising and falling FM sweeps of the same frequency range, as have been used in this study, do recruit different (but overlapping) tonotopic areas in field A1 of the auditory cortex (Ohl *et al.*, 2000b). Except for the P1 subcomponent there were no differences between cortical AEPs evoked by rising or falling FM tones. This finding can be mostly attributed to the spatial averaging of the cortical signal: rising FM sweeps in particular activate a more rostral area on the tonotopic map of the primary ACX (Ohl *et al.*, 2000b). It could be that the preparations included more electrode locations proximate to the higher frequency (2 kHz) and therefore the spatial average over ACX electrodes yielded a higher potential amplitude for rising FM tones. According to the results from Ohl *et al.* (2000b), the same trend should have been visible in the N1 wave, too. As a matter of fact, N1 amplitudes evoked by rising FM sweeps showed a small trend for being larger than those evoked by falling FM sweeps [ $t = -1.7$ ,  $p = 0.099$ ].

Remarkably, the AEPs in the striatum were of larger amplitude when stimulated by upwards modulated tones. Speculatively, this could be related to the saliency of sweep direction in naturally behaving gerbils. Mongolian gerbils utilize several vocalization calls, among others low-frequency multi-harmonic calls in antagonistic situations, for instance during food competition, or high-frequency-ultrasonic frequency-modulated calls during greeting of colony mates (Nishiyama *et al.*, 2011). Thus frequency-modulation comprises an important aspect in gerbil syllable structure and therefore the basis for these animals' vocalizations (Kobayasi & Riquimaroux, 2012). This group also found that rising frequency modulated syllables were mostly used by the animals in non-conflict situations, while

downward FM syllables appear to be used in minor conflict encounters (Kobayasi & Riquimaroux, 2012).

Comparisons of the stimulation train's first AEPs revealed that the time course of these deflections differed between both brain areas. After the first robust identifiable positive peak -here called P1- subsequent deflections in the ventral striatum peaked significantly earlier. While these differences do not represent ultimate proof about the specific activation cascades following auditory stimulation in the cortex or the ventral striatum, they indicate that activation sources for P1 could stem from the same source, while later processing would be enacted differentially. In rodents, surface P1 of the MAEP complex should firstly represent monosynaptic thalamo-cortical activations that then overlap with other vertical and horizontal synaptic inputs (Barth & Di, 1990; Happel *et al.*, 2010; Ohl *et al.*, 2000a). Auditory input could reach the ventral striatum via non-primary auditory pathways such as in the hippocampal formation and amygdala. The functions of these paths have been mainly related to behavioral cueing (Bickford *et al.*, 1993; Hu, 2003; LeDoux, 2000) and prepulse inhibition (Koch & Schnitzler, 1997; Swerdlow *et al.*, 1992). Recent work in the visual sensory domain has shown that striatal spiny neurons can be rapidly activated through subcortical visual pathways that relay signals from the superior colliculus via the thalamus, most likely allowing for synaptic changes due to biological relevant stimuli (Redgrave *et al.*, 2010; Schulz *et al.*, 2009). A similar auditory subcortical loop through the basal ganglia appears plausible (McHaffie *et al.*, 2005). Hence, these findings point towards an independence of the striatal AEP generation from the primary auditory pathway, similar to temporal and midline AEPs (Kraus *et al.*, 1987; McGee *et al.*, 1991).

### **1.4.2 Auditory gating**

The clear amplitude suppression, found in the ventral striatum, shows that gating phenomena in rodents also hold true for more complex stimuli,

thereby displaying an indifference towards the acoustic feature of frequency modulation direction. Together with the work by other groups this result implies auditory gating to be a more general mechanism in sensory processing and probably more related to changes of physical features and saliency of a stimulus than the features per se (Boutros & Belger, 1999; Boutros *et al.*, 1997; Brenner *et al.*, 2009; Moura *et al.*, 2010). It is possible that subcortical auditory evoked potentials rather transport sensory significance than sensory perceptual information: in the hippocampus, for example, potentials evoked by either auditory clicks or tooth pulp stimulation bore the same time course and amplitude, thus information from both sensory modalities appeared to reach identical synaptic fields within the hippocampus (Brankack & Buzsáki, 1986).

In the present study, auditory gating was assessed by standard gating ratios of potentials evoked by the first and second tone in a train of six identical FM sweeps. Strong gating of evoked potentials was observed in the ventral striatum while it was negligible in the auditory cortex. At the inter-stimulus interval used in this study (0.5 s), and in most gating experiments, the auditory cortex showed no significant suppression of FM tone evoked amplitudes (Figures 1.2, 1.3). Furthermore, there were no correlations between striatal gating and amplitudes in the cortex. This is in line with several animal studies which found no association of auditory gating in hippocampal CA3, medial septal nucleus and brainstem reticular nucleus with auditory cortex or thalamic medial geniculate nucleus evoked potentials (Bickford-Wimer *et al.*, 1990; Moxon *et al.*, 1999). Yet, human P50 gating has been related to the primary auditory cortex (Grunwald *et al.*, 2003), to alpha oscillations therein (Mathiak *et al.*, 2011), as well as hemodynamic responses in its left hemisphere (Mayer *et al.*, 2009). Work from others point towards the frontal lobe as the primary mediator of gating (Knott *et al.*, 2009; Korzyukov *et al.*, 2007) and patients with prefrontal cortex lesions displayed impaired auditory gating (Knight *et al.*, 1999). Rat medial prefrontal cortex has been shown to demonstrate strong gating, as well (Mears *et al.*, 2006, 2009), and should therefore, in future animal studies, be tested for its interventional role in the gating process with other brain

areas. A more recent imaging study (Boutros *et al.*, 2011) points out that sensory registration and suppressive mechanisms are most likely carried out by different brain areas and the present results hint into that direction as well.

Literature on human auditory gating is mainly centered on suppression effects on the pre-attentive P50 and P50m or the early-attentive N100 and N100m component recorded at the vertex electrode in EEG or MEG experiments, respectively. Both components show auditory gating (Boutros & Belger, 1999), while the later N100's suppression appears to be more prone to attentional factors (Gjini *et al.*, 2011; Rosburg *et al.*, 2009a). A direct comparison of human and murine EP components, acknowledged at least partial comparability of their AEP-components (Umbricht *et al.*, 2004). In animal studies, auditory cortex P1 and N1 have been mainly attributed to thalamo-cortical activation of primary auditory cortex neurons, while the P2/N2 complex generation appeared to also involve secondary cortical areas (Barth & Di, 1990; Ohl *et al.*, 2000a).

Data on striatal evoked potentials is sparse. The most extensive study was probably put forward by Ryan *et al.* (1986) who investigated striatal LFPs evoked by electrical stimulation of cortical areas and white matter. They conclude that striatal P1 most likely results from the synchronous depolarization of striatal cells, while N1 ("N2" in their nomenclature) results from intrastriate collateral inhibition and P2 represents the decline phase of tonic excitatory input. This fits well with the high variability found for the suppression of the P1 subcomponent, while the N1 and P2 waves were readily gated. In the present study, amplitude suppression of all three subcomponents investigated was similar.

### **1.4.3 Short-term habituation in the ventral striatum**

The T/C ratio for stimulus repetitions after the second tone were additionally analyzed for its decrement dynamics. Hypothetically, to classify the AEP behavior as "habituation" process, the repeated stimuli should show a



progressive decline due to the loss of novelty, while a neuronal model of the auditory percept is being built. A “bottom-up” process, on the contrary, should yield the immediate stabilization of the neural generators, and tones after S1 should reset their refractoriness. Hence the primary determinant of the amplitude decrement should be ISI (time between two response-eliciting tones) and not repetition number.

Although this study did not test for all of Thompson and Spencer’s classical criteria for habituation, there are at least two that were not met with the present data (Thompson & Spencer, 1966): The amplitude decrement in the striatum did not follow a linear or a negative exponential function of stimulus position (cf. characteristic #1 Rankin *et al.*, 2009) as comparisons between subsequent positions were not significant except for the first two stimuli. A floor effect can be excluded as with different ISIs, amplitudes were suppressed to an equal level within a train. According to Thompson & Spencer (1966) the frequency of stimulation should positively correlate with the rapidity of habituation, hence longer ISIs should produce a gradual amplitude decrement. Although there were significant ISI x STIMULUS POSITION interaction effects for the N1 and P2 subcomponents these were due only to the linear amplitude decrease between the first and the second stimulus and hence this criterion was also not met (see also Figure 1.4). Therefore our data are in line with results from Rosburg *et al.* (2004) and Boutros *et al.* (1997) and support the notion that striatal auditory gating is mainly based on the recovery of the neuronal generator pool (but see Ritter *et al.*, 1968). It has to be pointed out that the term “refractoriness”, although describing similar qualities, can only indirectly be related to refractory period of a single neuron, as it designates here the network properties of a whole neuronal pool.

This analysis additionally showed that amplitude changes in the striatum can sufficiently be analyzed by only looking at the change from the first to the second stimulus. Contrarily, dishabituation was found in several gating studies (Boutros *et al.*, 1997, 1999; Rosburg *et al.*, 2004) and embodies a characteristic of classical short-term habituation: “Presentation of another (usually strong) stimulus results in recovery of the habituated response

(dishabituation).” (cf. Rankin *et al.*, 2009). Unfortunately a change stimulus was not tested in the current setting which would have helped clarifying the network dynamics a bit better. If neuronal responses to such a hypothetical change stimulus would have elicited stronger “gating-in” responses is not clear. In spite of that, dishabituation effects not necessarily rule out refractoriness dynamics, as the change stimulus might activate slightly different neuronal networks than the previous stimuli. These discrepancies demonstrate, that a clear-cut classification of gating as a phenomenon relating to habituation or being solely based on refractoriness of its neuronal generator pool cannot be made. Moreover, both mechanisms do not by definition have to exclude each other.

#### **1.4.4 Estimated recovery times**

A study by Umbricht *et al.* (2004) set out to compare AEP decrement by stimulus onset asynchrony between men and mice using similar model fits as in the present study. In this study, fits for the P1, N1 and P2 subcomponents reached asymptotic levels between 3.3 and 6.5 s which is well in line with our findings for N1 and P2 gating in the Mongolian gerbil. They also fit human data that postulate an inter-trial interval of 8 s for the inhibitory mechanism during gating to fully recover (Zouridakis & Boutros, 1992). The effect of ISI on auditory gating was also investigated in a study by de Bruin *et al.* (2001), in which various vertex-recorded subcomponents of the rat AEP had not fully recovered before 5 s had elapsed.

In an older study by Dafny & Gilman (1974), testing various dopamine-associated agents on the recovery cycles, the later subcomponent P2 had already recovered within 600 ms within the control experiments. A follow-up by Dafny (1975) showed that among various tested structures, basal ganglia areas in rats exhibited the longest recovery times (1000 ms and 1400 ms for the caudate nucleus and the globus pallidus, respectively), although, in comparison to the recovery times of the present study, the durations are still short.

It has to be noted, that while the present data point towards a role of refractoriness of the neuronal generator pool, other mechanisms that have not been tested here are possible to function in parallel (Sable *et al.*, 2004).

# Chapter 2

## Time-frequency analysis of gating

### 2.1 Introduction

#### 2.1.1 The role of stimulus-locking in the physiology of auditory gating

Since it is still not clarified which brain networks take part in auditory gating and which structures effect the inhibition, or if the phenomenon is generated locally in different brain structures, a detailed description of the neuronal mechanism implicated in gating is not available. Instead of a manifest neuronal inhibition process, more recent studies have proposed temporal contiguity of neuronal responses to the evoking stimuli as a factor determining auditory gating.

Temporal variability in the response timing to the conditioning tone (S1) on a trial-by-trial basis have been shown to contribute to increased P50 gating ratios frequently found in schizophrenic subjects (Jin *et al.*, 1997; Patterson *et al.*, 2000). Similarly, such patients displayed lower low frequency responses than control subjects after S1 stimulation, which could be in direct relation to the diminished averaged S1 evoked potentials (Blumenfeld & Clementz, 2001). But phase-locking to the second stimulus appears also

to add to the P50 gating effect in healthy controls (Jin *et al.*, 1997). Jansen *et al.* (2003) reported that phase-synchronization in healthy subjects was increased after presentation of the auditory S1 stimulus in the 2-12 Hz frequency range and included the time span in which P50, N100 and P200 components are commonly observed. Schizophrenic patients were reported to show less phase-synchronization for the same parameters (Jansen *et al.*, 2004).

Phase-synchronization effects are in line with an understanding of the AEP as result of stimulus-related reorganization of the ongoing spontaneous EEG instead of additive afferent activity. More recent work has also suggested that stimulus-locking effects might as well be coupled with consistency effects: auditory gating could also be related to fewer responses to the test stimulus in healthy controls that would result in smaller amplitude grand averages (Hu *et al.*, 2009). Likewise it was shown that schizophrenic patients produced more incomplete responses to S1 (and S2) than control subjects (Jansen *et al.*, 2010).

If amplitude suppression in gating could be based on jittering phase-locking to the 2<sup>nd</sup> stimulus has not been tested in animals so far. Therefore a central objective of the present study was to investigate, whether auditory gating in the ventral striatum can be related to a temporal phase-locking mechanism rather than blocking afferent neuronal activity in the awake Mongolian gerbil.

### **2.1.2 Contribution of different frequency ranges to the auditory gating phenomenon**

The reduction in phase-locking after S1 presentation found in schizophrenic subjects as compared to healthy controls was most clearly seen in the theta-alpha frequency range and most likely corresponded to the N100 generation (Brockhaus-Dumke *et al.*, 2008). Another study extended this finding by showing that poor N100 gators had increased theta-alpha phase-locking after S2 (Rosburg *et al.*, 2009b). Those subjects also displayed less phase-locked

beta activity towards the first stimulus, indicating that here poor gating could be based on an encoding problem (Rosburg *et al.*, 2009b).

Not only amplitude effects and intensity-independent changes seem to constitute altered auditory gating, apparently also different frequency ranges might contribute to the auditory gating effect in health and disease (for a review see Uhlhaas *et al.*, 2008).

Due to conduction delays of brain matter, faster oscillations like gamma are generally reckoned to be local and oftentimes the first response after a sensory stimulus; slower waves are able to travel longer distances and hence are more likely to contribute to inter-area communication and synchronization up to memory modulations (Moran & Hong, 2011). Furthermore, cross-frequency coupling, e.g. theta-gamma interaction has been implicated in diverse cognitive processes, such as working memory (Moran & Hong, 2011). Smaller alpha and gamma responses to S1 have been detected in patients, as well as lower induced alpha activity directly preceding S2 presentation (Popov *et al.*, 2011). Both, induced gamma bursts and evoked gamma oscillations were reduced by stimulus repetition in human intracranial recordings (Trautner *et al.*, 2006). Likewise, overall increased gamma power was found in schizophrenic subjects with concurrent impairment of gating in the theta-alpha frequency range (Moran *et al.*, 2012). Theta-alpha oscillations during resting conditions seem to be elevated in schizophrenic subjects and even their first degree relatives and correlated strongly with insufficient suppression in this frequency range during sensory gating (Hong *et al.*, 2012). Interestingly, gating in the theta-alpha frequency range was estimated highly heritable as compared to the traditional P50 gating in such patients (Hong *et al.*, 2008).

The matter is even more obfuscated by findings that associate beta oscillations with normal functioning and malfunctioning auditory gating: evoked gamma-to-beta transitions have been thought to mark stimulus-driven salience of a cue, for example stimulus rarity, in sensory brain areas. Along this line, a study by Kisley & Cornwell (2006) showed that especially the evoked beta oscillations were modulated by ISI. Healthy subjects that displayed strong evoked beta oscillations after S1 stimulation

also showed the strongest P50 gating (Hong *et al.*, 2008). Complementary findings indicate that S1-evoked low beta power (12-20 Hz) is reduced in schizophrenic patients underlining their “saliency processing abnormalities” (Brenner *et al.*, 2009).

The above-mentioned reports only represent a glimpse on the influence of oscillatory activity on auditory gating in health and disease, highlighting the fact that time-frequency analysis within this task is only at its beginning, yet promising to entangle the physiological and systemic grounds for it. Given the manifold frequency influences on auditory gating, found in human literature, one goal within the present study was to examine the oscillatory influences of different frequency bands (delta to gamma) on amplitude suppression in the gerbil.

Time-frequency analysis can be employed to differentiate power modulation that is phase-locked (evoked) to the stimulus within single trials and power that is non-phase-locked (induced) and therefore mostly lost in average-based data analysis (Kalcher & Pfurtscheller, 1995; Klimesch *et al.*, 1998, Figure 2.1). In addition, phase information can be used to calculate cross-signal coherence, a measure that reveals information about the mutual interaction of two oscillators (Fries, 2005; Herrmann *et al.*, 2005). Within the present study this information was used to examine the contribution of the auditory cortex to the gating effect in the ventral striatum, by analyzing phase-locking between both areas.

The objectives of the second part of the present study can be summarized as follows:

1. Analysis of the role of stimulus-locking in the physiological process of auditory gating by investigating evoked and induced activity in the auditory cortex and ventral striatum respectively: An auditory gating effect, based on temporally jittering responses was expected to be expressed in increased or equal induced energy after S2 presentation, as compared to the evoked activity after the test stimulus.

2. The time-frequency analysis of the data from auditory cortex and ventral striatum was used to assess influences of discrete frequency bands on evoked and induced activities after S1 and S2 stimulations. As no distinct frequency band can be precisely held responsible for the gating process, the full range from delta to gamma oscillations were investigated. If stimulus-locking played a role during auditory gating, the recovery of the evoked activities were expected to compare to the AEPs while the recovery of induced activity should have been markedly shorter.
3. As elaborated in Chapter 1, the neural networks underlying auditory gating are far from being identified. To fully make use of the time-frequency analysis, phase information was extracted and used to examine phase-locking activity of the auditory cortex and the ventral striatum during auditory gating across trials. If gating was directly mediated by the cortical structure, a synchronization between both areas was anticipated.

## **2.2 Methods**

### **2.2.1 Subjects and procedures**

Subjects and procedures were the same as in Chapter 1 (cf. Section 1.2.1). For the analysis of evoked and induced activity only data with 0.5 s ISIs were used.

### **2.2.2 Data Analysis**

#### **2.2.2.1 Preprocessing**

Trials showing obvious movement artifacts were discarded. To compensate for both, possible inter-animal-differences, as well as, between-area-differences in signal strengths, signals were z-transformed to their own



baseline (1 s at the beginning of a trial). For the wavelet analysis, the channel showing the largest response was selected for each brain region.

#### **2.2.2.2 Wavelet transform**

To analyze evoked and induced activity a continuous wavelet transform was applied, utilizing wavelet tools from Torrence & Compo (1998) for Matlab (<http://paos.colorado.edu/research/wavelets/software.html>; MATLAB, The MathWorks, Natick, MA, USA). The Morlet mother wavelet was used, a complex exponential modulated by a Gaussian, with a non-dimensional frequency of 6, yielding approximately three oscillations within the Gaussian envelope (Torrence & Webster, 1999). This particular wavelet was chosen because of its good balance between time and frequency resolution and because a complex mother wavelet will return information about both, amplitude and phase of the signal (Grinsted *et al.*, 2004; Torrence & Compo, 1998). The wavelet transform represents a convolution of the time series of interest with the normalized and scaled mother wavelet. With a non-dimensional frequency of 6, the wavelet scales are nearly equal to Fourier periods (factor 1.03, Grinsted *et al.*, 2004). For the calculation of the wavelet transform a total of 105 logarithmically spaced scales was used, equivalent to a Fourier frequency range of 0.03 - 268.89 Hz. Zero padding of the data provided that our frequency range of interest (2 - 256 Hz) was not affected by edge artifacts. Wavelet transforms were calculated for every trial of the 0.5 s ISI train with rising FM tones, including a pre- and post-stimulus time of 1 s each (one trial amounting to a 5 s epoch). Baseline epochs of the same length were calculated likewise from parts of the recording session without stimulus presence.

#### **2.2.2.3 Induced and Evoked activity**

For each signal, the wavelet transform yielded a matrix of complex wavelet coefficients, one value for each frequency and time-point ( $W(t, f)$ ). Wavelet power was calculated as  $|W(t, f)|^2$  (Torrence & Compo, 1998). Hence the mean of power values over trials (TSP: total-signal-power) can be obtained

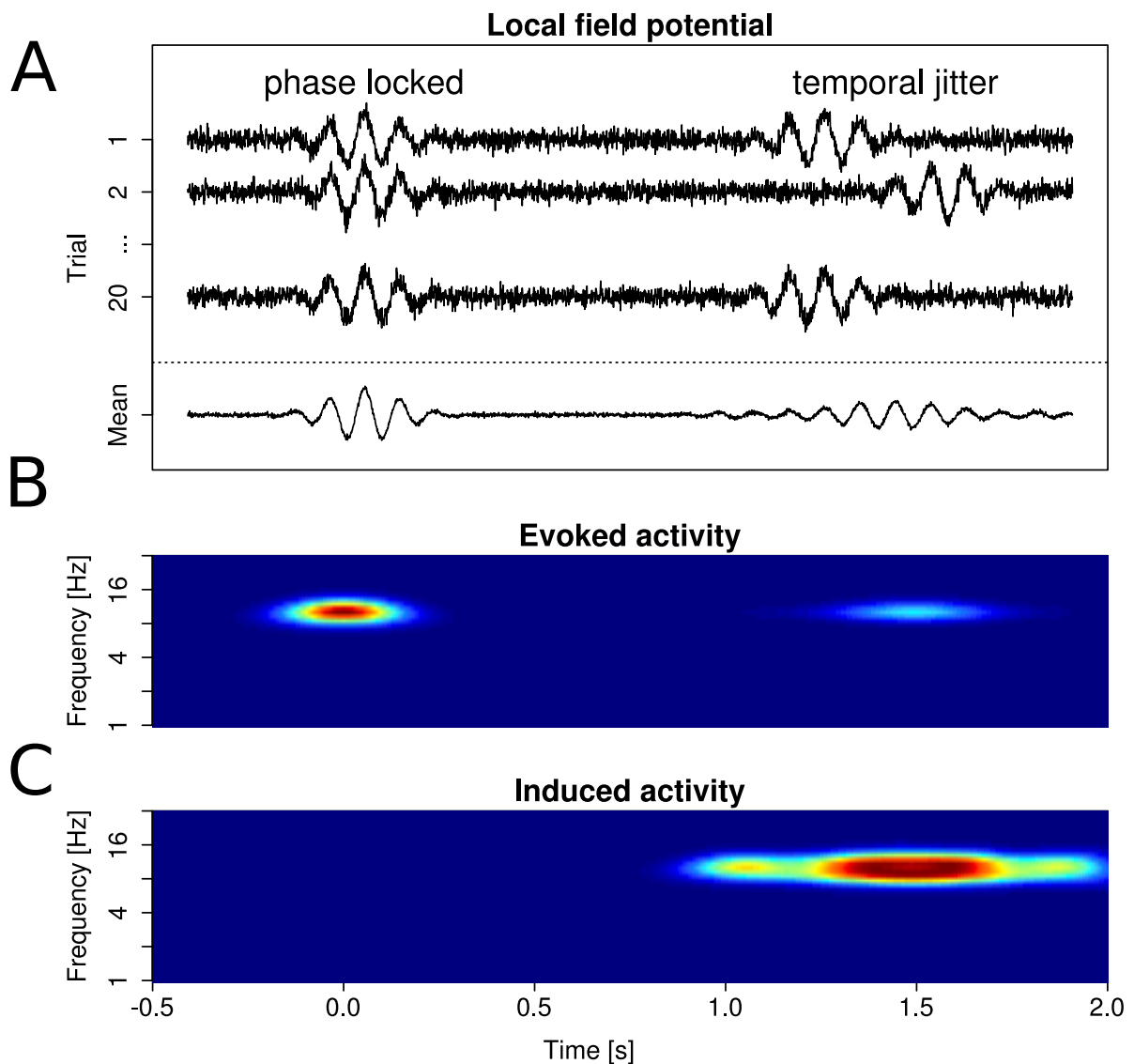


**Figure 2.1: Schematic display how averaging of local field potentials blurs information on non-phase-locked (induced) activity.** (A) Deflections of the local field potentials (artificially generated) can occur as stimulus-locked in time (here at 0.0 s) or as stimulus induced with a temporal jitter around the onset (here at 1.5 s). Typical averaging (“Mean”: bottom trace) results in decreased amplitudes for the latter kind of activity. Time-frequency analysis can distinguish between both kinds of energy (B, C). Evoked activity (B) is a measure for the stimulus-locked power, hence only a fraction of stimulus related activity that appears with temporal jitters towards the onset in single trials will show up in the spectrogram. This kind of activity is better captured in the non-phase-locked induced activity (C), which is calculated by subtracting the fraction of evoked power from the total-signal-power (modified from [Herrmann \*et al.\*, 2005](#)).

by calculating:

$$TSP(t, f) = \frac{1}{n} \sum (\Im^2 + \Re^2),$$

with  $\Im$  and  $\Re$  representing the respective imaginary and real part of the wavelet coefficient at time  $t$  and frequency  $f$  and  $n$  the number of trials. TSP contains both phase-locked and non-phase-locked energy. To obtain the fraction of activity that is phase-locked and therefore synchronized across trials (Figure 2.1 A “phase locked”), averaging of the imaginary and real parts of the wavelet coefficients before calculating the power will yield the trial-averaged evoked activity (EA):

$$EA(t, f) = \left( \frac{\sum \Im}{n} \right)^2 + \left( \frac{\sum \Re}{n} \right)^2.$$

This kind of activity strongly resembled the evoked potential in which all non-phase-locked components are cancelled out (Figure 2.1 A “Mean”, Figure 2.1 B). Activity that is event-related but does not appear with constant timing towards that event (INDA; Figure 2.1 A “temporal jitter”) can be obtained by subtracting the phase-locked fraction from the TSP (Figure 2.1 C):

$$INDA(t, f) = TSP(t, f) - EA(t, f).$$

All measures were normalized to the median baseline TSP. Spectra are displayed as grand averages over animals (Figure 2.2). To calculate group spectra, averages were first taken for each animal over trials and then over subjects for the respective measure of interest. To determine significance thresholds for these grand average spectra, evoked and induced activity of the baseline signals without sound presentation were used: for every frequency a distribution of power values over the 5 s baseline trial epoch was generated and the 95% confidence intervals of the distribution determined. Values outside this interval were deemed significantly higher or lower than baseline (respectively black and white contour lines in Figure 2.2);

additionally only patches with more than 50 contiguous points were accepted as truly significant.

#### 2.2.2.4 Recovery times of induced and evoked activities

Recordings from longer ISIs were used to determine recovery behavior of evoked and induced activities. For this purpose 200 ms from tone onset of the first and second tone of an FM sweep train were wavelet transformed as described above; likewise the induced and evoked activity was calculated and normalized to the median of the total-signal-power. T/C ratios were calculated as the ratio of the respective power values of the second and the first stimulus. The identical two-parameter model as in Section 1.3.4 was then applied to the median population data, using the same routines.

Recovery times were estimated with bootstrapping (sampling with  $k = 999$ ), as the time the T/C ratio reached 90% of the asymptote value (cf. Section 1.2.3.3). Where the bootstrap algorithm was not applicable, because the randomly chosen bootstrap sets did not allow for a convergence of the model fitting algorithm, recovery time was calculated from the estimated fit parameters (Appendix B Table 3).

#### 2.2.2.5 Phase-locking

To calculate the between-area phase-locking index (PLI) for each animal the instantaneous phase ( $\phi$ ) of the striatal and cortical channels was determined in each trial from the inverse tangent ( $arg$ ) of the wavelet coefficient  $W(t, f)$ :

$$\phi(t, f) = arg(W(t, f)).$$

The instantaneous phase difference ( $\Delta\phi$ ) was obtained by subtracting the striatal from the cortical phase. The average PLI for each animal across trials was then calculated by:

$$PLI(t, f) = \frac{1}{N} \left| \sum_{k=1}^N e^{i\Delta\phi(t,f)} \right|,$$

with  $k = 1, \dots, N$  designating the number of trials. For averaging across animals, the PLI was Fisher transformed, the mean calculated and transformed back. As for the calculation of the induced and evoked activity, baseline PLIs were calculated to determine time-frequency epochs of significant phase-locking (see above).

### **2.2.3 Statistical analysis**

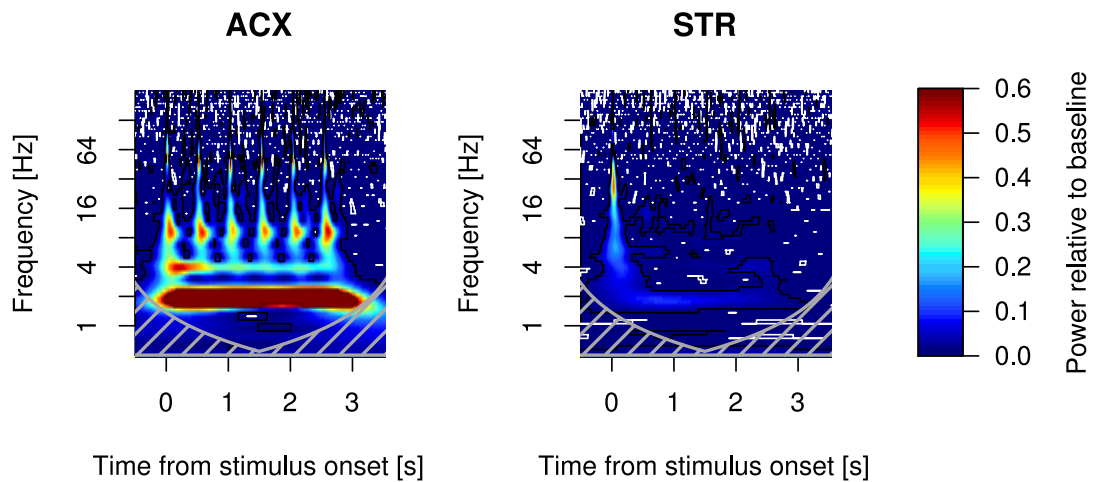
Statistics were computed using R (R Foundation for Statistical Computing, Vienna, Austria) and SPSS (PASW Statistics 18, SPSS, Inc., Chicago). Total-signal-power and fractions of induced and evoked activity were compared between areas with paired t-tests. Furthermore, gating effects and frequency band influences on evoked and induced activity were tested for each area with a repeated-measure ANOVA (Table 2.1, Figure 2.4) with factors FREQUENCY (levels: “delta”, “theta”, “alpha”, “beta” and “gamma”) and STIMULUS POSITION (levels: “S1” and “S2”). Frequency bands were defined within the following ranges: 1-4 Hz (delta), 4-8 Hz (theta), 8-12 Hz (alpha), 12- 30 Hz (beta) and 30-80 Hz (gamma). Greenhouse-Geisser corrections were applied when appropriate (Table 2.1). Significant interaction effects were analyzed *post-hoc* with paired t-tests. Similarly, phase-locking in different frequency bands were tested for effects of FM STIMULUS PRESENCE (levels: “during” and “after” stimulation) and STIMULUS POSITION (levels: “S1” and “S2”) with a repeated-measure ANOVA and *post-hoc* paired t-tests (Table 2.2; Figure 2.8). This was done for the 0.5 ISI (rising FM) as well as the 1.2 ISI (falling FM). For all statistical computations a significance level of 0.05 was chosen.

## **2.3 Results**

### **2.3.1 Induced and evoked activity**

The wavelet-transformed data was used to assess phenomena relating to stimulus-locking within auditory gating. Particularly, phase-locked (evoked)

## Evoked Activity



## Induced Activity

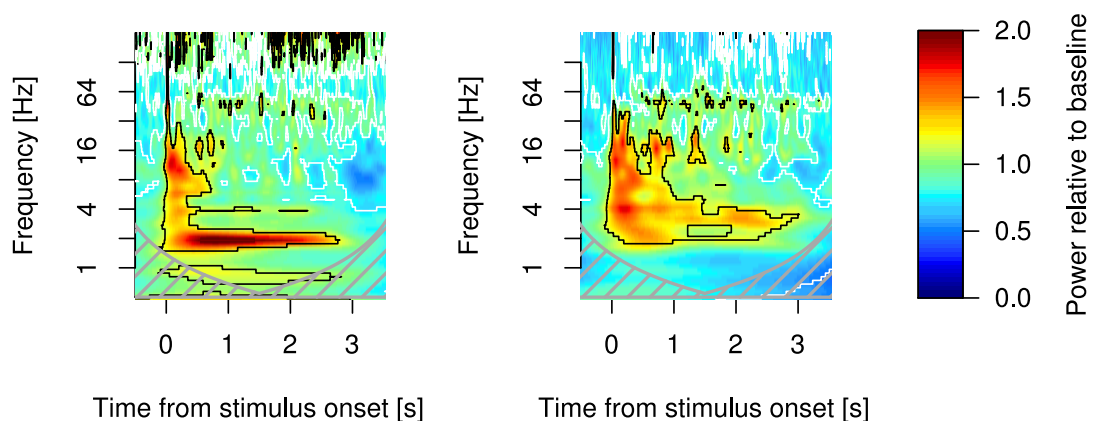


**Figure 2.2: Trains of frequency-modulated (FM) tones stimulated primarily evoked activity in the auditory cortex but mainly induced activity in the striatum.** Shown are grand averages of evoked and induced activity in the cortex (*left panels*) and striatum (*right panels*). Top row displays the evoked, stimulus-locked, activity. Activity in the auditory cortex (*left*) coupled exactly to the repetition rate (2 Hz). In the striatum (*right panels*) a strong evoked response was only present during the first stimulus presentation (0-0.2 s). Evoked activity in the 2 Hz band could also be found in this area, as well as some significant patches in the beta range. Induced activity is displayed in the bottom row. In the auditory cortex (*left panels*) strong induced activity was found in the beta and alpha frequency range (4-16 Hz). In the striatum (*right panels*) induced activity was found in the theta-gamma range and there were also prominent rhythmic beta patches after each FM stimulus which decreased in their extent. Shown is the whole train of six stimuli. Areas with black or white contours respectively indicate regions with significantly higher or lower power values than baseline ( $p = 0.05$ ). Areas outside the wavelet-transform cone of influence are shaded in gray.

and non-phase-locked (induced) stimulus-related energy was analyzed. Time-frequency plots of evoked activity directly mirrored local field potential evoked responses. While the cortical responses strongly coupled to the stimulation with repetitive FM tones, a large evoked response in the striatum was only found for the first stimulus presentation within a train (Figure 2.2, top row). However, a comparison with the induced activity (Figure 2.2, bottom row) revealed that a large portion of the stimulus related energy was expressed as induced activity in the striatum (Figure 2.3).

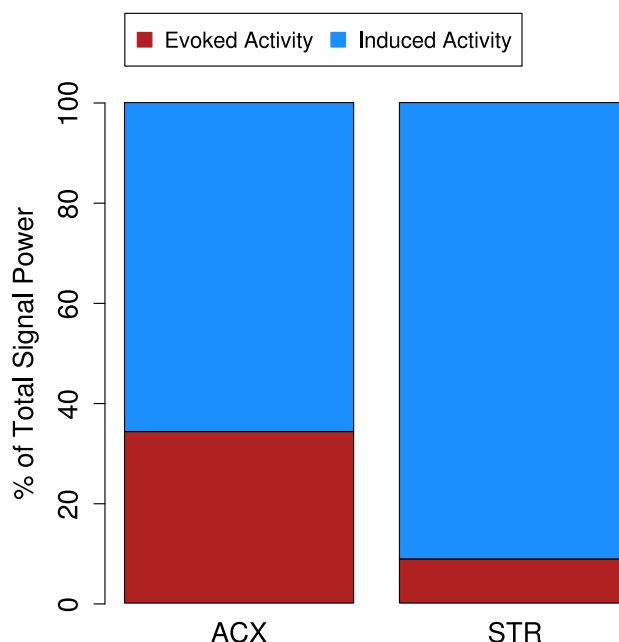


**Figure 2.3: Total-signal-power was split differently between evoked and induced activity in the auditory cortex and ventral striatum.** During stimulation the fraction of induced activity in the striatum accounted for nearly 90% of the total-signal-power while in the cortex the value was only 66%. Data are means. ACX: auditory cortex; STR: ventral striatum.

Analyzing the whole train of stimulation (0-3 s after first tone onset) in the frequency range of 2-256 Hz showed that evoked activity in the cortex exceeded the one in the ventral striatum [34 + 3.6% vs. 9 + 1.4% of total-

signal-power, mean + SE,  $t = 8$ ,  $p < 0.000$ ], while induced activity was larger in the striatum during the whole train [ $91 + 1.4\%$  vs.  $66 + 3.6\%$  of TSP, mean + SE,  $t = -8$ ,  $p < 0.000$ ]. Cortical and striatal total-signal-power did not differ significantly from one another [ $t = 1.1$ ,  $p > 0.05$ ].

To specifically assess gating effects from S1 to S2 for both brain areas

**Table 2.1: Repeated-measure ANOVA for FREQUENCY band and STIMULUS POSITION effects on induced and evoked activity in the auditory cortex and ventral striatum.** Greenhouse-Geisser epsilons are cited where appropriate corrections were made.

Activity	Area	Effect	df	F	$\epsilon$	p
<b>evoked activity</b>	ACX	FREQUENCY	(1.25, 17.50)	17.68	0.328	<0.000
		STIMULUS POSITION	(1,14)	0.00	-	0.971
		FREQUENCY x STIMULUS POSITION	(2.1, 29.36)	4.42	0.619	0.020
	STR	FREQUENCY	(1.87, 26.18)	3.87	0.467	0.036
		STIMULUS POSITION	(1,14)	27.95	-	<0.000
		FREQUENCY x STIMULUS POSITION	(4, 56)	3.40	-	0.015
<b>induced activity</b>	ACX	FREQUENCY	(2.20, 30.83)	5.49	0.658	0.008
		STIMULUS POSITION	(1,14)	28.06	-	<0.000
		FREQUENCY x STIMULUS POSITION	(4, 56)	6.61	-	<0.000
	STR	FREQUENCY	(1.46, 20.47)	3.31	0.366	0.070
		STIMULUS POSITION	(1,14)	2.75	-	0.120
		FREQUENCY x STIMULUS POSITION	(2.34, 32.77)	1.27	0.585	0.299



and different frequency bands, repeated-measure ANOVAs were calculated for induced and evoked activities with factors FREQUENCY and STIMULUS POSITION (Table 2.1, see experimental procedures). Evoked activity in both brain areas was influenced by FREQUENCY band and the interaction of STIMULUS POSITION with FREQUENCY band, but a significant main effect for STIMULUS POSITION was only found in the ventral striatum. These results were tested in more detail with paired t-tests (Figure 2.4): There was no gating effect of evoked activity in all frequency bands in the auditory cortex [ $-2.1 < t < 2.1$ , all  $p > 0.05$ ], but the power of evoked activity in each frequency band in the ventral striatum was reduced from S1 to S2 [all  $t > 2.8$ , all  $p < 0.05$ ; Figure 2.4 *top row*].

There were no effects from either factor or their combination on induced activity in the striatum, but cortical induced activity was influenced by FREQUENCY band, STIMULUS POSITION and their interaction (Table 2.1). *Post-hoc* paired t-tests revealed that induced activity in the cortex was diminished from S1 to S2 in the delta, theta and alpha frequency range [all  $t > 3.6$ , all  $p < 0.007$ ; Figure 2.4 *bottom row*].

### **2.3.2 Recovery time of induced and evoked activities**

To compare recovery dynamics of the time-frequency analyzed activities to the dynamics of the evoked potentials, asymptotic exponential functions were fit to evoked and induced activities at different ISIs, as well (see Section 1.3.4 / Figure 1.5). Fits were estimated for different frequency ranges (Appendix B Table 3); results presented within this section refer to a broad band frequency range of 2-268 Hz. Data points from rising and falling FM sweeps were pooled.

At the used ISIs an inhibitory gating effect for evoked activity was only found within the ventral striatum. Nonetheless, to have a qualitative comparison, the model was also fitted to cortical data points (Figure 2.5, *top row, left panel*). When the model was fitted to the original dataset from the auditory cortex, there was no convergence of the algorithm for data points from the evoked activity. Established parameters showed that cortical data

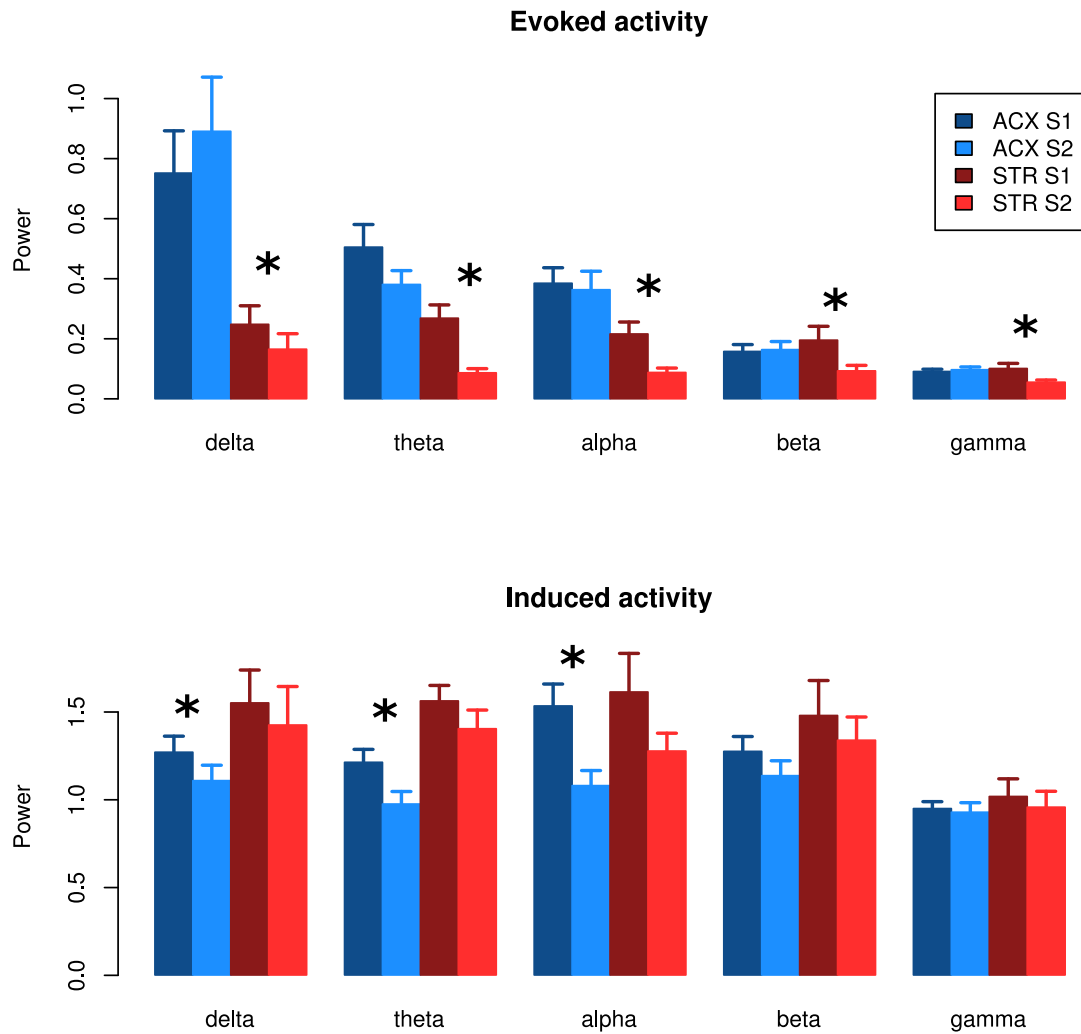


**Figure 2.4: Only evoked activity was subject to auditory gating in the striatum.** The figure displays evoked (*top row*) and induced activity (*bottom row*) in both brain areas for separate frequency bands. In contrast to the evoked activity, induced activity in the striatum changed non-significantly from the first to the second stimulus presentation (see Table 2.1). ACX: auditory cortex, STR: ventral striatum, S1: first stimulus, S2: second stimulus.\*: paired t-test  $p < 0.05$ . Data are means with SE.

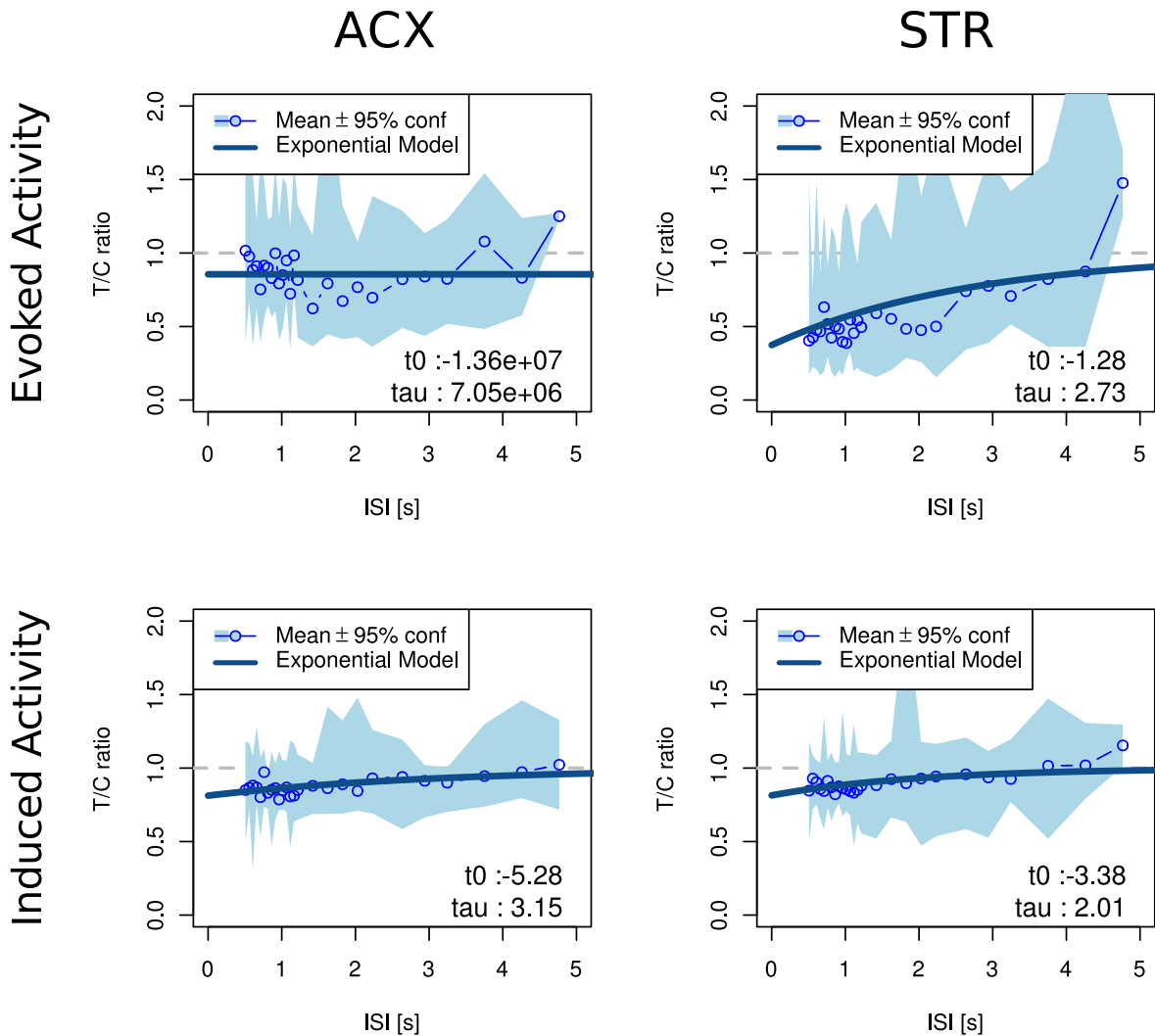


**Figure 2.5: Gating dynamics were only seen for evoked activity in the ventral striatum in the 2-268 Hz range.** Mean population data points (blue circles) with 95% confidence intervals (blue shaded area behind the curve). The fitted curve is displayed by the continuous blue line. The exponential model was fitted to the test-conditioning (T/C) ratio of the activity values during the first and second stimulus presentation (cf. Section 1.3.4). A convergence of the two-parameter model fit was not obtained for the evoked activity in the auditory cortex (*left panel, top row*) since the points were already in the stationary part of the assumed model. Gating dynamics for induced activity (*bottom row*) were comparable between both brain areas. Parameters from the exponential fits are displayed for both areas.

points hardly laid in the non-stationary part of the curve (Figure 2.5, top row, left panel). When fitted to the original striatal evoked activity dataset, the model proved to be highly convergent [ $t_0 = -1.28$ ,  $t = -2.8$ ,  $p = 0.005$ ;  $\tau = 2.73$ ,  $t = 5.25$ ,  $p < 0.001$ ; residual standard error = 0.35 on 434 df]. The model also converged for both brain areas' induced activity datasets (Figure 2.5 bottom row). Weak gating effects were found for earlier ISIs with a slightly stronger trend for cortical induced activity [ACX:  $t_0 = -5.28$ ,  $t = -2.68$ ,  $p = 0.008$ ;  $\tau = 5.15$ ,  $t = 3.24$ ,  $p = 0.001$ ; residual standard error = 0.17 on 434 df; Figure 2.5 bottom row, left panel; STR:  $t_0 = -3.38$ ,  $t = -2.22$ ,  $p = 0.03$ ;  $\tau = 2.01$ ,  $t = 2.87$ ,  $p = 0.004$ ; residual standard error = 0.19 on 434 df]. The model was used to bootstrap recovery times for both activities, i.e. the ISI time to approach the asymptote at an 90% confidence interval. While striatal evoked activity attained a recovery time of 5 s, induced activity recovered faster (1.2 s), which was in a comparable range to recovery time of cortical induced activity (2 s, Figure 2.5). Recovery times for different frequency ranges are summarized in Appendix B Table 4 but generally showed the same trend as the broad band frequency range presented here.

### 2.3.3 Between-area coherence determined by phase-locking

Phase-locking between the auditory cortex and ventral striatum was tested for two ISIs: 0.5 and 1.2 s. The phase-locking index was averaged over animals (Figure 2.7). Significant patches were determined by using the 5% and 95% quantiles of the distribution of PLI values during baseline recording. Most notably, for the ISI of 0.5 s phase-coupling in the theta (4-8 Hz) and alpha frequency band (8-12 Hz) was significantly decreased compared to baseline during S1 presentation and in the alpha and lower beta frequency band (12-16 Hz) during S2 presentation, thus pointing towards a uniform distribution of phases at these time-points (Mormann *et al.*, 2000). For the longer ISI (Appendix B Figure 2), this held true, as well.

Increased synchrony was expectedly found in the delta frequency range which contained the repetition frequency of the stimulus presentation in a

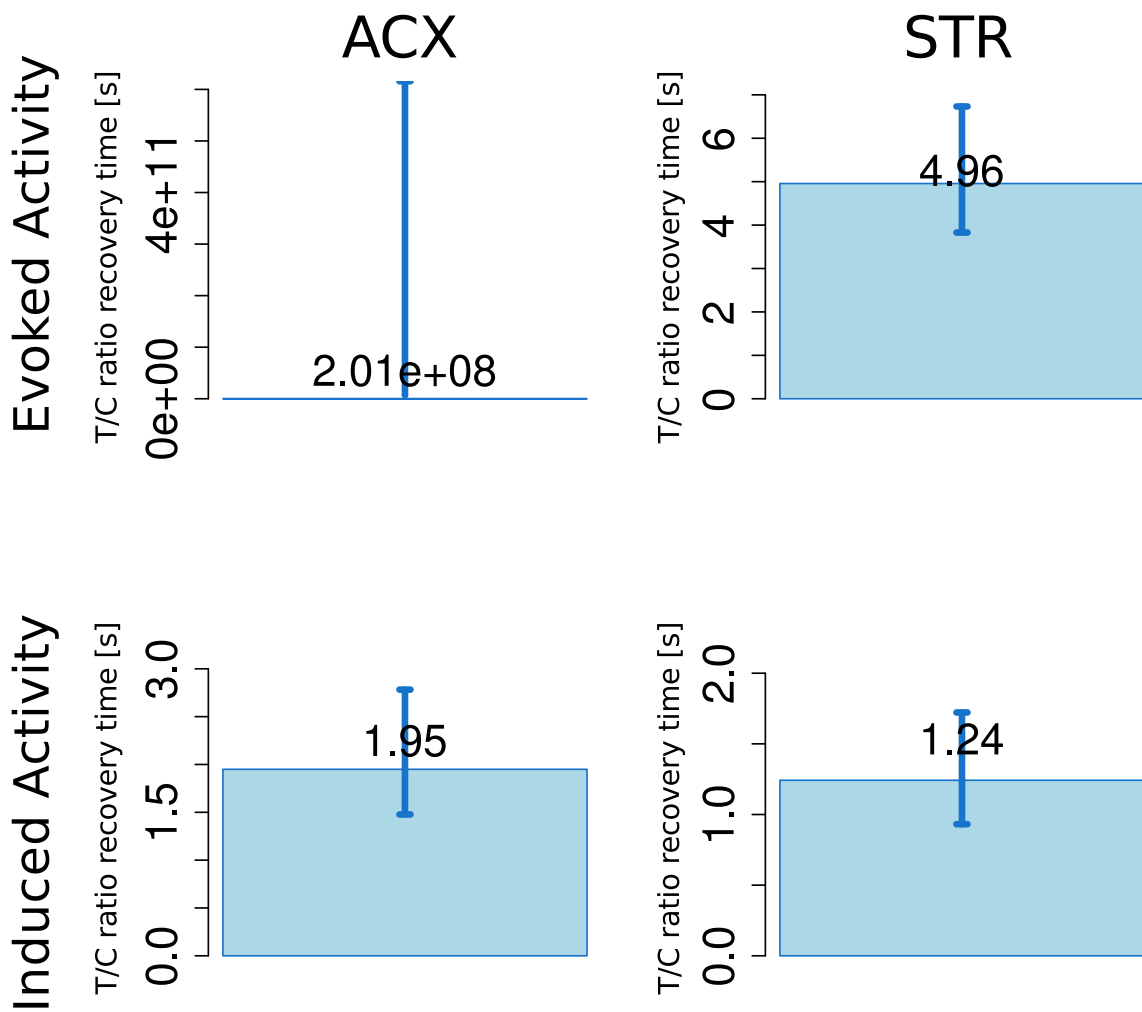


**Figure 2.6: Estimated recovery time of striatal evoked activity for repetitive frequency modulated (FM) tone stimulation exceeded 4 s.** Induced activity in both brain areas needed approximately 2 s to reach 90% of the full activity values (*bottom row*). Displayed are the bootstrapped median and 95% confidence intervals. Note different abscissa scaling.

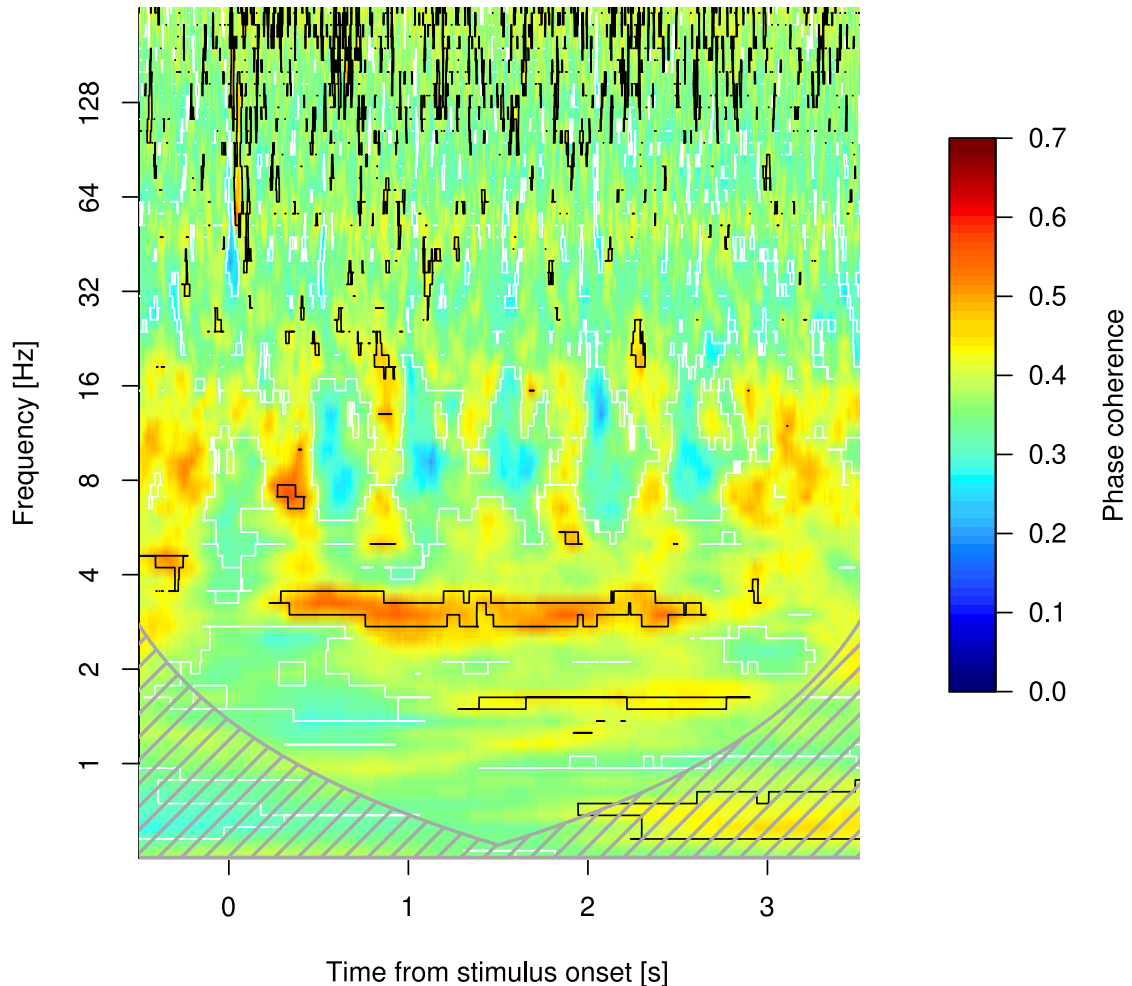


**Figure 2.7: Stimulation with frequency modulated tones resulted in diminished phase synchrony between auditory cortex and ventral striatum.** Time-points of stimulation (0, 0.5, ..., 2.5 s) corresponded to significantly lower phase-locking index (PLI) values in the theta, alpha and lower beta band compared to baseline. Increased continuous phase-locking in delta band, starting from the first stimulus offset corresponded to phase-locking values between 0.5 - 0.6. Displayed is the average PLI over all animals. Areas with black or white contours respectively indicate regions with significantly higher or lower PLI values as compared to baseline ( $p = 0.05$ ). Areas outside the wavelet-transform cone of influence are shaded in gray.

**Table 2.2: Repeated-measure ANOVA for STIMULUS PRESENCE and POSITION effects on between-area phase-locking.**

Frequency range	Effect	df	F	p
<b>delta</b>	STIMULUS PRESENCE	(1, 14)	13.40	0.003
	STIMULUS POSITION	(1, 14)	8.20	0.012
	STIMULUS PRESENCE x POSITION	(1, 14)	0.10	0.777
<b>theta</b>	STIMULUS PRESENCE	(1, 14)	11.20	0.005
	STIMULUS POSITION	(1, 14)	1.00	0.325
	STIMULUS PRESENCE x POSITION	(1, 14)	0.40	0.556
<b>alpha</b>	STIMULUS PRESENCE	(1, 14)	5.20	0.038
	STIMULUS POSITION	(1, 14)	3.20	0.096
	STIMULUS PRESENCE x POSITION	(1, 14)	0.30	0.620
<b>beta</b>	STIMULUS PRESENCE	(1, 14)	2.00	0.175
	STIMULUS POSITION	(1, 14)	0.20	0.652
	STIMULUS PRESENCE x POSITION	(1, 14)	7.30	0.017
<b>gamma</b>	STIMULUS PRESENCE	(1, 14)	0.20	0.630
	STIMULUS POSITION	(1, 14)	0.30	0.605
	STIMULUS PRESENCE x POSITION	(1, 14)	2.40	0.145

trial. It started at the offset of the first stimulus and lasted till the offset of the last stimulus in the train. This synchrony was not seen in the longer ISI measurement (Appendix B Figure 2). Phase-locking was tested in different frequency bands for effects of FM stimulus presence and stimulus position with a repeated-measure ANOVA and *post-hoc* paired t-tests (Table 2.2; Figure 2.8).

Including FREQUENCY band as a factor yielded no significant main effect (Appendix B Tables 5, 6), therefore ANOVAs were calculated for each frequency band separately (Table 2.2, Appendix B Table 7). Synchrony between both areas in the delta, theta and alpha frequency bands was highly decreased during FM tone stimulation compared to the time period after tone offset and baseline. In the delta frequency band phase-locking increased from S1 to S2 of the FM tone train. In the beta frequency band there was a significant FM STIMULUS PRESENCE x POSITION interaction: while phase-

locking during FM presence was indifferent between S1 and S2 [ $t = 1$ ,  $p = 0.32$ ], it was higher in the post-stimulus episode after S2 compared to S1 [ $t = -2.8$ ,  $p = 0.015$ ]. With longer ISI stimulation FM tone presence had a significant effect on phase-coherence in the theta range [ $F(1,14) = 9.9$ ,  $p = 0.007$ ; Appendix B Table 7, Figure 3].

## 2.4 Discussion

Local field potentials were simultaneously recorded in the auditory cortex and ventral striatum of awake gerbils during stimulation with trains of FM tones. Auditory gating was assessed by time-frequency analyses. Furthermore, while total-signal-power was very similar in both areas, this energy was mainly expressed as non-phase-locked induced activity in the ventral striatum, and as stimulus-locked evoked activity in the auditory cortex. To the author's knowledge this is the first animal study applying time-frequency analyses in an auditory gating paradigm, but human studies in the last years have stressed the importance of oscillations and temporal variability of neuronal responses within this task (Brockhaus-Dumke *et al.*, 2008; Hong *et al.*, 2008; Patterson *et al.*, 2000; Popov *et al.*, 2011; Rosburg *et al.*, 2009b; Uhlhaas *et al.*, 2008).

### 2.4.1 Induced and evoked activity

Assessing the total-signal-power within a broad frequency band in both areas showed no significant difference between the ventral striatum and the auditory cortex. Thus the energy that originated from the auditory stimulation remained at comparable levels in both brain areas. Interestingly, the total-signal-power was split differently into stimulus-locked (evoked) and induced energy within each area (Figure 2.3). The fraction of induced energy was nearly 25% higher in the striatum than in the auditory cortex.

The main finding of the present study was that auditory gating in the striatum was based on the evoked activity at S2 presentation, while there were no decrements of evoked power in the auditory cortex. The major



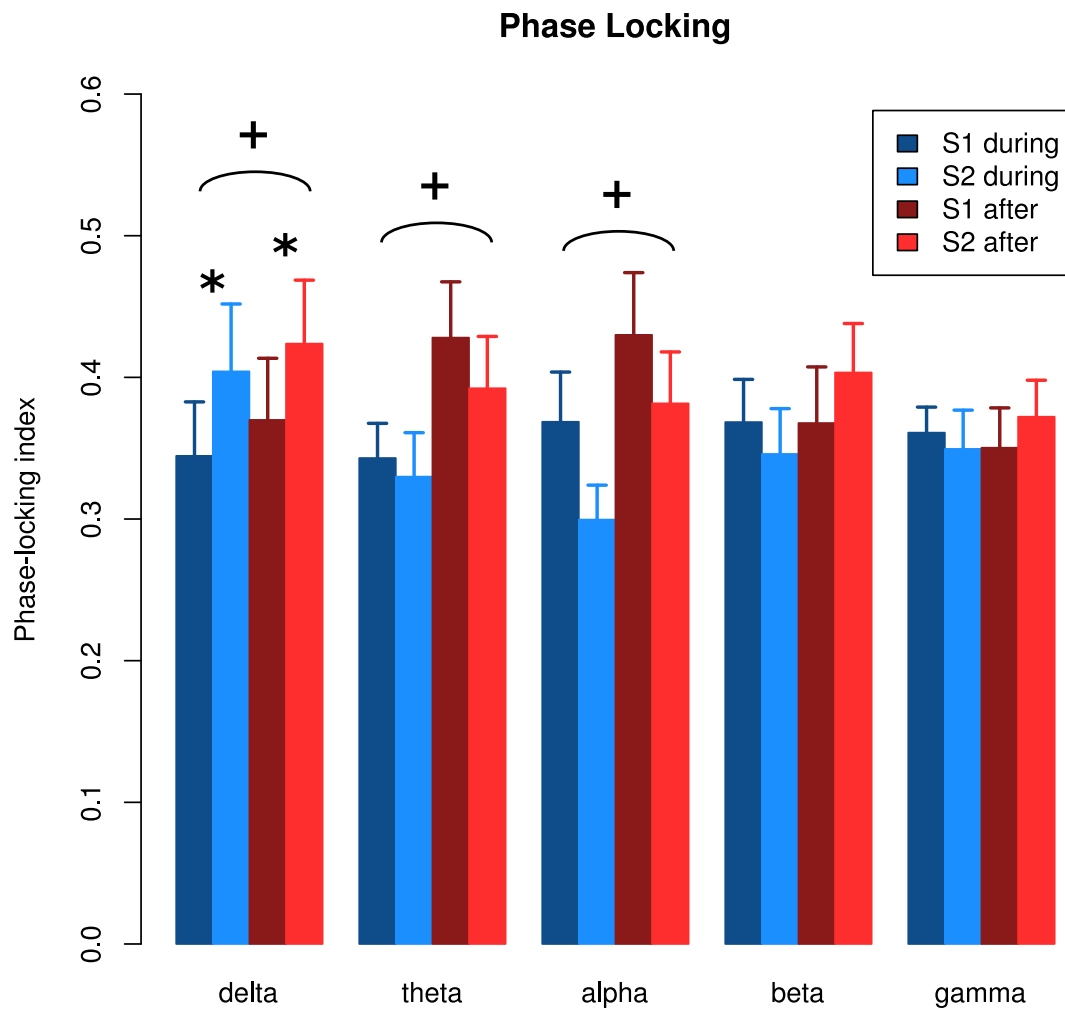


**Figure 2.8: Phase-locking between the cortex and striatum was significantly decreased during tone presence in lower frequency bands.** Blue colored bars display phase-coherence during frequency-modulated (FM) tone presence and red colored bars in the absence of FM tones (offset-to-onset time). \*: main effect STIMULUS POSITION between stimulus one (S1) and two (S2)  $p < 0.02$ , +: main effect comparing presence and absence of FM stimuli,  $p < 0.05$ . Not shown is the significant FM PRESENCE  $\times$  STIMULUS interaction effect in the beta frequency band (see text). S1: first stimulus, S2: second stimulus. Data are means + SE.

part of the energy in the striatum was contributed by induced activity, while, at the same time, the total-signal-power of both areas remained comparable. This leads to the conclusion that gating in the striatum can be explained by temporal de-synchronization during the second stimulus and not by suppression of synaptic input or reduction of striatal mass activity. Interestingly dysfunctional auditory gating in schizophrenic subjects has been related to temporal variability of the S1 response (Jansen *et al.*, 2004; Jin *et al.*, 1997; Patterson *et al.*, 2000). While these findings stress the importance of temporal variability in the diseased brain, the present data suggest, that temporal variability might form the basis of healthy functioning gating as well (cf. Jansen *et al.*, 2003). Thus in a gating experiment S1 appears to induce mechanisms that mainly trigger de-synchronized neuronal responses during subsequent repeated stimuli.

Evoked potentials in the striatum represent synaptic activity, stemming mainly from glutamatergic  $\alpha$ -amino-3-hydroxy-5-methyl-4-isoxazolepropionic acid (AMPA) receptors and  $\gamma$ -aminobutyric acid (GABA) mediated inhibitory modulations (Galiñanes *et al.*, 2011). Blocking of AMPA receptors reduced the evoked potentials completely, whereas blocking of GABAergic synapses resulted in a relatively small amplitude reduction and longer duration of evoked potentials (Galiñanes *et al.*, 2011). Therefore stimulus-locking in the ventral striatum could be linked to proper functioning of GABAergic modulation. Also, the observed auditory gating in the striatum could be based on de-synchronized inputs to striatal synapses, or locally regulated by GABAergic neurotransmission, or a combination of both.

Many studies have described a differential involvement of various frequency bands in sensory gating and its pathological disturbance. For example, phase-locking was found to be lowered in schizophrenic patients in the theta and alpha band and in poor gators in the beta band (Brockhaus-Dumke *et al.*, 2008; Rosburg *et al.*, 2009b). Gamma to beta transitions have been shown to mark stimulus driven salience in paired-stimuli designs (Kisley & Cornwell, 2006) and reduced evoked beta and gamma activity has been reported in schizophrenic patients during sensory gating (Brenner *et al.*, 2009; Popov *et al.*, 2011). The multitude of ranges involved and

the interdependence of low and high frequency oscillations calls for an analysis of the full frequency spectrum, rather than focusing on a single band (reviewed in Moran & Hong, 2011; Uhlhaas *et al.*, 2008). Striatal evoked activity was gated in all frequency ranges analyzed (2-80 Hz) and therefore we could not attribute a significant role of a specific frequency band in the gating process, as has been recently discussed, for example, for beta oscillations in human studies (Hong *et al.*, 2008; Kisley & Cornwell, 2006). On the other hand, cortical induced activity was significantly suppressed at S2 in the lower frequency range (2-12 Hz; Figure 2.4), indicating that this range might especially contribute to input phase synchrony during S2 observed in the auditory cortex. Human vertex AEPs during S1 presentation were due to increased phase synchronization in the low (2-8 Hz) frequency range, as well (Jansen *et al.*, 2003). Notably, the reduction in induced activity at S2 in the cortex barely compared to auditory gating of evoked activity in the ventral striatum in magnitude, where the suppression reached nearly 50% (48% suppression of low frequency (2-12 Hz) striatal evoked activity; 20% suppression of auditory cortex induced activity).

#### **2.4.2 Recovery times of induced and evoked activity**

With an approximation of 5 s, recovery times for the evoked activity in the striatum matched the estimate for the evoked potential recovery times (considering the estimated variances as well, cf. Section 1.3.4). From a different perspective, the recovery time of neuronal activity after auditory stimulation has been associated with echoic memory, the initial sensory memory storage of an acoustic event (Cowan, 1984; Lu *et al.*, 1992). Lu *et al.* (1992) measured the decay of the human N100m and compared it to the decay time for the remembrance of the loudness of played tones: they found a perfect correlation. Interestingly their N100m (and P180m) attained asymptotic values in times comparable to the ones measured in the present study for the ventral striatum evoked activity (and AEP subcomponents). Auditory sensory memory is thought to consist of two phases: a short phase (250-300 ms) involved in stimulus registration and trace formation,

and a longer phase that bears the representation (“store”) of the analyzed stimulus (Cowan, 1984). Given the N1 and P2 recovery time reflects such a thing as echoic memory and the finding in the present data that there is no AEP suppression within 0.5 - 4 s ISIs within the primary auditory cortex, this would lead to the conclusion that the representation of the previously analyzed stimulus does not prevent new trace formation or stimulus analysis of succeeding stimuli within this area, while this might be happening for repetitive identical stimuli in the ventral striatum. It has to be stressed, however, that auditory cortex functioning has been proven to encompass more than just stimulus registration and analysis: during the last years its flexible, task-dependent principle of operation has become evident (Ohl & Scheich, 2005; Scheich *et al.*, 2007).

A recovery model could be fit to the data of broad-band induced power from both areas, the auditory cortex and the ventral striatum. This means that, on average, in both areas there was more induced power during the S1 presentation than during the S2 presentation and this was more evident for short ISIs. Firstly it has to be emphasized that the suppression range was much smaller compared to the one found for the evoked energy in the ventral striatum (or the AEPs there). Nonetheless this could mean that the conditioning stimulus in both areas triggered a higher degree of non-phase-locked activity than the test tone.

### **2.4.3 Coherence and phase-locking**

The phase-locking index indicates the degree to which two signals bear a constant phase relationship (a phase-locking index of one infers a constant phase relationship over all trials). Two signals could be in phase for example if signal A peaks at the regarded timepoint, while signal B moves towards a through with a phase angle of approximately 45°; this behavior would need to be repeated during the chosen timepoint in every trial to obtain a perfect phase-locking. Phase-locking between the auditory cortex and the ventral striatum was modulated by the acoustical stimulation of the animals with FM tone trains (Figure 2.7) in long (1.2 s) and short (0.5 s) ISI conditions. Notably,

during FM tone presentation the inter-area phase-locking was significantly decreased (Figure 2.8), i.e. the electrical signals within both areas were out of phase, especially in the theta (4-8 Hz) and alpha frequency band (8-12 Hz) during S1 presentation and lower beta frequency band (12-16 Hz) during S2 presentation. After tone offsets, phase-locking appeared to increase again, marginally rising above baseline phase-locking values. The found decreased coherence during single FM tone stimulation (with a duration of 200 ms) represents another indication that acoustical information might primarily reach both areas on different paths (cf. Section 1.4.2). It also suggests that during S2 presentation, during which the auditory gating in the striatum is enforced, and during which auditory-cortex – striatum phase-locking was not existent, both areas are subjected to differential mechanisms: while the auditory cortex is destined to exactly follow the acoustical content of the stimuli, striatum-relevant acoustical features were probably already extracted during S1 presentation and then subjected to further local processing. Phase-locking appeared to increase after tone-offsets during both tested ISI conditions. During the short ISI condition, phase-locking in the FM presence was indifferent between S1 and S2 in the beta frequency band but it was higher in the post-stimulus episode after S2 compared to S1.

Exploiting the accessibility of simultaneous intracranial recordings, locally defined in the auditory cortex and ventral striatum, the present work provides more direct evidence that auditory gating could result from de-synchronized responding of neuronal populations, rather than reflecting a purely inhibitory mechanism that would reduce neuronal mass action. Furthermore, the characterization of the simultaneously measured gating dynamics in both areas indicates an independence of the two areas during gating.

## **Chapter 3**

# **The impact of FM tone discrimination learning on sensory gating**

### **3.1 Introduction**

#### **3.1.1 State and task influences in auditory gating: Attention, memory and stress**

Interestingly, like the physiology for auditory gating (see Chapter 2), its deeper functional aspects are not completely understood. While clinical research has focused mostly on the association of P50 gating abnormalities to psychiatric illnesses and their pharmacological manipulations, behavioral and physiological state influences have only sparsely been investigated.

The classical view on auditory gating claims that its fundamental function lies in the selection of incoming, task-relevant information (“gating in”) and the blocking of task-irrelevant information (“gating out”), and this mechanism, at least for the early human P50 wave is deemed to be pre-attentive in its nature (Boutros & Belger, 1999). However, while attention demanding tasks, that do not change gating, are said to prove its pre-attentive (and hence hard-wired) nature, it is also postulated that, as

gating filters out redundant information, it could represent a physiological manifestation of attention. Clearly, the term “attention” in the field of sensory gating is liable to circular reasoning. Not surprisingly the role of attentional influences on auditory gating and specific effects on different middle-latency evoked potentials are highly debated. While Jerger *et al.* (1992) have shown that selective attention had a manipulative effect only on the N100 amplitude and its suppression, but not on the earlier auditory P50 gating, in a study by Guterma *et al.* (1992) selective attention on the test stimulus (S2) or a concordant Go/NoGo motor response (a button press) was able to modify the P50 suppression effect. This “cognitively mediated process” was impaired in schizophrenic subjects (Guterma & Josiassen, 1994). A few studies have investigated auditory gating in the context of memory related tasks. Evidentially the transition from attention to memory is rather smooth, as the control of attention can be regarded as central to working memory. In line with this, middle-latency evoked potentials differed between subjects with low and high working memory span (Brumback *et al.*, 2004). P50, N100 and P200 gating values showed differential relationships with measures of response bias and working memory in the immediate and delayed memory task (Lijffijt *et al.*, 2009). It was interpreted that auditory gating could thereby serve to protect higher order cognition. Implicit (artificial grammar) and explicit (Wechsler memory scale) learning scores were found to correlate with N100 gating in healthy controls, while schizophrenic subjects were impaired in both tasks (Hsieh *et al.*, 2004). Altogether literary proof is scarce and heterogeneous on this subject and the impact of attentional variables on auditory gating are not clarified in detail, as all experimental setups hardly allow for determining attention as the sole state variable. Furthermore, the already scant literature is almost exclusively restricted to human studies. The common view supports the notion that strong sensory gating capability supports better performance in tasks requiring selective attention and working memory, but might not be a direct correlate thereof.

Acute stressors seem to have the most robust influence on auditory gating. After a cold-pressor test procedure, in which subjects had to immerse

their hands into icy water for a short period of time, P50 gating was found transiently reduced for five of ten subjects (Johnson & Adler, 1993). Psychological stress, like the loud mental arithmetic task was also able to diminish both P50 and N100 gating, by altering the conditioning evoked potential (EP) amplitude (White & Yee, 1997; Yee & White, 2001).

Animal studies on the interrelation of stress and auditory gating all rely on acute physical stressors, like immobilization or fear conditioning which both led to transiently weakened gating (Mears *et al.*, 2009; Süer *et al.*, 2004). A 24-h maternal deprivation stress on postnatal day 9 led to reduced auditory gating and acoustic startle habituation in the adult Wistar rats (Ellenbroek *et al.*, 2004).

In the striatum, acute stress by saline injections strengthened auditory gating of unit firing rates and evoked potentials, while chronic stress (food deprivation) led to an impairment of gating on the unit level but increased evoked potential gating (Cromwell *et al.*, 2007). The latter study illustrates that modulations of auditory gating can indeed act on different time-scales and different neuronal levels, which complicates a clear dis-entanglement of state and trait influences all the more.

### **3.1.2 Testing behavioral influences on auditory gating in the Mongolian gerbil**

#### **3.1.2.1 Auditory discrimination learning in the shuttle-box**

A behavioral task that encompasses at least two of the mentioned state-variables, namely attention and stress, shown to influence gating, is auditory discrimination learning in a Go/NoGo paradigm in the shuttle-box. Within this task gerbils learn to differentiate the modulation direction of FM tones and are even able to transfer the category of modulation direction to novel stimuli (Wetzel *et al.*, 1998). Within a two-compartmental shuttle-box, divided by a small hurdle, animals indicate a successful discrimination by changing the compartment as response to the presentation of the “Go” conditioned stimulus (CS+) (in this case frequency upward modulated tones)



but suppressing a shuttle-response as reaction to the “NoGo” conditioned stimulus (CS-) (a frequency downward modulated tone). If, on CS+ trials, the animals fail to cross the hurdle within a certain time window, they receive a mild foot-shock and the trials are scored as “miss”; conversely if the animals shuttle during a CS- trial they are punished as well (“false alarm”). The initial learning in the shuttle-box is of Pavlovian nature when the animals learn to associate the conditioned stimulus (CS) with the unconditioned stimulus (US), the foot shock (Cain & LeDoux, 2008). Within this phase animals normally overcome their anxiety and adopt an escape strategy in which they shuttle after having received the foot-shock. Simultaneously, animals acquire the discrimination between the CS+ and CS- conditional stimuli, and learn to suppress shuttling in response to the CS-, which would be followed by a foot shock as well. Once the animals transit from escape reactions to an active avoidance, i.e. changing the compartment as response to the CS+ (CR: conditioned response), a strong association of CS-US has been formed and the Go/NoGo reaction strategy has been developed.

### **3.1.2.2 Putative involvement of the auditory cortex and the ventral striatum in the Go/NoGo auditory discrimination task**

Ohl *et al.* (1999) have shown that the auditory cortex plays a central role in discrimination learning of FM tones, but not pure tones. Bilateral ablation of the auditory cortex corrupted the acquisition of the discrimination in the first place, but also impaired the retention of the FM categorization by a marked increase in false alarm responses in pre-trained animals. High-resolution electro-corticographical recordings in this area revealed that the formation of “rising” and “falling” FM tone category is accompanied by a sudden change in behavior and a marked change in the dynamics of cortical stimulus representation (Ohl *et al.*, 2001).

Sound specific auditory learning involves a tonotopically organized cortico-thalamic cortico-collicular loop that is modulated mainly via cholinergic but also serotonergic and dopaminergic transmission (reviewed in Xiong *et al.*, 2009). Learning in the sweep direction discrimination task, in particular, has

been shown to depend on dopamine (DA) signaling and protein synthesis within the auditory cortex (Kraus *et al.*, 2002; Schicknick *et al.*, 2012). Auditory fear learning involves both, the lemniscal pathway (involving the ventral division of the medial geniculate body in the thalamus) and non-lemniscal circuit (involving the medial division of the medial geniculate body), but the perpetuation of discriminative fear and its extinction depended mainly on an intact non-lemniscal pathway that projects directly from the thalamus to the amygdala (Antunes & Moita, 2010).

On the other hand, amygdala and striatum appear to complement one another in procedures of appetitive and aversive conditioning (Delgado *et al.*, 2008). Two-way active avoidance acquisition, for example, has been demonstrated to depend upon dopamine signaling in the amygdala, but also the entire striatum (Darvas *et al.*, 2011). Using gene therapy to selectively restore DA signaling, Darvas *et al.* (2011) also showed that after prolonged training (possibly after habit formation) only dopamine in the striatum was needed to retain the active avoidance behavior. This finding underlines the striatum's central position in stimulus-response (SR) behavior. It has to be noted however, that the shift from "goal-directed" to "stimulus-response" behavior, mediated by the associative and sensorimotor striatal regions respectively, is most probably continuous and the process of habit formation and temporal involvement of striatal regions herein are still not clear (reviewed by Adams *et al.*, 2001; Ashby *et al.*, 2010).

The ventral part of this large brain structure has been mostly implicated in goal-directed behavior, in which the calculations of expected reward values and actual response outcomes (the "prediction error") become fundamental to decision making and action selection. Reinforcement theories that involve striatal activities, for instance by calculating this prediction error, oftentimes applied appetitive procedures. This complicates the image on shuttle-box learning, by posing the question if the avoidance of an aversive outcome can be regarded as rewarding itself. In studies involving human subjects the medial orbitofrontal cortex – a structure also implicated in prediction error processing – was equally recruited during money loss and during the reception of a monetary reward (Kim *et al.*, 2006). There is also good

evidence that aversive conditioning involves the ventral striatum and that negative prediction errors are coded by dopaminergic signaling similar to appetitive reward predictions (reviewed in [Delgado et al., 2008](#)).

Hence there is proof that the ventral striatum is involved in acquiring the auditory cue-significance associated with CS+ and CS- respectively in the FM tone discrimination task in the shuttle-box regardless of its primary aversive nature. Furthermore, in the ventral striatum, appropriate response selection would be fine-tuned according to reinforcement theories. The task is also tightly dependent on the auditory cortex, both during the acquisition and the retention ([Ohl et al., 1999](#)). An interplay between both brain areas appears most likely.

Reports on the interaction between auditory cortex and the ventral striatum are sparsely found. [Popescu et al. \(2009\)](#) investigated how gamma oscillations couple the basolateral amygdala and the ventral striatum during appetitive auditory discrimination learning in cats and also recorded from the auditory cortex. However they could not show any learning related changes in the gamma-coupling of cortex and striatum; on the other hand amygdalostriatal interactions in the gamma frequency range markedly increased during the course of learning. In a most recent study, [Znamenskiy & Zador \(2013\)](#) manipulated corticostriatal projections from the auditory cortex to the “auditory” caudal striatum using optogenetic-techniques. They could show that activation or inactivation of direct cortico-striatal projections were able to influence response bias and reaction times on a two-way auditory choice discrimination task.

Conclusively auditory cortico-striatal projections transmit sound information that these rats utilized to make decisions. If auditory gating has a role in this rather complex task is unclear. The other way round, how auditory gating could be affected by the auditory discrimination task is indistinct: variables of selective attention, mild stress and the formation of (procedural) memories all loom within the task.

According to the aforementioned facts, the following hypotheses related to the impact of discrimination training on auditory gating were put forward:

1. Using a train of identical frequency modulated tones as CS, attention needs to be paid only to the first tone (as minimum requirement) to identify the adequate response action, hence on average gating should be intact. It appears possible, however, that during the very initial sessions, when a proper CS+/CS- discrimination has not been attained, yet, attention on the single tones of a train could be elevated and gating diminished. Therefore, the timepoint at which animals properly discriminated between CS+ and CS- was determined, and comparison of AEP gating values before and after this timepoint have been made. If the task required additional attentional resources, gating should initially have been diminished. Also possible differences between the subcomponents were to be investigated to identify putative pre-attentiveness of single subcomponents.
2. Stress should increase during the first sessions in the avoidance paradigm, then gradually decrease as performance goes up (Johnson & Adler, 1993), escape reactions become true avoidances and the animals receive less shocks: hence gating scores could have been negatively correlated with stresslevel. A correlation analysis with performance and gating scores was calculated to clarify this.
3. Finally, it was of interest if discrimination training strengthened or modulated the auditory cortex – ventral striatum interaction. Therefore a comparison of phase-locking before and after the discrimination training had been calculated.

## **3.2 Methods**

### **3.2.1 Subjects and procedures**

Subjects were the same animals used for the experiments in Chapters 2 and 3 (cf. Section 1.2.1). For the phase-locking analyses (Section 3.3.4) a subgroup (n = 6) of these animals was used.

### 3.2.2 Behavioral Task

In the Go/NoGo task animals were trained in a shuttle-box to discriminate frequency modulation direction of presented tones by hurdle crossing. One training session consisted of 60 trials with equal ratios of pseudo-randomized CS+ (1-2 kHz) and CS- (2-1 kHz) stimuli (both 200 ms long with 5 ms on- and offset cosine squared ramps). CS+ and CS- cues were presented in trains with inter-stimulus intervals of 0.5 s (onset to onset). CS- stimuli were presented 12 times while CS+ stimuli were repeated 20 times; stimuli were silenced if the animal scored a hit or a false alarm, respectively, by crossing the hurdle. A false alarm was punished with a mild foot-shock through the grid floor (approximately 350  $\mu$ A; electrical stimulator model 2100, AM Systems Inc., Carlsborg, WA, USA); in the same way not changing the compartment during the CS+ condition (“miss”) was punished after 6 s. Animals were trained till they performed successful discrimination of the frequency modulation direction of stimuli.

Electrophysiological recordings were obtained continuously during the whole training procedure (cf. Section [1.2.1.3](#)).

### 3.2.3 Data Analysis

For the display of a learning curve, “Go” reactions were split according to trial condition (CS+ Trial / CS- Trial). For each session exact Fisher tests were calculated, to obtain session numbers that indicated a dependence of reaction from stimulus condition at the 0.05 significance level. As measure of performance, for each animal, the sensitivity index ( $d'$ ) of the receiver operator characteristics of each training session was calculated:

$$d' = z(\textit{hit rate}) - z(\textit{false alarm rate}),$$

where  $z$  is the inverse of the cumulative Gaussian function (quantile function). Performance ( $d'$  values) and reaction times to the CS+ were analyzed for their interrelation and their relation with session number using Pearsons' product correlation coefficient.

Reaction times for hits and false alarms were analyzed *post-hoc* with one-sided t-tests, hypothesizing that shuttle responses on the CS+ stimulus occurred later than those on the CS- trials. All behavior data was analyzed in R (R Foundation for Statistical Computing, Vienna, Austria).

### **3.2.4 Electrophysiological recordings**

LFP data, that was acquired during the training, was preprocessed similarly as described in Sections 1.2.2.1 and 1.2.2.2; only for the peak sorting a 30 Hz phase-neutral 6<sup>th</sup> order Butterworth filter was used. Calculation of amplitude suppression is described in Section 1.2.2.3 and was based on the averaged LFP trace per session and CS. Suppression scores for the first 4 session were subjected to a repeated-measure ANOVA with factors SESSION (levels: 1-4) and CS (levels: plus and minus) and their interaction to test for training effects on auditory gating.

### **3.2.5 Phase-locking after the training**

A subgroup of animals (n = 6) was tested for long-term influences of the training on auditory cortex – ventral striatum phase-locking. With this objective, the gating recordings were repeated one day after the animals had completed all discrimination trainings-sessions. Wavelet and coherence calculations were performed as described in Sections 2.2.2.2 and 2.2.2.5. Baseline values (1 s before the stimulation) were tested for changes due to training with repeated-measure ANOVA with factors FREQUENCY (levels: “delta”, “theta”, “alpha”, “beta”, “gamma”) and TIMEPOINT (levels: “before” and “after”). Greenhouse-Geisser corrections were applied where necessary. Paired t-tests were used as *post-hoc* analysis.

Phase-locking during the first stimulus was analyzed for effects of the factors FREQUENCY, CS and TIMEPOINT. This time *post-hoc* analyses were performed using repeated-measures ANOVAs for each frequency band with factors CS and TIMEPOINT. All ANOVA calculations were performed in SPSS (PASW Statistics 18, SPSS, Inc., Chicago).

## **3.3 Results**

### **3.3.1 Behavioral performances**

#### **3.3.1.1 Learning curve**

During the discrimination training, median population discrimination performance reached significance in the third training-session (Figure 3.1). Individual data reinstated that the first significant discrimination performance was reached after 3 sessions [ $2.73 \pm 0.25$ , mean  $\pm$  SE,  $n = 15$ ] on average.

#### **3.3.1.2 Discrimination performance and reaction times to CS+**

Performance ( $d'$ ) values, and hence discrimination between CS+ and CS-, increased with training [ $t = 2.39$ ,  $df = 116$ ,  $p = 0.019$ ,  $r = 0.22$ ; Figure 3.2 A]. Reaction times towards the CS+ correlated negatively with number of sessions, hence reaction times decreased with training [ $t = -4.52$ ,  $df = 116$ ,  $p < 0.001$ ,  $r = -0.39$ ; Figure 3.2 B]. The population median of the CS+ reaction time for the second session was already below 6 seconds, the threshold between true avoidance and escape reaction (foot-shock onset). Both performance values showed a strong negative correlation (Figure 3.3).

Analysis of reaction times to cross to the other compartment on CS+ and CS- stimuli showed that during the initial learning of the discrimination task, false alarm reactions occurred significantly faster than jumps on the CS+ stimuli [sessions 1 - 6; all  $t > 2.2$ , all  $p < 0.03$  one-sided t-tests] (Figure 3.4).

### **3.3.2 Auditory Gating during the training**

To analyze if training in the FM tone discrimination task influenced suppression scores, gating of evoked potentials was evaluated for each subcomponent of the evoked potential for the first four sessions during the behavioral training. The first four sessions were chosen because almost all animals had acquired a significant discrimination performance within the first three sessions. While striatal evoked potentials were constantly gated

during the training with suppression scores close to 50%, cortical potentials were hardly suppressed (Figure 3.5). For all components of the AEP (P1, N1, P2) there were no significant influences by either the factor SESSION, nor CS nor an interaction effect of both factors (Table 3.1). Also there were no apparent difference in gating between subcomponents. Individual variations of subcomponent gating is displayed in Figures. 4, 5 in the Appendix C.

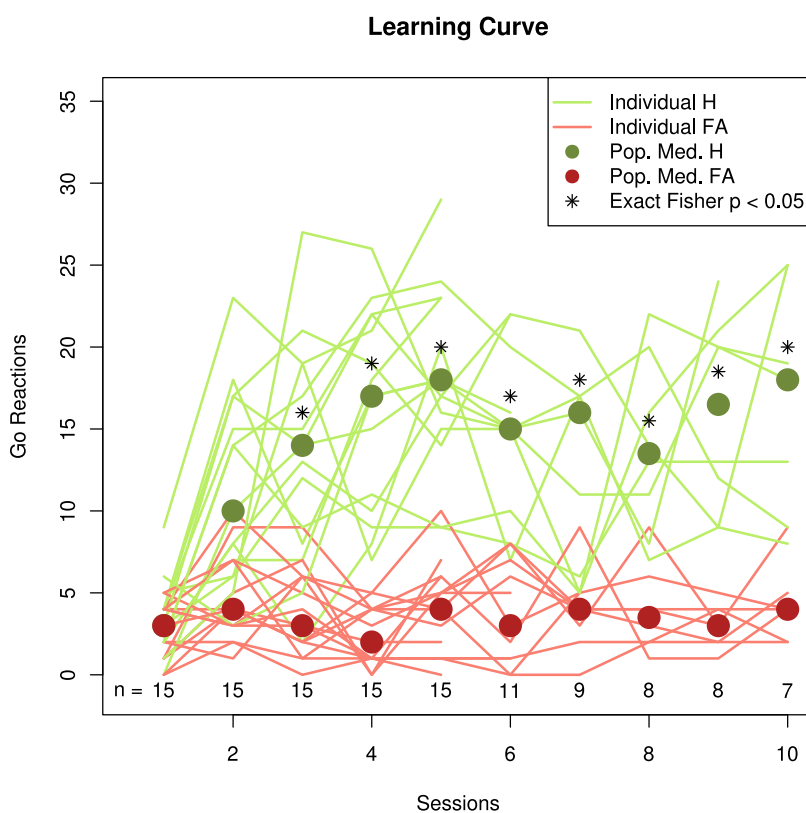


**Figure 3.1: Successful discrimination of frequency modulated (FM) tones was attained after three training sessions.** Shown is the population median learning curve as “Go” reactions per session in dependence of the stimuli (red: CS-, green: CS+). Since animals were not trained for equal number of sessions, but until they were able to discriminate correctly, n numbers are given for each data point. Individual performances are plotted as thin lines below. \*: sessions with significant difference between numbers of hits and false alarms (exact Fisher test); H: hit; FA: false alarm.



**Table 3.1: Training effects on striatal auditory gating.** Repeated-measure ANOVA of effects by the factors SESSION and CS on amplitude suppression in the ventral striatum and the auditory cortex. Greenhouse-Geisser epsilons are cited where appropriate corrections have been made.

Area	Component	Effect	df	F	$\epsilon$	p
<b>Auditory cortex</b>	P1	SESSION	(1.1, 4.4)	0.38	0.366	0.764
		CS	(1, 4)	0.50	-	0.520
		SESSION x CS	(3, 12)	0.75	-	0.545
	N1	SESSION	(1.5, 16.4)	0.33	0.498	0.664
		CS	(1, 11)	1.69	-	0.220
		SESSION x CS	(3, 33)	0.54	-	0.657
	P2	SESSION	(3, 33)	0.22	-	0.880
		CS	(1, 11)	1.20	-	0.300
		SESSION x CS	(3, 33)	0.18	-	0.910
<b>Striatum</b>	P1	SESSION	(1.2, 5.9)	0.55	0.391	0.517
		CS	(1, 5)	1.38	-	0.293
		SESSION x CS	(3, 15)	0.54	-	0.660
	N1	SESSION	(3, 18)	1.63	-	0.217
		CS	(1, 6)	4.87	-	0.069
		SESSION x CS	(3, 18)	0.29	-	0.833
	P2	SESSION	(3, 21)	1.40	-	0.273
		CS	(1, 7)	0.19	-	0.677
		SESSION x CS	(3, 21)	1.60	-	0.211

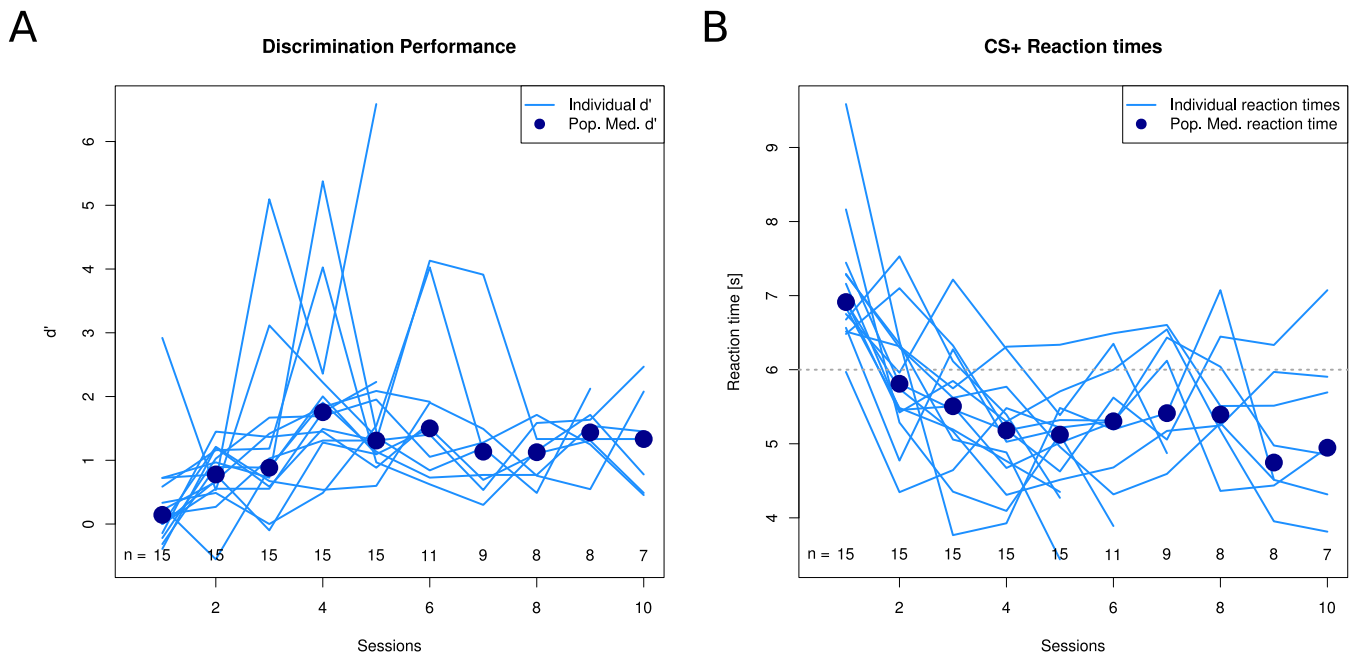


**Figure 3.2: Discrimination performances and CS+ reaction times changed with training.** (A) CS+ versus CS- discrimination performance increased with training. Displayed are the population median  $d'$  values plotted over individual  $d'$  curves (light blue). (B) CS+ reaction times decreased with training. A reaction time below 6 seconds marks trials that are counted as true avoidance reaction (gray stippled line). Animal numbers are given at the bottom of the plot for each median data point.

### 3.3.3 Gating and performance

It is possible that testing auditory gating in a session-wise procedure blurs effects that are not strictly linear with sessions. Individual performances naturally jitter from session to session, while average discrimination performance steadily increases with training (cf. Figure 3.2 A). To be able to capture these individual variations, correlations of the striatal AEP suppression scores with performance were calculated. Discrimination performance was measured as  $d'$  (Section 3.2.3). There were no significant correlations of discrimination performance with AEP suppression scores in the ventral striatum [all  $p > 0.05$ ; Figure 3.6].

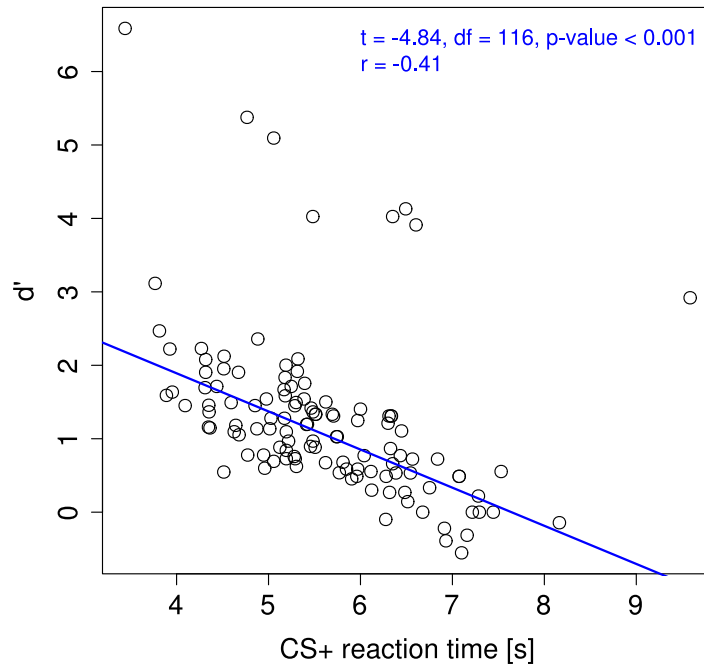


**Figure 3.3: Better discrimination performance correlated strongly with faster reaction times to the CS+.** A linear fit and the correlation statistics are also displayed.

### 3.3.4 Training influence on auditory cortex – ventral striatum phase-locking

A subgroup of animals ( $n = 6$ ) was tested after termination of the discrimination training for their auditory gating values (passive task, cf. Chapter 2). Phase coherence was determined before and after the training and values were subjected to statistical analysis. Figure 3.7 displays the grand average of phase-locking values to the passive stimulation with trains of CS+ and trains of CS- tones (upward and downward frequency modulated tones, respectively) before and after the training.

### Go Reaction Times

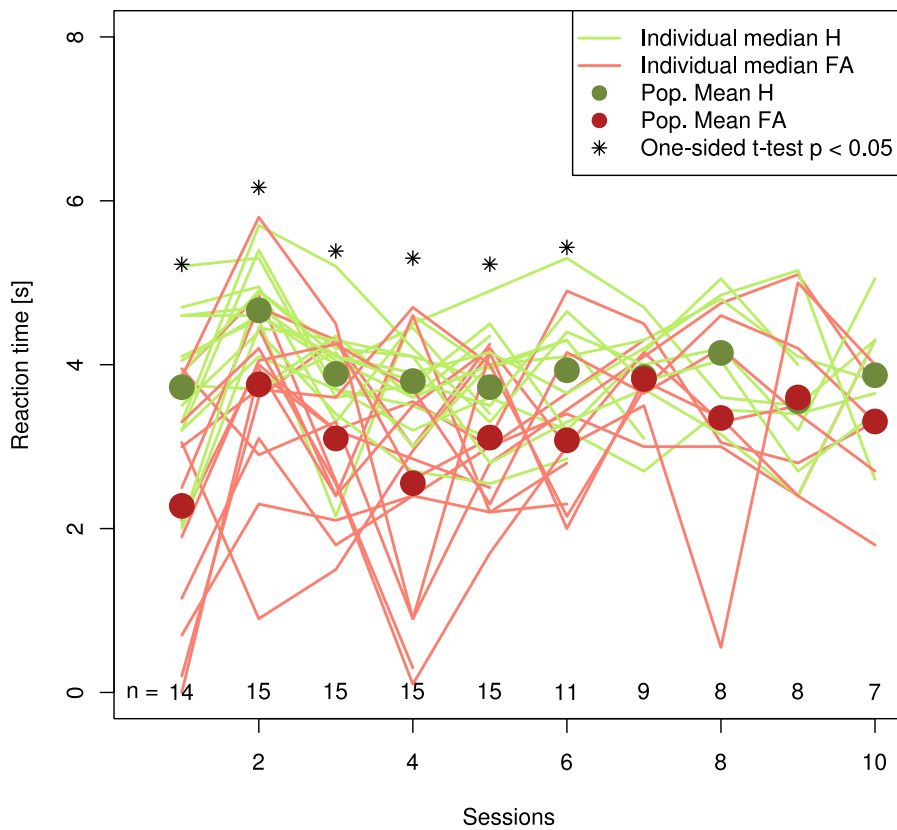


**Figure 3.4: Reaction times of “Go” responses were slower during CS+ trials during the discrimination.** Displayed are the population average go reaction times during CS+ (red dots) and CS- trials (green dots). Since animals were not trained for an equal number of session, n numbers are given for each data point. Individual median reaction times are plotted as thin lines below. \*: significantly larger reaction times during CS+ trials (one-sided t-test). H: hit, FA: false alarm.

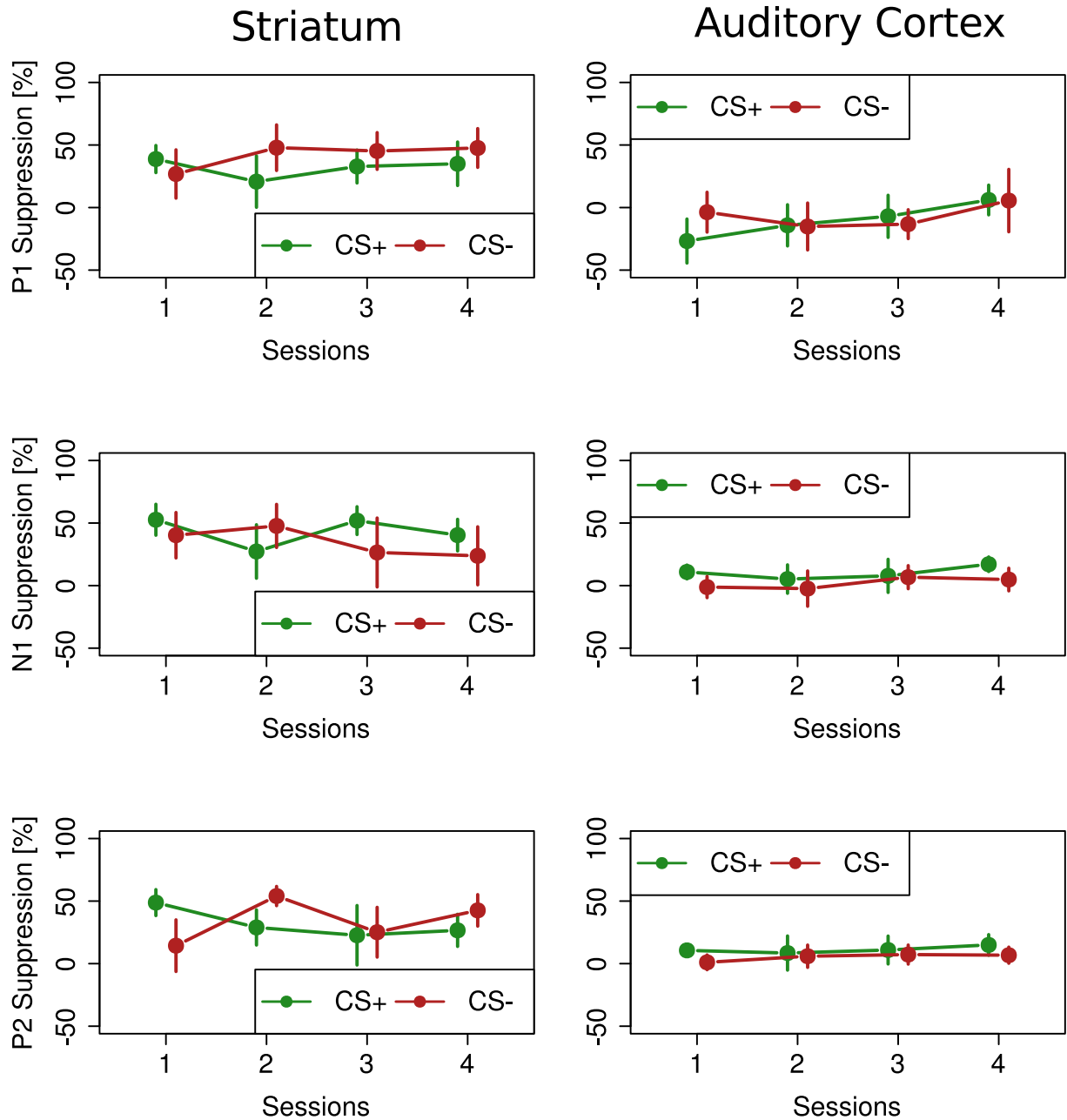


**Figure 3.5: Amplitude suppression during discrimination training in the ventral striatum and auditory cortex.** Suppression scores in the striatum remained positive and mostly above 40% during the training, hence amplitudes were still suppressed after the first stimulus. Also during training gating was not evident in the cortex, as suppression scores varied around 0%, or even showed light facilitation (negative suppression scores) for the P1 sub-component of the AEP. In both areas, repeated-measure ANOVA yielded no effects for either factor SESSION or CS. Data are means of averaged sessions per animal  $\pm$  SE.

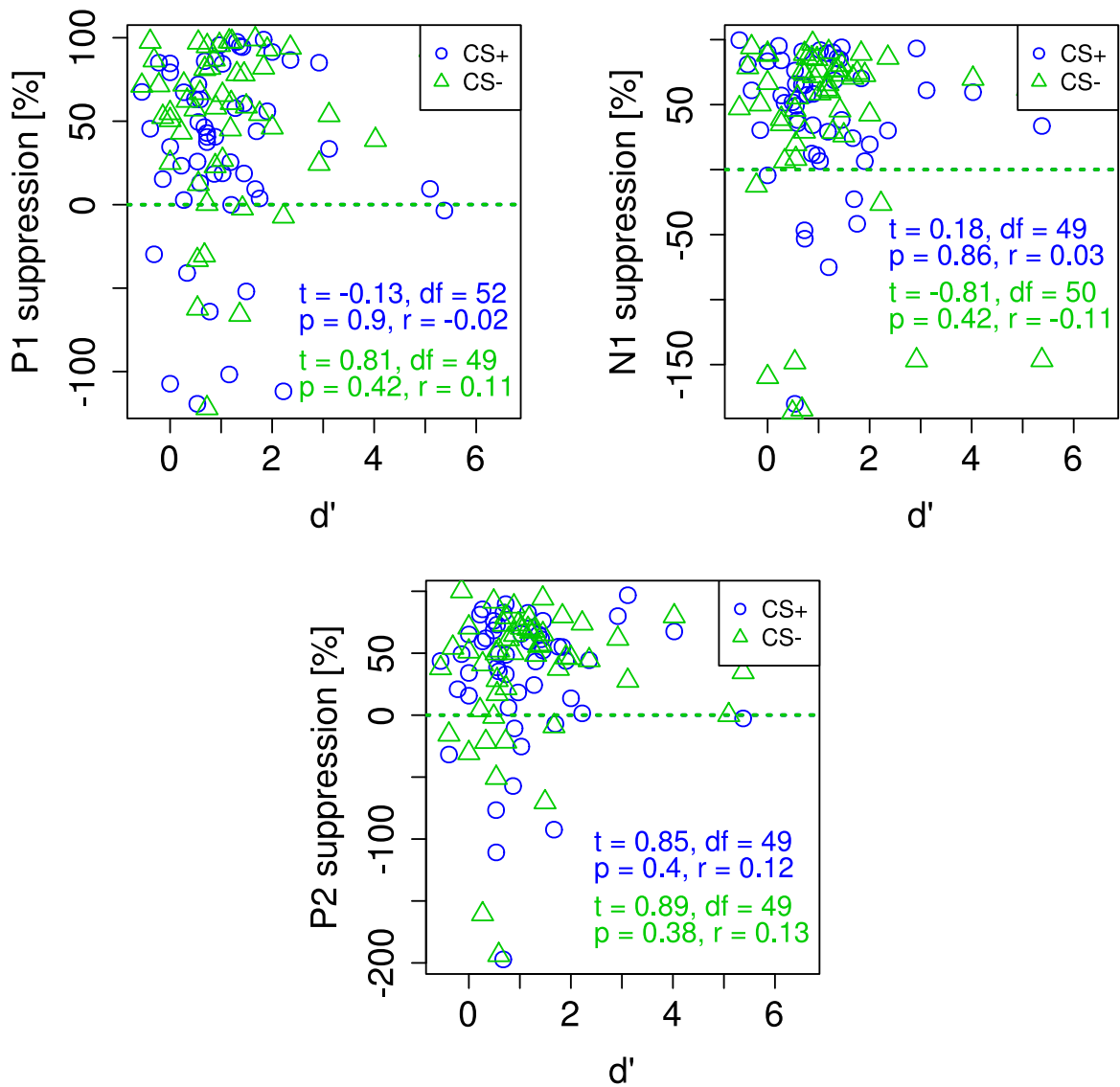


**Figure 3.6: AEP suppression did not correlate with discrimination performance.** Shown are  $d'$  correlations with the suppression of all three investigated subcomponents in the ventral striatum.

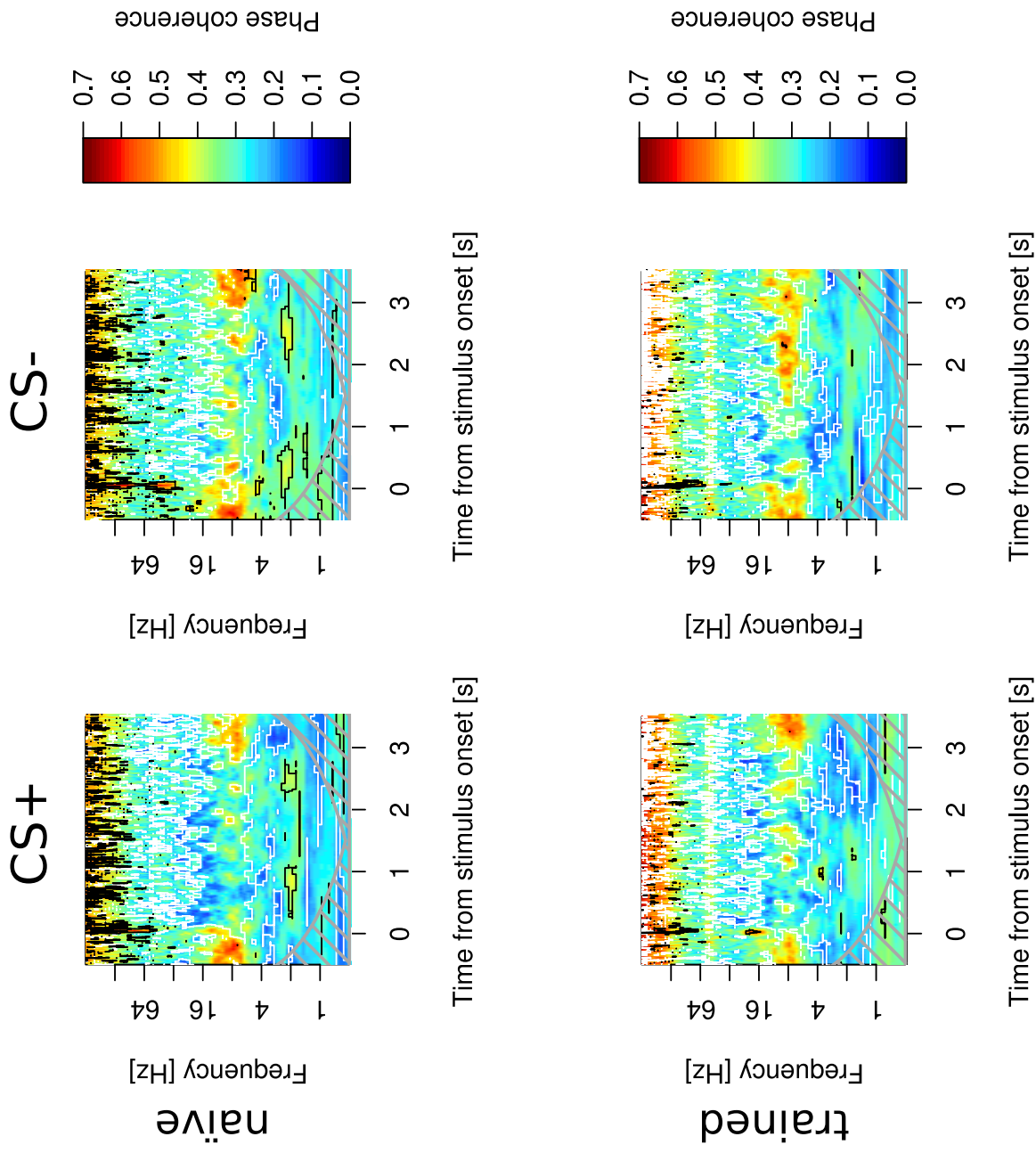


**Figure 3.7: Phase-locking before and after discrimination training.** Upper panels naive animals, lower panels trained animals; left panels CS+, right panels CS-. Grand average of phase-locking index. Contour lines display values that were significantly higher or lower than grand-average baseline phase-locking values. The wavelet cone of influence is shaded in gray.

Firstly it was controlled if baseline PLI values, without sound stimulation, had changed after the training. Baseline values were subjected to repeated-measure ANOVA with factors TIMEPOINT and FREQUENCY to check if possible changes were related to only narrow frequency bands; for this analysis baseline periods before stimulation with rising or falling FM tones were pooled. Therefore two values per animal were included in the data pool. Baseline PLI was influenced by factor FREQUENCY [ $p < 0.001$ ] and an interaction effect of TIMEPOINT with FREQUENCY [ $p < 0.001$ ], but not TIMEPOINT as a factor itself (Table 3.2). A *post-hoc* paired t-test revealed that there was a trend towards an increase of alpha band PLI values [ $t = 2.12$ ,  $df = 11$ ,  $p = 0.058$ ] after the training, while gamma band PLI decreased significantly [ $t = -2.91$ ,  $df = 11$ ,  $p = 0.014$ ].

Hypothetically, during stimulation only the first stimulus carries all the information necessary for the animal to elaborate its appropriate response action. Therefore PLI was analyzed during the stimulation with the first tone for influences of the factors FREQUENCY, CS and TIMEPOINT of training. Only the factor FREQUENCY band had an impact on PLI values irrespective of the timepoint before or after training (Table 3.3); therefore phase-locking during stimulation was re-analyzed split by frequency bands using repeated-measure ANOVA again. This analysis revealed only a CS effect in the gamma band with higher PLI values for the CS- tone than for the CS+ (Table 3.4).

---

**Table 3.2: Training effects on baseline phase-locking.** Repeated-measure ANOVA of effects by the factors TIMEPOINT and FREQUENCY on baseline phase-locking between the auditory cortex and the ventral striatum. Greenhouse-Geisser epsilons are cited where appropriate corrections have been made.

<b>Effect</b>	<b>df</b>	<b>F</b>	<b><math>\epsilon</math></b>	<b>p</b>
TIMEPOINT	(1, 11)	0.00	-	0.984
FREQUENCY	(1.45, 15.93)	62.38	0.36	<0.001
TIMEPOINT x FREQUENCY	(4, 44)	6.47	-	<0.001



**Table 3.3: Training effects on phase-locking during FM tone stimulation.** Repeated-measure ANOVA of effects by the factors SESSION and CS and TIMEPOINT on phase-locking scores during the first tone presentation. Greenhouse-Geisser epsilons are cited where appropriate corrections have been made.

<b>Effect</b>	<b>df</b>	<b>F</b>	<b>ε</b>	<b>p</b>
TIMEPOINT	(1,5)	0.06	-	0.822
FREQUENCY	(4, 20)	4.27	-	0.012
CS	(1, 5)	1.97	-	0.219
TIMEPOINT x FREQUENCY	(2.04, 10.19)	1.28	0.51	0.319
TIMEPOINT x CS	(1, 5)	0.53	-	0.499
FREQUENCY x CS	(4, 20)	0.84	-	0.518
TIMEPOINT x FREQUENCY x CS	(4, 20)	1.28	-	0.313

**Table 3.4: Training effects on phase-locking during FM tone stimulation split by frequency.** Repeated-measure ANOVA of effects by the factors TIMEPOINT and CS on phase-locking scores during the first tone presentation.

<b>Frequency</b>	<b>Effect</b>	<b>df</b>	<b>F</b>	<b>p</b>
<b>delta</b>	TIMEPOINT	(1, 5)	0.09	0.773
	CS	(1, 5)	3.76	0.110
	TIMEPOINT x CS	(1, 5)	0.55	0.494
<b>theta</b>	TIMEPOINT	(1, 5)	0.30	0.610
	CS	(1, 5)	3.62	0.115
	TIMEPOINT x CS	(1, 5)	0.00	0.974
<b>alpha</b>	TIMEPOINT	(1, 5)	3.06	0.140
	CS	(1, 5)	4.67	0.083
	TIMEPOINT x CS	(1, 5)	0.09	0.777
<b>beta</b>	TIMEPOINT	(1, 5)	0.49	0.517
	CS	(1, 5)	0.09	0.775
	TIMEPOINT x CS	(1, 5)	1.56	0.267
<b>gamma</b>	TIMEPOINT	(1, 5)	5.20	0.071
	CS	(1, 5)	7.63	0.040
	TIMEPOINT x CS	(1, 5)	3.89	0.106

Altogether the training appeared not to have changed phase-locking during tone stimulation between the auditory cortex and the ventral striatum. Baseline values in the alpha band showed a trend towards increased phase-locking after training, however, and gamma phase-locking between the areas had significantly decreased.

## **3.4 Discussion**

### **3.4.1 Auditory evoked potential suppression during discrimination training**

In the last section of the study, auditory gating was tested for its susceptibility to training effects in an auditory discrimination task. For this purpose animals were trained in a shuttle-box on a Go/NoGo paradigm in which they learned to discriminate frequency upward modulated tones from frequency downward modulated tones. To avoid mild foot-shocks animals adopted the strategy to shuttle on the CS+ (upward modulated tone) and stay in the current compartment on CS- trials. On average animals acquired the task within three days (one training session of 60 trials per day), when the median number of “go” responses during a session on a CS+ trial (hits) surmounted those in CS- trials (false alarms) significantly (Figure 3.1). At this point, the median  $d'$  value was close to one and median reaction times on CS+ trials lay below 6 s (shock onset), hence the mean number of animals performed true avoidance strategies.

Auditory suppression scores were measured during the training for the first four sessions, hence the data included two sessions with non-significant discrimination and two sessions in which animals had acquired a proper response-strategy within the Go/NoGo task. Calculating a repeated-measure ANOVA yielded no effect of the factor SESSION for ventral striatum auditory gating for all three measured subcomponent of the AEP (Figure 3.5, Table 3.1). These findings indicate two things: on the one hand they most likely support the idea that auditory gating serves an internal filtering mechanism

with rather robust settings, that was barely influenced by attentional factors or other modulations through discrimination learning. On the other hand, such hypothetical attentional influences might be limited to only a sparse number of trials of initial training sessions. To obtain an evoked potential that allows for the identification of different subcomponents, however, it is necessary to average over a larger number of trials. Therefore it is possible that subtle effects are averaged out by individual variances. Figure 4 of Appendix C (page 103) shows that even gating scores averaged by sessions for each animal displayed a high variance. Speculatively, Figure 3.5 (*left panels*) hints at a trend-wise increase of amplitude suppression during the CS- trials within the ventral striatum, with a stronger suppression of all three subcomponents regarding the first two sessions and suppression slightly decreasing for CS+ trials for all three subcomponents. One could conjecture, that during the acquisition phase of discrimination training evoked potentials from CS+ tones might have been transiently less suppressed than CS- AEPs, signifying a differential filtering of these two salient cues. Hence the CS+ cue could signify a more salient event to the animal insofar as it required immediate motor responses. At this point there is insufficient data to come to clear conclusions about attentional influences.

Moreover, the results generally underline findings from a human subject study that showed P50 gating to be pre-attentive and not modifiable through attention-demanding tasks (Jerger *et al.*, 1992). More recent studies implicate high correlations of measures of attentional vigilance with P50 suppression in EEG (Wan *et al.*, 2008), while others demonstrated an attention effect for scalp and intracranial N100, but not P50 (Rosburg *et al.*, 2009a). Yadon *et al.* (2009) have linked auditory gating with a focus on cognitive inhibition, “the restriction of attentional access, deletion of no-longer-relevant information from attention and working memory and restraint over habitual or prepotent response tendencies”, arguing on the basis of the load theory (Lavie *et al.*, 2004), that P50 suppression was negatively related to interference resolution - the need to ignore irrelevant information - in the Stroop task and positively to response inhibition in a Go/NoGo task. The relatively small number of animals trained in the

present study did not allow for the evaluation of gating effects split by trial responses, because the numbers of false alarms were relatively low already from the beginning (Figure 3.1). Probably, response inhibition would better be detected in a comparison between false alarm and correct rejection responses. On the other hand, strong effects on auditory gating would also be reflected when the data was split between CS categories (Table 3.1), but this was not seen here.

The fact that gating of the later P2 component of the present study appeared equally unaffected by the task, questions the comparability of later animal AEPs and human AEPs (Budd *et al.*, 2012; Umbricht *et al.*, 2004), such as the N100, that was demonstrated to be altered by attention tasks in human subjects (Jerger *et al.*, 1992; White & Yee, 1997).

### **3.4.2 Relation of gating scores with discrimination performances**

To more strongly consider individual learning performances, that not necessarily increase with session number (Gallistel *et al.*, 2004), it was checked if AEP suppression showed correlations with discrimination performances. For no subcomponent of the evoked striatal potentials were there any significant correlations with  $d'$  (Figure 3.6). This finding is in line with the above mentioned results and in support of a pre-attentive mechanism that denies the influences of mild stress and cognitive effects as they appear during the shuttle-box experiments (Jerger *et al.*, 1992; White & Yee, 1997). Arguably the stress level during the Go/NoGo task is rather moderate and limited to the very early trials when animals make the most mistakes. The aversive foot-shock is also controllable by escape shuttling behavior. This is in contrast to the animal studies that have investigated auditory gating after acute stress situations, such as fear conditioning, sodium-chloride injections or three hours of constraint stress (Cromwell *et al.*, 2007; Mears *et al.*, 2009; Süer *et al.*, 2004). Active avoidance learning has been characterized as “escape from fear” learning in which hitting the safe compartment can actually be regarded as rewarding and reinforcing (Cain

*et al.*, 2010; Rogan *et al.*, 2005).

It is highly likely that (positive) stress and raised attentional load do play a role in the initial acquisition phase of the Go/NoGo discrimination task. These two behavioral components are hard to delineate within the task, as they probably occur in temporal contiguity. Future investigations could base the experiments on a larger number of animals to obtain higher statistical power or measure additional physiological features adherent to mild stress, such as heart rate.

### **3.4.3 Long-term changes in cortico-striatal phase-locking**

With a subgroup of animals gating was measured after the discrimination training had been completed. Since there were no apparent changes in the gating score during the training, it was of special interest, if the training had changed cortico-striatal interaction in the long term. This was tested by analyzing phase-locking before and after the training. After training light - but not significant - elevation in the alpha band phase-locking during baseline condition without acoustical stimulation and a decrease in gamma coherence was detected. During passive tone stimulation, however no changes after the training were seen for the first stimulus of a train of six FM tones.

It could well be that the animals do differentiate between in-training and passive stimulation context, which they can assess relatively quickly once they do not receive a foot-shock after the CS+. It appears plausible that, considering that there were also no task effects on auditory gating, the brain would maintain its baseline activity and not change phase-locking between areas. Yet a small (non-significant) increase in the baseline alpha range was seen and a reduction in the gamma frequency range. Jensen & Mazaheri (2010) have proposed that alpha oscillation serve to inhibit task irrelevant brain areas, but could also prime areas for subsequent processing, thus the elevation in coherent baseline alpha could have primed both areas for functioning in the Go/NoGo task. Gamma oscillations have been associated with a many brain-physiological functions, e.g. short-term representations of

novel sensory objects or encoding those into memory (e.g. [Haenschel et al., 2000](#); [Jeschke et al., 2008](#)). Simply put, the decrease in baseline gamma coherence within the present study could signify a loss of general novelty effects, but at this point no further speculations seem appropriate.

Appetitive auditory discrimination training has been shown to modulate and increase coherent amygdalo-striatal gamma oscillations ([Popescu et al., 2009](#)), especially during CS+ stimulation. In their supplemental material the group also demonstrated that auditory cortex–striatal coupling remained at a stable low level and was not altered during the training. Given the fact that both training methods work with different stimuli (pure tones versus frequency modulated tones in the present study) and different reinforcers (appetitive liquid reward versus aversive foot-shock) the comparability of both studies remains restricted. Yet the results cautiously point into the same direction: Long-term training effects between both investigated brain areas could not be observed here. This emphasizes that the task itself represents no features that alter brain physiology, as has been shown for paradigms involving chronic stress (cf. [Mears et al., 2009](#)).

# Chapter 4

## Conclusions

In the present study, auditory gating was analyzed in the ventral striatum and in the auditory cortex simultaneously in awake, freely behaving Mongolian gerbils. Auditory evoked potential and time-frequency analysis was used to characterize this effect in the animal subject. Furthermore, task influences on auditory gating were assessed with an auditory discrimination paradigm in a shuttle-box.

From the auditory evoked potential analysis it became clear that FM sweep evoked potentials in both brain areas follow different dynamics: while the cortex responded to each stimulus repetition with a full AEP, the striatal AEPs were liable to auditory gating, displaying a suppression of approximately 60% for each AEP subcomponent upon repeated tone stimulation. These findings have two implications: firstly, in classical auditory gating paradigms click stimuli are used, that lack the spectro-temporal complexity that potentially requires auditory cortex processing. Therefore, in the present study, frequency-modulated tones were presented as test and conditioning stimuli. Yet, the lack of amplitude suppressions in the cortex support the notion that filtering within the tested time-scales does not apply to the auditory cortex. Secondly, since these more complex stimuli are clearly subject to auditory gating, at least in the striatum, stimulus features do not affect this robust filter mechanism of the brain.

Analyzing between-area phase-locking during passive tone-train stimulation revealed that phase-locking between the auditory cortex and the ventral

striatum during tone stimulus presence was significantly decreased, followed by an increase in the low frequency range after tone offset. The model that one could envision based on these results is the following: auditory information would reach both brain areas on different paths, possibly branching at the level of the thalamus (Matsumoto *et al.*, 2001). Feedback from the auditory cortex about the auditory cue could reach the striatum after tone offset and explain the found increase in phase coherence. It is not clear however, if the cortex directly projects to the striatum in this case, or if there are intermediate structures, like the prefrontal cortex, that ultimately direct gating. A way to test this would be to reversibly or irreversibly silence the auditory or prefrontal cortex (or both) and check for intact gating. Alternatively, gating develops from inherent properties of striatal neuronal networks, in which cholinergic interneurons have been shown to exert a dominant inhibitory control function (English *et al.*, 2012; Witten *et al.*, 2010). In favor of this hypothesis, short-term habituation experiments showed that suppression in the striatum can be best explained by the decrease of response amplitudes between the first and the second stimulus presentation, but the recovery of the striatal AEP was estimated to exceed 4 s. Taken together these results support a refractory mechanism of the AEP generator pool that, given the long recovery time estimates, is probably coupled to additional inhibitory mechanisms, most likely striatal interneuronal signaling. In order to gain a more precise understanding of the behavioral relevance of auditory gating, dishabituation experiments could be conducted while recording simultaneously from both, the cortex and ventral striatum.

Time-frequency transformation of the recorded signals showed that total-signal-power in both, the auditory cortex and the ventral striatum, was comparable during tone-train stimulation. However, the total-signal power was differently split into stimulus-locked activity and stimulus induced activity, with the latter being significantly higher in the striatum than in the cortex. Gating of striatal evoked activity was found in a frequency range from 1-80 Hz, while induced energy was not gated in this area. This finding allows to infer that the reduced striatal amplitudes in response to repeated stimuli



are generated because of temporally jittering responses to these tones. To substantiate this result, AEPs to the test stimulus could be further analyzed for their trial-to-trial variability, EP completeness (i.e. the full development of identified subcomponents of the AEP, [Hu et al., 2009](#); [Jansen et al., 2010](#)). Additionally, computer algorithms could be used to perform EP alignments ([Patterson et al., 2000](#)). Possibly, stimulus-locking beyond the first stimulus is not relevant for the features that are extracted during cue processing in the striatum, e.g. temporal structure of the stimulus. This explanation would also match general processing deficits found in schizophrenic subjects, which have often been described as sensory flooding.

Finally, discrimination learning in an aversive Go/NoGo paradigm showed no effect on AEP gating or long term phase-locking between the auditory cortex and the ventral striatum. Intuitively, during the shuttle-box training a stimulus-response association is formed that is reinforced by successful foot-shock avoidance. All information needed to perform hits and correct rejections in the task, are already given during the first stimulus presentation in the train of FM tones, that were used as CS+ and CS- cues. The paradigm differs from other animal studies that demonstrated changes in auditory gating due to inevitable chronic stressors, and hence might be better suited to model real world situations. The finding further implicates that in a controllable situation, auditory gating functions robustly and subtle changes in the brain physiology due to learning cannot alter this process. To gain a deeper understanding of the role of attention during gating, future investigations could alter the CS stimuli in a way that attention had to be paid not to the first stimulus but to the second or a later tone within a stimulation train.

Auditory gating is a concept that came into existence from human EEG studies. Work in animal subjects with locally defined electrodes has helped to show that this concept applies to certain brain regions, such as the hippocampus, amygdala or prefrontal cortex. The present study added to the notion that this process might be rather generated locally than transmitted between areas. Furthermore it seems plausible that this inhibitory process

serves different causes, according to the brain area's behavioral purposes. Only if systemic approaches in animals studies are combined with the knowledge from human studies, can the mechanism of auditory gating be disclosed. The identification of the function in healthy organisms represents the basis for developing measures for the betterment in the affected mental illnesses.

Single findings of the present study are listed below:

**FM sweep-evoked potentials in the auditory cortex and striatum displayed different time-courses of activation.** Wave shapes differed after the P1 peak and might reflect that both brain areas were activated through sounds on differing pathways, that only partially overlap.

**Significant amplitude suppression was only seen in the ventral striatum.** Stimulation with identical repetitive sounds that were separated by an inter-stimulus interval of at least 500 ms only yielded auditory gating in the ventral striatum but not in the auditory cortex.

**Spectro-temporal complex stimuli are liable to auditory gating.** This finding for once underpins the fact the stimulus parameters play a subordinate role during auditory gating and that fine-grained cortical processing might not be necessary here.

**The suppression dynamics are best explained by a refractory phase of the AEP generator pool.** Although theories that favor habituation as basis of the auditory gating mechanism, cannot definitely be ruled out, the present data are in support of a rather passive process.

**Estimation of recovery times are in favor of additional mechanisms.** The very long recovery times that were estimated within this study for the N1 and P2 subcomponents indicate that additional inhibitory processes might be operating.

**Stimulation with FM sounds triggers comparable activity in the auditory cortex and the ventral striatum.** Total-signal-power and therefore mass neural activity was equally high within both brain areas during auditory stimulation.

**Striatal total-signal-power contained more induced activity than cortical TSP during auditory stimulation.** This shows that the normal functioning auditory gating effect could be explained by phase-desynchronization and hence jitters in neuronal responses in animal subjects as well ([Woldeit et al., 2012](#)).

**No specific LFP frequency band in the ventral striatum mediates auditory gating.** Striatal auditory gating was detected in all frequency ranges of the evoked activity; yet, suppression of induced activity from S1 to S2 in the cortex was mainly found in the frequency range below 12 Hz (below beta frequency range), the frequency range that could be responsible for phase-locked LFP responses.

**Inter-area phase-locking was significantly decreased during tone stimulation.** This finding added to the notion that both areas are rather independent from each other during sound analysis.

**Auditory discrimination learning had no influence on AEP gating in the Mongolian gerbil.** There were no measurable changes during the training on auditory gating scores, that would prove selective attention or stress effects on the process.

**Discrimination training did not alter long-term phase-locking between cortex and striatum.** Animal subjects might well be able to distinguish training versus passive stimulation contexts and training in the Go/NoGo paradigm is likely not to disturb the brain's equilibrium state.

# **Appendix A**

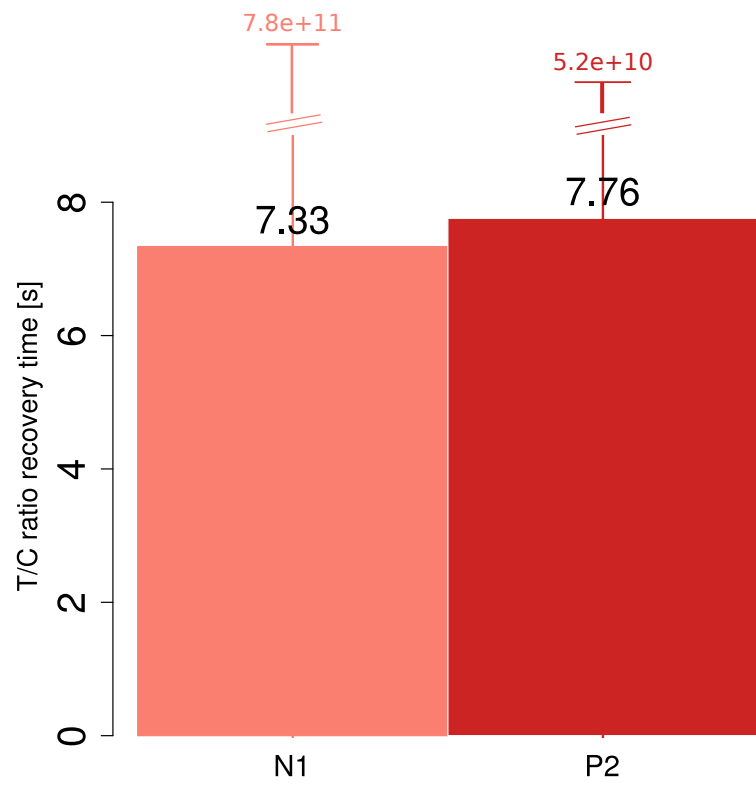


**Figure 1: Median recovery times estimated on individual subject exponential fits.** Recovery of N1 and P2 was comparable with population data estimates, but displayed large inter-individual variance. Note that the 95% confidence intervals are not displayed completely (N1-95%: [1.9,  $7.8 \times 10^{11}$ ] ; P2-95%: [1.3,  $5.2 \times 10^{10}$ ]),

**Table 1: Average amplitudes split by the used test factors.**

ISI	Area	FM	Component	Stimulus Position					
				1st	2nd	3rd	4th	5th	6th
<b>short</b>	ACX	rising	P1	4.75	4.02	3.25	3.45	3.34	3.29
			N1	9.88	8.87	8.43	7.61	8.14	7.61
			P2	10.07	8.78	8.93	7.65	8.14	7.73
		falling	P1	4.38	3.22	2.71	2.79	2.90	2.74
			N1	12.33	9.32	8.08	8.23	8.20	8.61
			P2	13.00	11.45	10.96	10.52	9.69	10.67
	STR	rising	P1	3.99	0.94	1.02	0.62	1.40	0.81
			N1	6.90	1.72	1.47	1.28	1.26	0.95
			P2	7.98	3.32	3.34	2.45	2.46	2.72
		falling	P1	2.50	0.78	0.58	0.80	0.67	1.12
			N1	5.72	1.04	1.23	1.32	1.06	1.14
			P2	7.38	2.31	3.45	2.88	3.17	3.16
<b>intermediate</b>	ACX	rising	P1	4.14	2.74	2.40	2.71	3.34	3.39
			N1	10.23	7.72	7.49	7.24	7.41	7.48
			P2	11.63	8.31	8.30	8.30	7.70	7.00
		falling	P1	3.57	2.72	2.63	1.72	2.27	2.66
			N1	10.59	7.63	7.96	7.08	7.83	7.16
			P2	11.75	10.09	10.49	10.37	9.46	8.73
	STR	rising	P1	2.67	1.04	0.76	0.79	1.41	1.25
			N1	5.78	1.71	1.96	1.66	1.69	2.09
			P2	8.09	3.63	3.13	2.54	2.79	3.07
		falling	P1	2.44	1.64	1.39	0.82	0.86	1.39
			N1	5.35	1.85	1.98	1.50	1.60	2.03
			P2	7.98	4.17	4.03	3.71	2.92	3.23
<b>long</b>	ACX	rising	P1	4.55	4.20	3.97	3.93	4.47	4.22
			N1	11.73	10.36	11.82	11.79	10.90	10.61
			P2	12.46	11.93	12.58	12.39	12.51	11.84
		falling	P1	4.55	4.20	3.97	3.93	4.47	4.22
			N1	11.73	10.36	11.82	11.79	10.90	10.61
			P2	12.46	11.93	12.58	12.39	12.51	11.84
	STR	rising	P1	3.44	2.27	2.27	2.99	2.89	2.58
			N1	6.42	5.13	5.80	6.13	5.74	5.88
			P2	8.39	7.19	7.26	7.41	6.45	7.83
		falling	P1	2.76	1.47	1.96	2.16	2.21	2.74
			N1	5.71	3.66	3.53	3.98	4.50	5.53
			P2	7.10	5.56	6.01	6.28	7.73	7.47

**Table 2: Average latencies split by the used test factors.**

ISI	area	FM	Component	Stimulus Position					
				1st	2nd	3rd	4th	5th	6th
<b>short</b>	ACX	rising	P1	33	26	26	27	28	26
			N1	85	82	88	75	81	80
			P2	217	227	227	215	224	213
		falling	P1	27	26	26	25	24	26
			N1	77	82	80	80	81	82
			P2	222	215	225	213	219	219
	STR	rising	P1	27	26	25	28	24	25
			N1	50	43	55	52	55	45
			P2	145	148	146	152	164	166
		falling	P1	27	22	18	17	20	29
			N1	53	41	54	54	37	57
			P2	143	147	157	149	151	153
<b>intermediate</b>	ACX	rising	P1	31	28	27	30	28	30
			N1	78	86	84	77	80	93
			P2	216	223	229	224	219	228
		falling	P1	33	27	26	26	28	28
			N1	76	83	78	78	80	85
			P2	216	207	224	214	212	220
	STR	rising	P1	29	26	27	26	29	29
			N1	49	46	47	46	48	47
			P2	147	136	152	151	149	136
		falling	P1	27	24	24	24	26	19
			N1	52	50	48	49	40	41
			P2	138	148	158	166	160	151
<b>long</b>	ACX	rising	P1	28	31	36	32	37	35
			N1	77	78	77	84	78	80
			P2	216	233	234	234	235	224
		falling	P1	28	31	33	34	33	36
			N1	77	81	84	83	85	88
			P2	228	226	223	211	230	227
	STR	rising	P1	29	28	28	27	31	31
			N1	48	51	48	51	52	53
			P2	157	153	151	134	145	164
		falling	P1	28	31	28	31	32	32
			N1	52	55	53	58	53	58
			P2	155	147	164	143	157	152

# Appendix B



**Table 3: Summary of model parameters from the exponential fits.** Given are the models' convergence properties, as well as the two parameters' estimates. Only the fit on the striatal evoked activity and both areas' induced activity in the 2-268 Hz range converged with both parameters. NA: not available.

Activity	Area	Frequency	Convergence	Residual standard error	Degrees of freedom	t0			$\tau$			
						estimate	t	p	estimate	t	p	
EA	ACX	all	F	<b>0.31</b>	<b>434</b>	<b>-1.36E+007</b>	<b>0.00</b>	<b>1.000</b>	<b>7.05E+006</b>	<b>0.00</b>	<b>1.000</b>	
		delta	T	0.61	434	-4.90	-0.48	0.633	2.32	0.58	0.564	
		theta	F	0.66	434	-1.11E+011	0.00	1.000	4.13E+010	0.00	1.000	
		alpha	F	1.25	434	-6.64E+010	0.00	1.000	2.62E+010	0.00	1.000	
		beta	F	0.69	434	-1.31E+013	0.00	1.000	6.83E+006	0.00	1.000	
		gamma	F	NA	434	0.49	NA	NA	-0.01	NA	NA	
		fast	T	0.32	434	-3.26	-1.28	0.201	1.92	1.67	0.097	
		<b>STR</b>	<b>all</b>	<b>T</b>	<b>0.35</b>	<b>434</b>	<b>-1.28</b>	<b>-2.80</b>	<b>0.005</b>	<b>2.73</b>	<b>5.25</b>	<b>0.000</b>
			delta	F	1.66	434	8.01	0.08	0.940	-0.92	-0.04	0.970
			theta	T	1.81	434	-0.76	-0.36	0.717	1.27	0.79	0.430
		alpha	T	1.34	434	0.10	0.24	0.809	0.82	1.78	0.076	
		beta	T	0.67	434	-1.51	-1.35	0.179	2.35	2.29	0.023	
		gamma	T	0.45	434	-9.15	-1.20	0.230	8.45	1.38	0.169	
		fast	T	0.31	434	-26.06	-0.51	0.611	12.37	0.54	0.592	
INDA	ACX	all	T	<b>0.17</b>	<b>434</b>	<b>-5.28</b>	<b>-2.68</b>	<b>0.008</b>	<b>3.15</b>	<b>3.24</b>	<b>0.001</b>	
		delta	T	0.29	434	-2.69	-1.45	0.149	1.67	1.96	0.051	
		theta	T	0.27	434	-4.73	-1.93	0.055	3.15	2.38	0.018	
		alpha	T	0.37	434	-2.67	-1.63	0.104	2.12	2.25	0.025	
		beta	T	0.32	434	-6.40	-1.42	0.158	3.20	1.67	0.095	
		gamma	F	0.25	434	-3.23E+008	0.00	1.000	1.05E+008	0.00	1.000	
		fast	T	0.25	434	-1.38	-1.36	0.174	0.95	2.17	0.031	
		<b>STR</b>	<b>all</b>	<b>T</b>	<b>0.19</b>	<b>434</b>	<b>-3.38</b>	<b>-2.22</b>	<b>0.027</b>	<b>2.01</b>	<b>2.87</b>	<b>0.004</b>
			delta	T	0.31	434	-0.77	-0.69	0.490	0.56	1.33	0.183
			theta	T	0.29	434	-1.85	-1.95	0.051	1.57	2.94	0.003
		alpha	T	0.40	434	-1.98	-1.33	0.186	1.56	1.95	0.052	
		beta	T	0.59	434	-1.57	-0.54	0.587	1.01	0.83	0.407	
		gamma	T	0.22	434	-4.48	-1.00	0.317	1.88	1.22	0.224	
		fast	T	0.17	434	-11.68	-0.83	0.407	4.09	0.91	0.361	

**Table 4: Estimated recovery times of evoked and induced activities.** Given are bootstrapped recovery times with 95% interquartile confidence intervals, when possible. Additionally recovery times calculated from the exponential fits are given with confidence intervals, when model confidence could be estimated. EA: evoked activity, INDA: induced activity, NA: not available.

Activity	Area	Frequency	Bootstrap analysis			Exponential fit		
			Estimate [s]	2.50%	97.50%	Estimate [s]	2.50%	97.50%
EA	ACX	all	2.01E+008	2.73	6.09E+011	2.60E+006	NA	NA
		delta	NA	NA	NA	0.43	NA	NA
		theta	-8.27E+000	-1.53E+011	1.64E+011	-1.60E+010	NA	NA
		alpha	-9.43E+008	-3.14E+012	1.33E+012	-6.00E+009	NA	NA
		beta	7.97E+007	-6.15E+005	5.83E+012	2.64E+006	NA	NA
	gamma	NA	NA	NA	0.47	NA	NA	
	fast	1.15	0.28	1.86	1.18	-17.16	19.06	
	STR	all	4.96	3.83	6.73	5.00	2.16	8.53
		delta	NA	NA	NA	5.89	NA	NA
		theta	NA	NA	NA	2.17	-43.68	42.30
alpha		NA	NA	NA	1.98	-1.26	6.82	
beta		3.99	1.97	9.21	3.89	-5.49	17.98	
ACX	ACX	gamma	9.87	5.06	2.18E+007	10.30	NA	NA
		fast	2.45	-16.58	1.98E+010	2.43	NA	NA
		all	1.95	1.48	2.78	1.98	-7.28	11.60
		delta	1.16	0.69	1.73	1.15	-6.60	8.74
		theta	2.51	1.65	4.94	2.51	-11.70	18.17
	alpha	2.27	1.34	3.97	2.22	-7.85	13.56	
	beta	2.55	1.57	8.40	2.62	-85.83	104.69	
	gamma	-3.27E+006	-4.22E+011	-0.47	-8.20E+007	NA	NA	
	fast	0.81	0.22	1.07	0.81	-3.95	5.28	
	INDA	STR	all	1.24	0.93	1.72	1.25	-5.34
delta			NA	NA	NA	0.53	-4.10	4.19
theta			1.75	1.31	2.53	1.76	-2.78	6.63
alpha			1.63	1.08	2.65	1.61	-6.50	10.23
beta			NA	NA	NA	0.74	NA	NA
gamma		-0.16	-3.12	0.57	-0.16	-36.01	27.52	
fast		-2.09	-3.77E+010	0.44	-2.26	NA	NA	

**Table 5: Repeated-measure ANOVA on between-area phase-locking during the 0.5 s ISI testing for FREQUENCY band influences, STIMULUS PRESENCE and POSITION effects.**

<b>Effect</b>	<b>Df</b>	<b>F</b>	<b>ε</b>	<b>p</b>
FREQUENCY	(1.991, 27.869)	0.36	0.498	0.697
STIMULUS POSITION	(1,14)	0.05	-	0.833
STIMULUS PRESENCE	(1, 14)	7.01	-	0.019
FREQUENCY x STIMULUS POSITION	(2.171, 30.390)	5.08	0.543	0.011
FREQUENCY x STIMULUS PRESENCE	(2.440, 34.160)	4.22	0.610	0.017
STIMULUS POSITION x STIMULUS PRESENCE	(1, 14)	0.65	-	0.434
FREQUENCY x STIMULUS POSITION x STIMULUS PRESENCE	(4, 56)	1.82	-	0.137

**Table 6: Repeated-measure ANOVA on between-area phase-locking during the 1.2 s ISI testing for FREQUENCY band influences, STIMULUS PRESENCE and POSITION effects.**

<b>Effect</b>	<b>Df</b>	<b>F</b>	<b>ε</b>	<b>p</b>
FREQUENCY	(2.294, 32.122)	0.94	0.574	0.412
STIMULUS POSITION	(1,14)	2.16	-	0.164
STIMULUS PRESENCE	(1, 14)	3.08	-	0.101
FREQUENCY x STIMULUS POSITION	(2.450, 34.306)	0.48	0.613	0.661
FREQUENCY x STIMULUS PRESENCE	(1.882, 26.343)	2.82	0.470	0.080
STIMULUS POSITION x STIMULUS PRESENCE	(1, 14)	0.02	-	0.903
FREQUENCY x STIMULUS POSITION x STIMULUS PRESENCE	(4, 56)	1.18	-	0.332

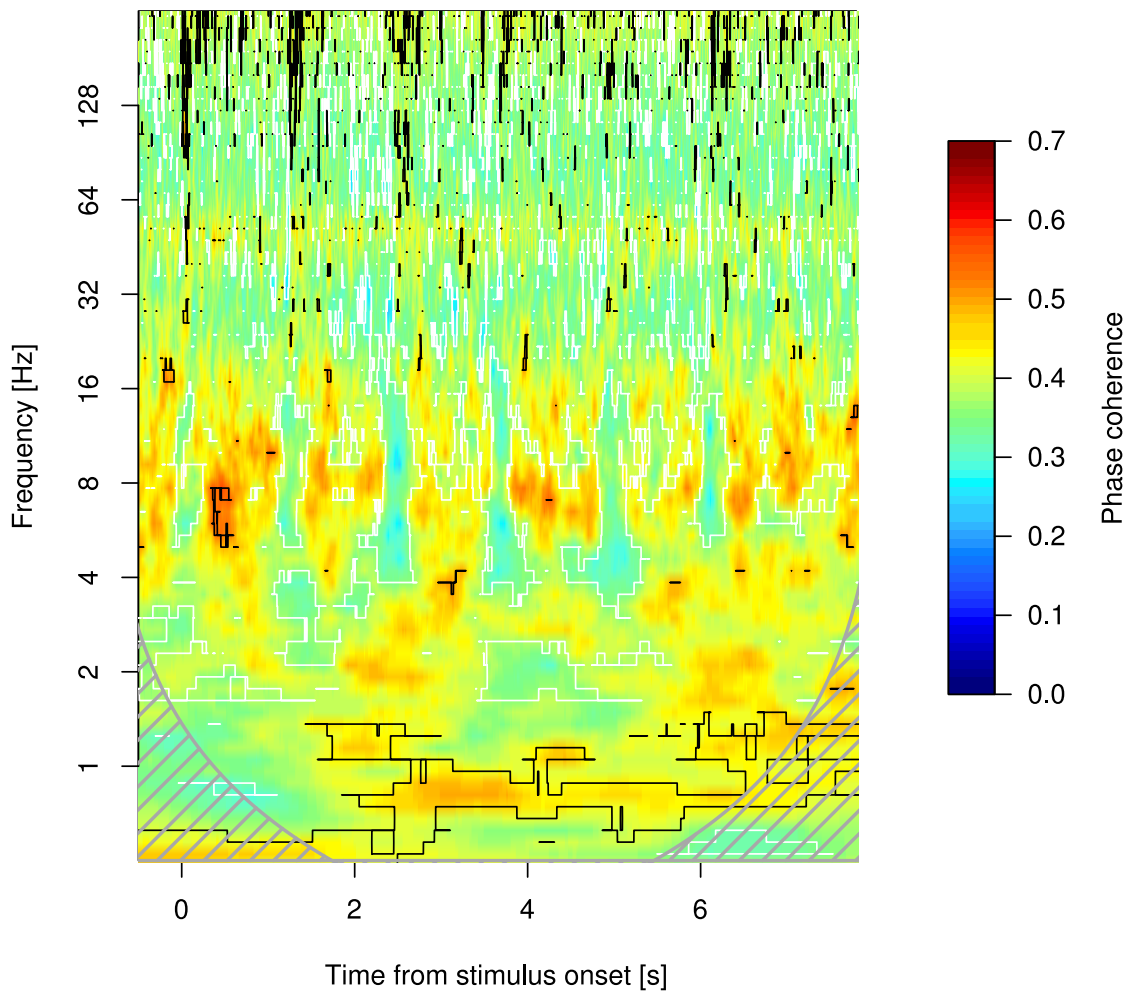


**Figure 2: Stimulation with with FM tones and a longer interstimulus interval (ISI) resulted in diminished phase synchrony between auditory cortex and ventral striatum, as well.** Time-points of stimulation (0, 1.2, ..., 7 s) corresponded to significantly lower phase-locking index (PLI) values in the theta, alpha and lower beta band compared to baseline. Displayed is the average PLI over all animals. Areas with black or white contours respectively indicate regions with significantly higher or lower PLI values as compared to baseline ( $p = 0.05$ ). Areas outside the wavelet-transform cone of influence are shaded in gray.

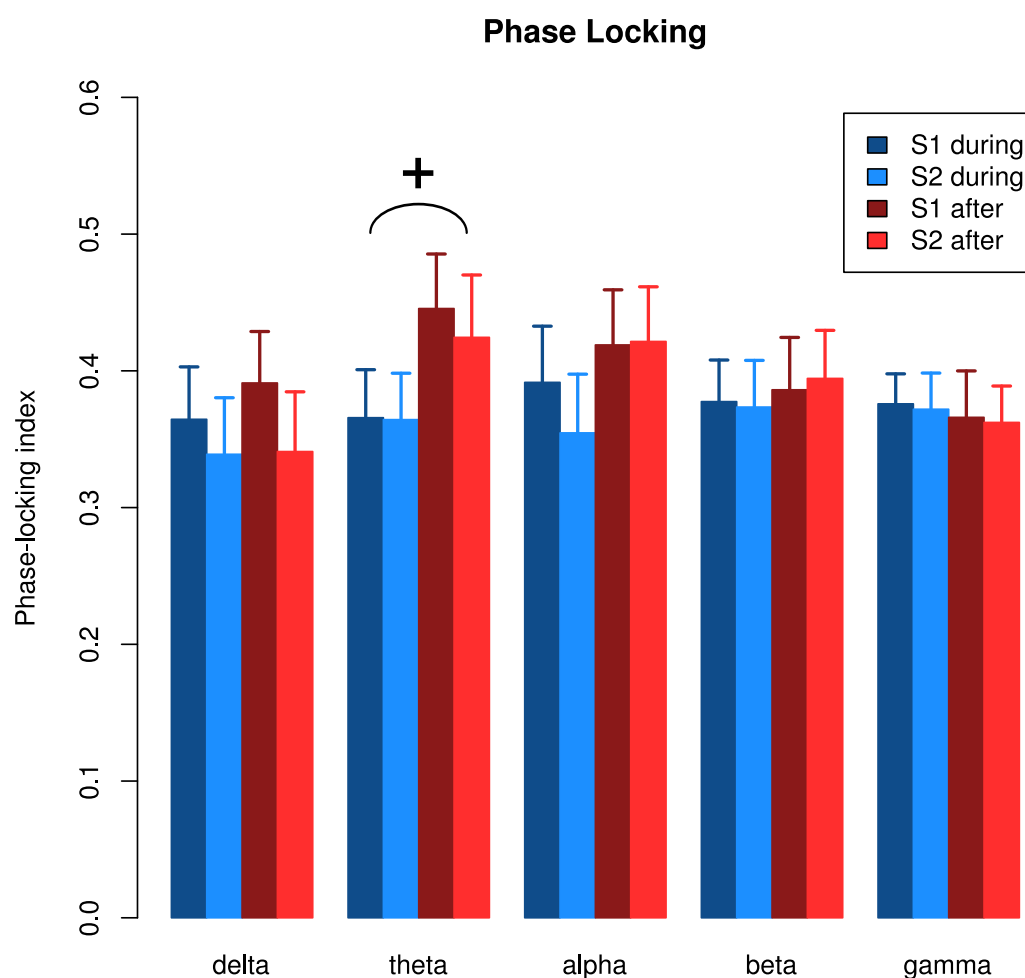


**Figure 3: Phase-locking between the cortex and striatum was significantly decreased during tone presence only in the theta band for the longer ISI stimulation.** Blue colored bars display phase-coherence during frequency-modulated (FM) tone presence and red colored bars in the absence of FM tones (offset-to-onset time). +: main effect comparing presence and absence of FM stimuli,  $p = 0.007$ . S1: first stimulus, S2: second stimulus. Data are means + SE.

**Table 7: Repeated-measure ANOVA for STIMULUS PRESENCE and POSITION effects on between-area phase-locking during the 1.2 s ISI.**

<b>Frequency range</b>	<b>Effect</b>	<b>df</b>	<b>F</b>	<b>p</b>
<b>delta</b>	STIMULUS PRESENCE	(1, 14)	2.07	0.172
	STIMULUS POSITION	(1, 14)	1.68	0.216
	STIMULUS PRESENCE x POSITION	(1, 14)	2.05	0.175
<b>theta</b>	STIMULUS PRESENCE	(1, 14)	9.90	0.007
	STIMULUS POSITION	(1, 14)	0.13	0.724
	STIMULUS PRESENCE x POSITION	(1, 14)	0.79	0.389
<b>alpha</b>	STIMULUS PRESENCE	(1, 14)	1.39	0.258
	STIMULUS POSITION	(1, 14)	0.87	0.366
	STIMULUS PRESENCE x POSITION	(1, 14)	1.71	0.212
<b>beta</b>	STIMULUS PRESENCE	(1, 14)	0.80	0.387
	STIMULUS POSITION	(1, 14)	0.02	0.879
	STIMULUS PRESENCE x POSITION	(1, 14)	0.16	0.695
<b>gamma</b>	STIMULUS PRESENCE	(1, 14)	0.70	0.418
	STIMULUS POSITION	(1, 14)	0.35	0.563
	STIMULUS PRESENCE x POSITION	(1, 14)	0.00	0.992

# Appendix C

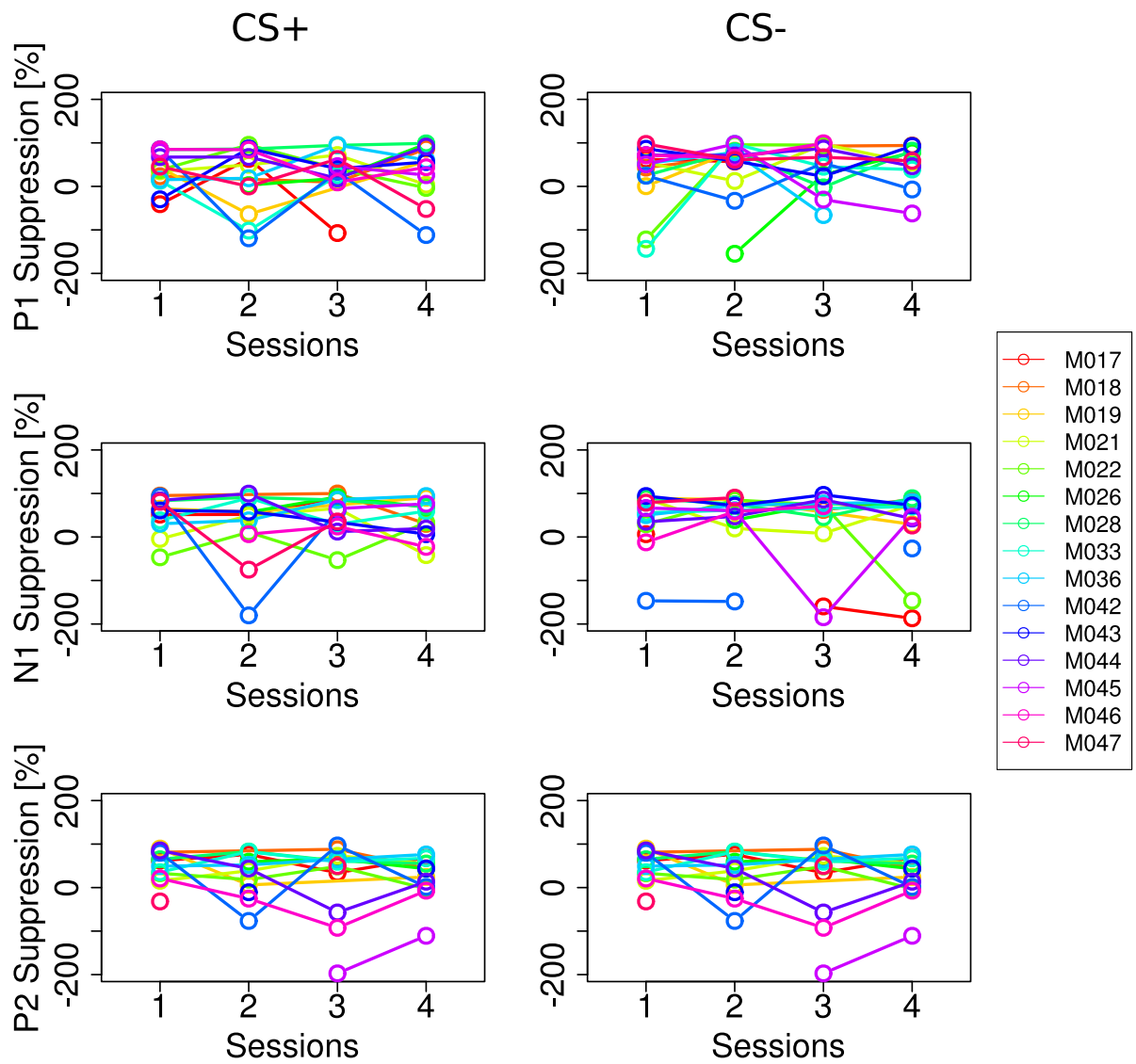


**Figure 4: Individual suppression scores for the CS+ and CS- during discrimination training in the ventral striatum.**



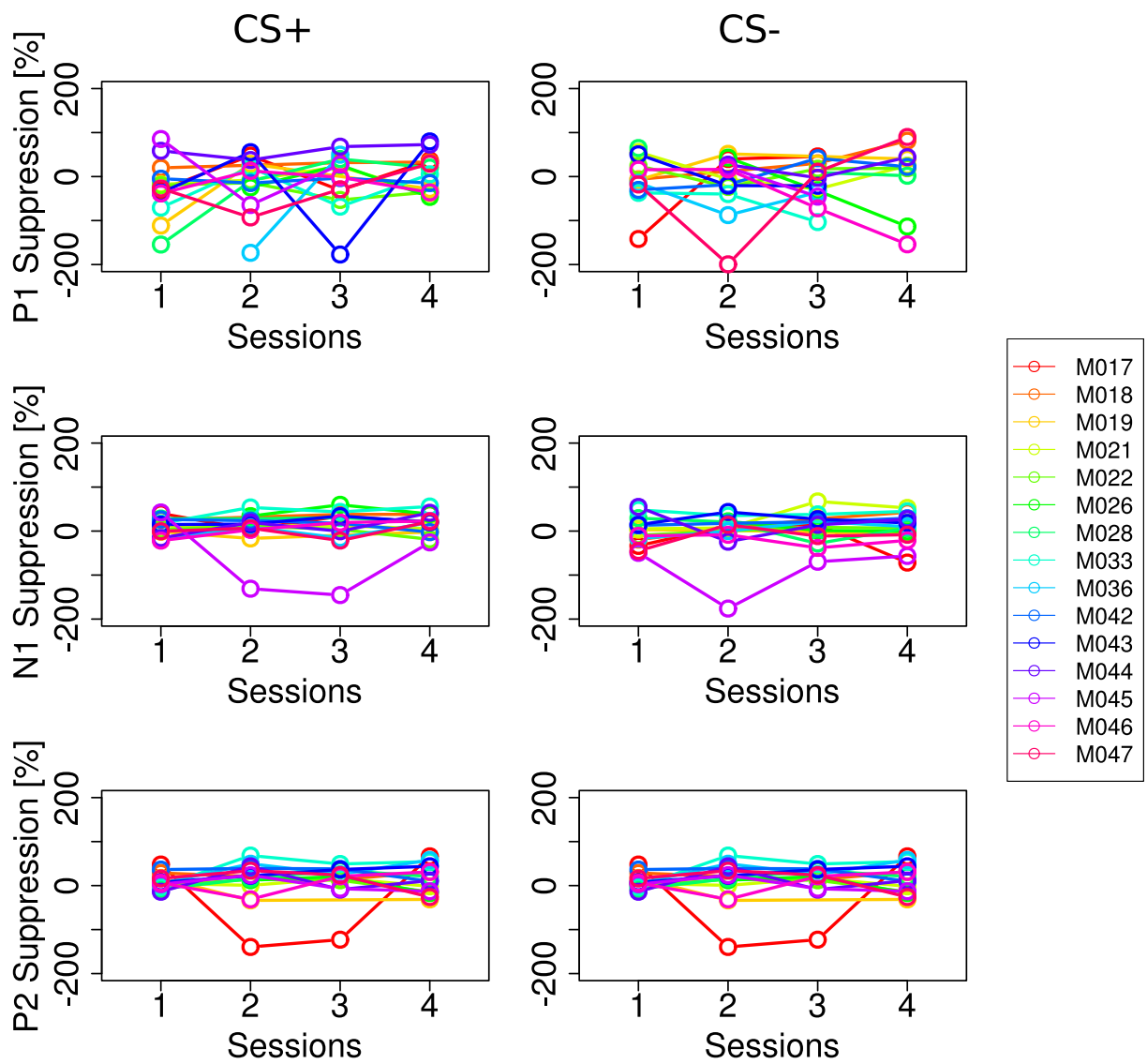


**Figure 5: Individual suppression scores for the CS+ and CS- during discrimination training in the auditory cortex.**

## References

- Adams, S., Kesner, R.P. & Ragozzino, M.E. (2001). Role of the medial and lateral caudate-putamen in mediating an auditory conditional response association. *Neurobiology of learning and memory*, **76**, 106–16. [65](#)
- Adler, L.E., Waldo, M.C. & Freedman, R. (1985). Neurophysiologic studies of sensory gating in schizophrenia: comparison of auditory and visual responses. *Biological psychiatry*, **20**, 1284–96. [3](#), [4](#)
- Adler, L.E., Rose, G. & Freedman, R. (1986). Neurophysiological studies of sensory gating in rats: effects of amphetamine, phencyclidine, and haloperidol. *Biological psychiatry*, **21**, 787–98. [4](#), [5](#), [8](#)
- Adler, L.E., Olincy, A., Waldo, M., Harris, J.G., Griffith, J., Stevens, K., Flach, K., Nagamoto, H., Bickford, P., Leonard, S. & Freedman, R. (1998). Schizophrenia, sensory gating, and nicotinic receptors. *Schizophrenia bulletin*, **24**, 189–202. [5](#)
- Alexander, G.E., DeLong, M.R. & Strick, P.L. (1986). Parallel organization of functionally segregated circuits linking basal ganglia and cortex. *Annual review of neuroscience*, **9**, 357–81. [2](#)
- Anonymous (1985). Schizophrenia – A mother’s agony over her son’s pain. *Chicago Tribune*, 5:1–3. [1](#)
- Antunes, R. & Moita, M.A. (2010). Discriminative auditory fear learning requires both tuned and nontuned auditory pathways to the amygdala. *The*

*Journal of neuroscience: the official journal of the Society for Neuroscience*, **30**, 9782–7. [65](#)

Arnfred, S.M., Eder, D.N., Hemmingsen, R.P., Glenthøj, B.Y. & Chen, A.C. (2001). Gating of the vertex somatosensory and auditory evoked potential P50 and the correlation to skin conductance orienting response in healthy men. *Psychiatry research*, **101**, 221–35. [3](#)

Ashby, F.G., Turner, B.O. & Horvitz, J.C. (2010). Cortical and basal ganglia contributions to habit learning and automaticity. *Trends in cognitive sciences*, **14**, 208–15. [65](#)

Barth, D. & Di, S. (1990). Three-dimensional analysis of auditory-evoked potentials in rat neocortex. *Journal of neurophysiology*, **64**. [29](#), [31](#)

Bickford, P.C., Luntz-Leybman, V. & Freedman, R. (1993). Auditory sensory gating in the rat hippocampus: modulation by brainstem activity. *Brain research*, **607**, 33–8. [29](#)

Bickford-Wimer, P.C., Nagamoto, H., Johnson, R., Adler, L.E., Egan, M., Rose, G.M. & Freedman, R. (1990). Auditory sensory gating in hippocampal neurons: a model system in the rat. *Biological psychiatry*, **27**, 183–92. [6](#), [7](#), [30](#)

Blumenfeld, L.D. & Clementz, B.A. (2001). Response to the first stimulus determines reduced auditory evoked response suppression in schizophrenia: single trials analysis using MEG. *Clinical neurophysiology: official journal of the International Federation of Clinical Neurophysiology*, **112**, 1650–9. [35](#)

Boutros, N.N. & Belger, A. (1999). Midlatency evoked potentials attenuation and augmentation reflect different aspects of sensory gating. *Biological psychiatry*, **45**, 917–22. [4](#), [30](#), [31](#), [61](#)

Boutros, N.N., Bonnet, K.A., Millana, R. & Liu, J. (1997). A parametric study of the N40 auditory evoked response in rats. *Biological psychiatry*, **42**, 1051–9. [4](#), [7](#), [30](#), [32](#)

- Boutros, N.N., Belger, A., Campbell, D., D'Souza, C. & Krystal, J. (1999). Comparison of four components of sensory gating in schizophrenia and normal subjects: a preliminary report. *Psychiatry research*, **88**, 119–30. [32](#)
- Boutros, N.N., Gjini, K., Urbach, H. & Pflieger, M.E. (2011). Mapping repetition suppression of the N100 evoked response to the human cerebral cortex. *Biological psychiatry*, **69**, 883–9. [31](#)
- Brankack, J. & Buzsáki, G. (1986). Hippocampal responses evoked by tooth pulp and acoustic stimulation: depth profiles and effect of behavior. *Brain research*, **378**, 303–14. [30](#)
- Brenner, C.A., Kieffaber, P.D., Clementz, B.A., Johannesen, J.K., Shekhar, A., O'Donnell, B.F. & Hetrick, W.P. (2009). Event-related potential abnormalities in schizophrenia: a failure to "gate in" salient information? *Schizophrenia research*, **113**, 332–8. [30](#), [38](#), [57](#)
- Brockhaus-Dumke, A., Mueller, R., Faigle, U. & Klosterkoetter, J. (2008). Sensory gating revisited: relation between brain oscillations and auditory evoked potentials in schizophrenia. *Schizophrenia research*, **99**, 238–49. [36](#), [55](#), [57](#)
- Brosch, M. & Schreiner, C. (1997). Time course of forward masking tuning curves in cat primary auditory cortex. *Journal of Neurophysiology*, 923–943. [6](#)
- Brosch, M., Schulz, A. & Scheich, H. (1999). Processing of sound sequences in macaque auditory cortex: response enhancement. *Journal of Neurophysiology*, 1542–1559. [6](#)
- Brumback, C., Low, K., Gratton, G. & Fabiani, M. (2004). Sensory ERPs predict differences in working memory span and fluid intelligence. *NeuroReport*, **15**, 373–376. [62](#)
- Budd, T.W. & Michie, P.T. (1994). Facilitation of the N1 peak of the auditory ERP at short stimulus intervals. *Neuroreport*, **5**, 2513–6. [8](#)

- Budd, T.W., Barry, R.J., Gordon, E., Rennie, C. & Michie, P.T. (1998). Decrement of the N1 auditory event-related potential with stimulus repetition: habituation vs. refractoriness. *International journal of psychophysiology: official journal of the International Organization of Psychophysiology*, **31**, 51–68. [8](#)
- Budd, T.W., Nakamura, T., Fulham, W.R., Todd, J., Schall, U., Hunter, M., Hodgson, D.M. & Michie, P.T. (2012). Repetition suppression of the rat auditory evoked potential at brief stimulus intervals. *Brain research*, **1498**, 59–68. [8](#), [10](#), [83](#)
- Cadenhead, K.S., Light, G.A., Geyer, M.A. & Braff, D.L. (2000). Sensory gating deficits assessed by the P50 event-related potential in subjects with schizotypal personality disorder. *The American journal of psychiatry*, **157**, 55–9. [5](#)
- Cain, C. & LeDoux, J. (2008). Brain mechanisms of Pavlovian and instrumental aversive conditioning. *Handbook of Behavioral Neuroscience*, **17**, 103–124. [64](#)
- Cain, C., Choi, J. & LeDoux, J. (2010). Active avoidance and escape learning. In G.F. Koob, M. Le Moal & R.F. Thompson, eds., *Encyclopedia of Behavioral Neuroscience*, 1–9, Academic Press, Oxford. [83](#)
- Cowan, N. (1984). On short and long auditory stores. *Psychological bulletin*. [58](#), [59](#)
- Cromwell, H.C. & Woodward, D.J. (2007). Inhibitory gating of single unit activity in amygdala: effects of ketamine, haloperidol, or nicotine. *Biological psychiatry*, **61**, 880–9. [6](#)
- Cromwell, H.C., Anstrom, K., Azarov, A. & Woodward, D.J. (2005). Auditory inhibitory gating in the amygdala: single-unit analysis in the behaving rat. *Brain research*, **1043**, 12–23. [6](#)

- Cromwell, H.C., Klein, a. & Mears, R.P. (2007). Single unit and population responses during inhibitory gating of striatal activity in freely moving rats. *Neuroscience*, **146**, 69–85. [6](#), [9](#), [63](#), [83](#)
- Cromwell, H.C., Mears, R.P., Wan, L. & Boutros, N.N. (2008). Sensory gating: a translational effort from basic to clinical science. *Clinical EEG and neuroscience: official journal of the EEG and Clinical Neuroscience Society (ENCS)*, **39**, 69–72. [4](#), [6](#)
- Dafny, N. (1975). Selective field potential changes induced by L-DOPA. *Experimental neurology*, **49**, 189–202. [33](#)
- Dafny, N. & Gilman, S. (1973). L-DOPA and reserpine: effects on evoked potentials in basal ganglia of freely moving rats. *Brain research*, **50**, 187–91. [6](#)
- Dafny, N. & Gilman, S. (1974). Monoamine effects on neuronal recovery cycles in globus pallidus, caudate nucleus, and substantia nigra. *Journal of neural transmission*, **35**, 275–81. [6](#), [33](#)
- Darvas, M., Fadok, J.P. & Palmiter, R.D. (2011). Requirement of dopamine signaling in the amygdala and striatum for learning and maintenance of a conditioned avoidance response. *Learning & memory (Cold Spring Harbor, N.Y.)*, **18**, 136–43. [65](#)
- de Bruin, N.M., Ellenbroek, B.A., van Schaijk, W.J., Cools, A.R., Coenen, A.M. & van Luijtelaar, E.L. (2001). Sensory gating of auditory evoked potentials in rats: effects of repetitive stimulation and the interstimulus interval. *Biological psychology*, **55**, 195–213. [8](#), [33](#)
- Delgado, M.R., Li, J., Schiller, D. & Phelps, E.A. (2008). The role of the striatum in aversive learning and aversive prediction errors. *Philosophical transactions of the Royal Society of London. Series B, Biological sciences*, **363**, 3787–800. [65](#), [66](#)
- Ellenbroek, B.A., de Bruin, N.M.W.J., van Den Kroonenburg, P.T.J.M., van Luijtelaar, E.L.J.M. & Cools, A.R. (2004). The effects of early maternal

- deprivation on auditory information processing in adult Wistar rats. *Biological psychiatry*, **55**, 701–7. [63](#)
- English, D.F., Ibanez-Sandoval, O., Stark, E., Tecuapetla, F., Buzsáki, G., Deisseroth, K., Tepper, J.M. & Koos, T. (2012). GABAergic circuits mediate the reinforcement-related signals of striatal cholinergic interneurons. *Nature neuroscience*, **15**, 123–30. [87](#)
- Freedman, R., Waldo, M., Bickford-Wimer, P. & Nagamoto, H. (1991). Elementary neuronal dysfunctions in schizophrenia. *Schizophrenia research*, **4**, 233–43. [3](#)
- Fries, P. (2005). A mechanism for cognitive dynamics: neuronal communication through neuronal coherence. *Trends in cognitive sciences*, **9**, 474–80. [38](#)
- Fuerst, D.R., Gallinat, J. & Boutros, N.N. (2007). Range of sensory gating values and test-retest reliability in normal subjects. *Psychophysiology*, **44**, 620–6. [4](#)
- Galiñanes, G.L., Braz, B.Y. & Murer, M.G. (2011). Origin and properties of striatal local field potential responses to cortical stimulation: temporal regulation by fast inhibitory connections. *PloS one*, **6**, e28473. [57](#)
- Gallistel, C.R., Fairhurst, S. & Balsam, P. (2004). The learning curve: implications of a quantitative analysis. *Proceedings of the National Academy of Sciences of the United States of America*, **101**, 13124–31. [83](#)
- Gjini, K., Burroughs, S. & Boutros, N. (2011). Relevance of Attention in Auditory Sensory Gating Paradigms in Schizophrenia. *Journal of psychophysiology*, **25**, 60–66. [31](#)
- Goto, Y. & Grace, A.A. (2008). Limbic and cortical information processing in the nucleus accumbens. *Trends in neurosciences*, **31**, 552–8. [7](#)
- Grace, A.A. (2000). Gating of information flow within the limbic system and the pathophysiology of schizophrenia. *Brain research. Brain research reviews*, **31**, 330–41. [7](#)

- Grinsted, A., Moore, J.C. & Jevrejeva, S. (2004). Application of the cross wavelet transform and wavelet coherence to geophysical time series. *Nonlinear Processes in Geophysics*, **11**, 561–566. [40](#)
- Gruber, A.J. & McDonald, R.J. (2012). Context, emotion, and the strategic pursuit of goals: interactions among multiple brain systems controlling motivated behavior. *Frontiers in behavioral neuroscience*, **6**, 50. [2](#)
- Gruber, A.J., Hussain, R.J. & O'Donnell, P. (2009). The nucleus accumbens: a switchboard for goal-directed behaviors. *PloS one*, **4**, e5062. [7](#)
- Grunwald, T., Boutros, N.N., Pezer, N., von Oertzen, J., Fernández, G., Schaller, C. & Elger, C.E. (2003). Neuronal substrates of sensory gating within the human brain. *Biological psychiatry*, **53**, 511–9. [30](#)
- Guterman, Y. & Josiassen, R.C. (1994). Sensory gating deviance in schizophrenia in the context of task related effects. *International journal of psychophysiology: official journal of the International Organization of Psychophysiology*, **18**, 1–12. [62](#)
- Guterman, Y., Josiassen, R. & Bashore, T. (1992). Attentional influence on the P50 component of the auditory event-related brain potential. *International Journal of psychophysiology: the official journal of the International Organization of Psychophysiology*, **12**, 197–209. [62](#)
- Haenschel, C., Baldeweg, T., Croft, R.J., Whittington, M. & Gruzelier, J. (2000). Gamma and beta frequency oscillations in response to novel auditory stimuli: A comparison of human electroencephalogram (EEG) data with in vitro models. *Proceedings of the National Academy of Sciences of the United States of America*, **97**, 7645–50. [85](#)
- Happel, M.F.K., Jeschke, M. & Ohl, F.W. (2010). Spectral integration in primary auditory cortex attributable to temporally precise convergence of thalamocortical and intracortical input. *The Journal of neuroscience: the official journal of the Society for Neuroscience*, **30**, 11114–27. [29](#)



- Herrmann, C.S., Grigutsch, M. & Busch, N.A. (2005). EEG oscillations and wavelet analysis. In T.C. Handy, ed., *Event-related potentials: a methods handbook.*, chap. 11, 229–259, MIT Press, Cambridge, MA. [38](#), [41](#)
- Hong, L.E., Buchanan, R.W., Thaker, G.K., Shepard, P.D. & Summerfelt, A. (2008). Beta (~16 Hz) frequency neural oscillations mediate auditory sensory gating in humans. *Psychophysiology*, **45**, 197–204. [37](#), [38](#), [55](#), [58](#)
- Hong, L.E., Summerfelt, A., Mitchell, B.D., O'Donnell, P. & Thaker, G.K. (2012). A shared low-frequency oscillatory rhythm abnormality in resting and sensory gating in schizophrenia. *Clinical neurophysiology: official journal of the International Federation of Clinical Neurophysiology*, **123**, 285–92. [37](#)
- Horvitz, J.C. (2002). Dopamine gating of glutamatergic sensorimotor and incentive motivational input signals to the striatum. *Behavioural brain research*, **137**, 65–74. [2](#)
- Hsieh, M.H., Liu, K., Liu, S.K., Chiu, M.J., Hwu, H.G. & Chen, A.C. (2004). Memory impairment and auditory evoked potential gating deficit in schizophrenia. *Psychiatry research neuroimaging*, **130**, 161–169. [62](#)
- Hu, B. (2003). Functional organization of lemniscal and nonlemniscal auditory thalamus. *Experimental brain research. Experimentelle Hirnforschung. Expérimentation cérébrale*, **153**, 543–9. [29](#)
- Hu, L., Boutros, N.N. & Jansen, B.H. (2009). Evoked potential variability. *Journal of neuroscience methods*, **178**, 228–36. [36](#), [88](#)
- Jansen, B.H., Agarwal, G., Hegde, A. & Boutros, N.N. (2003). Phase synchronization of the ongoing EEG and auditory EP generation. *Clinical neurophysiology: official journal of the International Federation of Clinical Neurophysiology*, **114**, 79–85. [36](#), [57](#), [58](#)
- Jansen, B.H., Hegde, A. & Boutros, N.N. (2004). Contribution of different EEG frequencies to auditory evoked potential abnormalities in schizophrenia.

*Clinical neurophysiology: official journal of the International Federation of Clinical Neurophysiology*, **115**, 523–33. [36](#), [57](#)

Jansen, B.H., Hu, L. & Boutros, N.N. (2010). Auditory evoked potential variability in healthy and schizophrenia subjects. *Clinical neurophysiology: official journal of the International Federation of Clinical Neurophysiology*, **121**, 1233–9. [36](#), [88](#)

Javitt, D.C., Jayachandra, M., Lindsley, R.W., Specht, C.M. & Schroeder, C.E. (2000). Schizophrenia-like deficits in auditory P1 and N1 refractoriness induced by the psychomimetic agent phencyclidine (PCP). *Clinical neurophysiology: official journal of the International Federation of Clinical Neurophysiology*, **111**, 833–6. [8](#)

Jensen, O. & Mazaheri, A. (2010). Shaping functional architecture by oscillatory alpha activity: gating by inhibition. *Frontiers in human neuroscience*, **4**, 186. [84](#)

Jerger, K., Biggins, C. & Fein, G. (1992). P50 suppression is not affected by attentional manipulations. *Biological psychiatry*, **31**, 365–77. [62](#), [82](#), [83](#)

Jeschke, M., Lenz, D., Budinger, E., Herrmann, C.S. & Ohl, F.W. (2008). Gamma oscillations in gerbil auditory cortex during a target-discrimination task reflect matches with short-term memory. *Brain research*, **1220**, 70–80. [85](#)

Jessen, F., Kucharski, C., Fries, T., Papassotiropoulos, A., Hoenig, K., Maier, W. & Heun, R. (2001). Sensory gating deficit expressed by a disturbed suppression of the P50 event-related potential in patients with Alzheimer's disease. *The American journal of psychiatry*, **158**, 1319–21. [5](#)

Jin, Y., Potkin, S.G., Patterson, J.V., Sandman, C.A., Hetrick, W.P. & Bunney, W.E. (1997). Effects of P50 temporal variability on sensory gating in schizophrenia. *Psychiatry research*, **70**, 71–81. [35](#), [36](#), [57](#)

Johnson, M.R. & Adler, L.E. (1993). Transient impairment in P50 auditory sensory gating induced by a cold-pressor test. *Biological psychiatry*, **33**, 380–7. [63](#), [67](#)

- Kalcher, J. & Pfurtscheller, G. (1995). Discrimination between phase-locked and non-phase-locked event-related EEG activity. *Electroencephalography and clinical neurophysiology*, **94**, 381–4. [38](#)
- Kim, H., Shimojo, S. & O’Doherty, J.P. (2006). Is avoiding an aversive outcome rewarding? Neural substrates of avoidance learning in the human brain. *PLoS biology*, **4**, e233. [65](#)
- Kisley, M.A. & Cornwell, Z.M. (2006). Gamma and beta neural activity evoked during a sensory gating paradigm: effects of auditory, somatosensory and cross-modal stimulation. *Clinical neurophysiology: official journal of the International Federation of Clinical Neurophysiology*, **117**, 2549–63. [37](#), [57](#), [58](#)
- Klimesch, W., Russeger, H., Doppelmayr, M. & Pachinger, T. (1998). A method for the calculation of induced band power: implications for the significance of brain oscillations. *Electroencephalography and clinical neurophysiology*, **108**, 123–30. [38](#)
- Knight, R.T., Staines, W.R., Swick, D. & Chao, L.L. (1999). Prefrontal cortex regulates inhibition and excitation in distributed neural networks. *Acta psychologica*, **101**, 159–78. [30](#)
- Knott, V., Millar, A. & Fisher, D. (2009). Sensory gating and source analysis of the auditory P50 in low and high suppressors. *NeuroImage*, **44**, 992–1000. [30](#)
- Kobayasi, K.I. & Riquimaroux, H. (2012). Classification of vocalizations in the Mongolian gerbil, *Meriones unguiculatus*. *The Journal of the Acoustical Society of America*, **131**, 1622–31. [28](#), [29](#)
- Koch, M. & Schnitzler, H.U. (1997). The acoustic startle response in rats—circuits mediating evocation, inhibition and potentiation. *Behavioural brain research*, **89**, 35–49. [29](#)
- Korzyukov, O., Pflieger, M.E., Wagner, M., Bowyer, S.M., Rosburg, T., Sundaresan, K., Elger, C.E. & Boutros, N.N. (2007). Generators of the

- intracranial P50 response in auditory sensory gating. *NeuroImage*, **35**, 814–26. [6, 30](#)
- Kraus, M., Schicknick, H., Wetzels, W., Ohl, F.W., Staak, S. & Tischmeyer, W. (2002). Memory consolidation for the discrimination of frequency-modulated tones in mongolian gerbils is sensitive to protein-synthesis inhibitors applied to the auditory cortex. *Learning & memory (Cold Spring Harbor, N.Y.)*, **9**, 293–303. [65](#)
- Kraus, N., Smith, D.I., McGee, T., Stein, L. & Cartee, C. (1987). Development of the middle latency response in an animal model and its relation to the human response. *Hearing research*, **27**, 165–76. [29](#)
- Krause, M., Hoffmann, W.E. & Hajós, M. (2003). Auditory sensory gating in hippocampus and reticular thalamic neurons in anesthetized rats. *Biological Psychiatry*, **53**, 244–253. [7](#)
- Lavie, N., Hirst, A., de Fockert, J.W. & Viding, E. (2004). Load theory of selective attention and cognitive control. *Journal of experimental psychology. General*, **133**, 339–54. [82](#)
- LeDoux, J. (2000). Emotion circuits in the brain. *Annual review of neuroscience*, 155–184. [29](#)
- Lijffijt, M., Lane, S. & Meier, S. (2009). P50, N100, and P200 sensory gating: relationships with behavioral inhibition, attention, and working memory. *Psychophysiology*, **46**, 1–20. [62](#)
- Loskota, W., Lomax, P. & Verity, M. (1974). *A stereotaxic atlas of the Mongolian gerbil (Meriones unguiculatus) brain*. Ann Arbor Science Publishers, Michigan. [12](#)
- Lu, Z.L., Williamson, S.J. & Kaufman, L. (1992). Behavioral lifetime of human auditory sensory memory predicted by physiological measures. *Science (New York, N.Y.)*, **258**, 1668–70. [58](#)

- Luntz-Leybman, V., Bickford, P.C. & Freedman, R. (1992). Cholinergic gating of response to auditory stimuli in rat hippocampus. *Brain research*, **587**, 130–6. [6](#)
- Mathiak, K., Ackermann, H., Rapp, A., Mathiak, K.A., Shergill, S., Riecker, A. & Kircher, T.T.J. (2011). Neuromagnetic oscillations and hemodynamic correlates of P50 suppression in schizophrenia. *Psychiatry research*, **194**, 95–104. [30](#)
- Matsumoto, N., Minamimoto, T., Graybiel, A.M. & Kimura, M. (2001). Neurons in the thalamic CM-Pf complex supply striatal neurons with information about behaviorally significant sensory events. *Journal of neurophysiology*, **85**, 960–76. [87](#)
- Mayer, A.R., Hanlon, F.M., Franco, A.R., Teshiba, T.M., Thoma, R.J., Clark, V.P. & Canive, J.M. (2009). The neural networks underlying auditory sensory gating. *NeuroImage*, **44**, 182–9. [30](#)
- McGee, T., Kraus, N., Comperatore, C. & Nicol, T. (1991). Subcortical and cortical components of the MLR generating system. *Brain research*, **544**, 211–20. [29](#)
- McHaffie, J.G., Stanford, T.R., Stein, B.E., Coizet, V. & Redgrave, P. (2005). Subcortical loops through the basal ganglia. *Trends in neurosciences*, **28**, 401–7. [29](#)
- Mears, R.P., Klein, A.C. & Cromwell, H.C. (2006). Auditory inhibitory gating in medial prefrontal cortex: Single unit and local field potential analysis. *Neuroscience*, **141**, 47–65. [6](#), [30](#)
- Mears, R.P., Boutros, N.N. & Cromwell, H.C. (2009). Reduction of prelimbic inhibitory gating of auditory evoked potentials after fear conditioning. *Behavioral neuroscience*, **123**, 315–27. [14](#), [30](#), [63](#), [83](#), [85](#)
- Moran, L.V. & Hong, L.E. (2011). High vs low frequency neural oscillations in schizophrenia. *Schizophrenia bulletin*, **37**, 659–63. [37](#), [58](#)

- Moran, Z.D., Williams, T.J., Bachman, P., Nuechterlein, K.H., Subotnik, K.L. & Yee, C.M. (2012). Spectral decomposition of P50 suppression in schizophrenia during concurrent visual processing. *Schizophrenia research*, **140**, 237–42. [37](#)
- Mormann, F., Lehnertz, K., David, P. & Elger, C. (2000). Mean phase coherence as a measure for phase synchronization and its application to the EEG of epilepsy patients. *Physica D: Nonlinear Phenomena*, **144**, 358–369. [51](#)
- Moura, G.S., Triñanes Pego, Y. & Carrillo-de-la Peña, M.T. (2010). Effects of stimuli intensity and frequency on auditory p50 and n100 sensory gating. *Advances in experimental medicine and biology*, **657**, 5–17. [30](#)
- Moxon, K.A., Gerhardt, G.A., Bickford, P.C., Austin, K., Rose, G.M., Woodward, D.J. & Adler, L.E. (1999). Multiple single units and population responses during inhibitory gating of hippocampal auditory response in freely-moving rats. *Brain research*, **825**, 75–85. [6](#), [7](#), [30](#)
- Nishiyama, K., Kobayasi, K.I. & Riquimaroux, H. (2011). Vocalization control in Mongolian gerbils (*Meriones unguiculatus*) during locomotion behavior. *The Journal of the Acoustical Society of America*, **130**, 4148–57. [28](#)
- Ohl, F.W. & Scheich, H. (2005). Learning-induced plasticity in animal and human auditory cortex. *Current opinion in neurobiology*, **15**, 470–7. [59](#)
- Ohl, F.W., Wetzel, W. & Wagner, T. (1999). Bilateral ablation of auditory cortex in Mongolian gerbil affects discrimination of frequency modulated tones but not of pure tones. *Learning & memory (Cold Spring Harbor, N.Y.)*, **6**, 347–62. [7](#), [64](#), [66](#)
- Ohl, F.W., Scheich, H. & Freeman, W.J. (2000a). Topographic analysis of epidural pure-tone-evoked potentials in gerbil auditory cortex. *Journal of neurophysiology*, **83**, 3123–32. [29](#), [31](#)
- Ohl, F.W., Schulze, H., Scheich, H. & Freeman, W.J. (2000b). Spatial representation of frequency-modulated tones in gerbil auditory cortex

- revealed by epidural electrocorticography. *Journal of physiology (Paris)*, **94**, 549–54. [28](#)
- Ohl, F.W., Scheich, H. & Freeman, W.J. (2001). Change in pattern of ongoing cortical activity with auditory category learning. *Nature*, **412**, 733–6. [64](#)
- Patterson, J.V., Jin, Y., Gierczak, M., Hetrick, W.P., Potkin, S., Bunney, W.E. & Sandman, C.A. (2000). Effects of temporal variability on p50 and the gating ratio in schizophrenia: a frequency domain adaptive filter single-trial analysis. *Archives of general psychiatry*, **57**, 57–64. [35](#), [55](#), [57](#), [88](#)
- Popescu, A.T.A., Popa, D. & Paré, D. (2009). Coherent gamma oscillations couple the amygdala and striatum during learning. *Nature neuroscience*, **12**, 1–8. [66](#), [85](#)
- Popov, T., Jordanov, T., Weisz, N., Elbert, T., Rockstroh, B. & Miller, G.A. (2011). Evoked and induced oscillatory activity contributes to abnormal auditory sensory gating in schizophrenia. *NeuroImage*, **56**, 307–14. [37](#), [55](#), [57](#)
- Potter, D., Summerfelt, A., Gold, J. & Buchanan, R.W. (2006). Review of clinical correlates of P50 sensory gating abnormalities in patients with schizophrenia. *Schizophrenia bulletin*, **32**, 692–700. [5](#)
- Rankin, C.H., Abrams, T., Barry, R.J., Bhatnagar, S., Clayton, D.F., Colombo, J., Coppola, G., Geyer, M.a., Glanzman, D.L., Marsland, S., McSweeney, F.K., Wilson, D.A., Wu, C.F. & Thompson, R.F. (2009). Habituation revisited: an updated and revised description of the behavioral characteristics of habituation. *Neurobiology of learning and memory*, **92**, 135–8. [32](#), [33](#)
- Recanzone, G.H. (2011). Perception of auditory signals. *Annals of the New York Academy of Sciences*, **1224**, 96–108. [1](#)
- Redgrave, P., Gurney, K. & Reynolds, J. (2008). What is reinforced by phasic dopamine signals? *Brain research reviews*, **58**, 322–39. [2](#)

- Redgrave, P., Coizet, V., Comoli, E., McHaffie, J.G., Leriche, M., Vautrelle, N., Hayes, L.M. & Overton, P. (2010). Interactions between the Midbrain Superior Colliculus and the Basal Ganglia. *Frontiers in neuroanatomy*, **4**, 1–8. [29](#)
- Ritter, W., Vaughan, H.G. & Costa, L.D. (1968). Orienting and habituation to auditory stimuli: a study of short term changes in average evoked responses. *Electroencephalography and clinical neurophysiology*, **25**, 550–6. [32](#)
- Rogan, M.T., Leon, K.S., Perez, D.L. & Kandel, E.R. (2005). Distinct neural signatures for safety and danger in the amygdala and striatum of the mouse. *Neuron*, **46**, 309–20. [84](#)
- Rosburg, T., Trautner, P., Korzyukov, O.A., Boutros, N.N., Schaller, C., Elger, C.E. & Kurthen, M. (2004). Short-term habituation of the intracranially recorded auditory evoked potentials P50 and N100. *Neuroscience letters*, **372**, 245–9. [8](#), [32](#)
- Rosburg, T., Trautner, P., Elger, C.E. & Kurthen, M. (2009a). Attention effects on sensory gating–intracranial and scalp recordings. *NeuroImage*, **48**, 554–63. [31](#), [82](#)
- Rosburg, T., Trautner, P., Fell, J., Moxon, K.A., Elger, C.E. & Boutros, N.N. (2009b). Sensory gating in intracranial recordings–the role of phase locking. *NeuroImage*, **44**, 1041–9. [36](#), [37](#), [55](#), [57](#)
- Rosburg, T., Zimmerer, K. & Huonker, R. (2010). Short-term habituation of auditory evoked potential and neuromagnetic field components in dependence of the interstimulus interval. *Experimental brain research. Experimentelle Hirnforschung. Expérimentation cérébrale*, **205**, 559–70. [8](#)
- Rossi, S., Bartalini, S., Ulivelli, M., Mantovani, A., Di Muro, A., Goracci, A., Castrogiovanni, P., Battistini, N. & Passero, S. (2005). Hypofunctioning of sensory gating mechanisms in patients with obsessive-compulsive disorder. *Biological psychiatry*, **57**, 16–20. [5](#)



- Ryan, L., Tepper, J., Young, S. & Groves, P. (1986). Frontal cortex stimulation evoked neostriatal potentials in rats: Intracellular and extracellular analysis. *Brain research bulletin*, **17**, 751–758. [31](#)
- Sable, J.J., Low, K.A., Maclin, E.L., Fabiani, M. & Gratton, G. (2004). Latent inhibition mediates N1 attenuation to repeating sounds. *Psychophysiology*, **41**, 636–42. [8](#), [34](#)
- Scheich, H., Brechmann, A., Brosch, M., Budinger, E. & Ohl, F.W. (2007). The cognitive auditory cortex: task-specificity of stimulus representations. *Hearing research*, **229**, 213–24. [2](#), [59](#)
- Schicknick, H., Reichenbach, N., Smalla, K.H., Scheich, H., Gundelfinger, E.D. & Tischmeyer, W. (2012). Dopamine modulates memory consolidation of discrimination learning in the auditory cortex. *The European journal of neuroscience*, **35**, 763–74. [65](#)
- Schulz, J.M., Redgrave, P., Mehring, C., Aertsen, A., Clements, K.M., Wickens, J.R. & Reynolds, J.N.J. (2009). Short-latency activation of striatal spiny neurons via subcortical visual pathways. *The Journal of neuroscience: the official journal of the Society for Neuroscience*, **29**, 6336–47. [2](#), [29](#)
- Shi, W.X. (2007). The auditory cortex in schizophrenia. *Biological psychiatry*, **61**, 829–30. [7](#)
- Süer, C., Dolu, N. & Ozesmi, C. (2004). The effect of immobilization stress on sensory gating in mice. *The International journal of neuroscience*, **114**, 55–65. [63](#), [83](#)
- Sutter, M.L. & Shamma, S.A. (2011). The Relationship of Auditory Cortical Activity to Perception and Behavior. In J.A. Winer & C.E. Schreiner, eds., *The Auditory Cortex*, chap. 29, 617–641, Springer US, Boston, MA. [1](#)
- Swedlow, N.R., Caine, S.B., Braff, D.L. & Geyer, M.a. (1992). The neural substrates of sensorimotor gating of the startle reflex: a review of recent findings and their implications. *Journal of psychopharmacology (Oxford, England)*, **6**, 176–90. [29](#)

- Thompson, R.F. & Spencer, W.A. (1966). Habituation: a model phenomenon for the study of neuronal substrates of behavior. *Psychological review*, **73**, 16–43. [8](#), [32](#)
- Torrence, C. & Compo, G. (1998). A practical guide to wavelet analysis. *Bulletin of the American Meteorological Society*, **79**, 61–78. [40](#)
- Torrence, C. & Webster, P. (1999). Interdecadal changes in the ENSO-monsoon system. *Journal of Climate*, **12**, 2679–2690. [40](#)
- Trautner, P., Rosburg, T., Dietl, T., Fell, J., Korzyukov, O.A., Kurthen, M., Schaller, C., Elger, C.E. & Boutros, N.N. (2006). Sensory gating of auditory evoked and induced gamma band activity in intracranial recordings. *NeuroImage*, **32**, 790–8. [37](#)
- Uhlhaas, P.J., Haenschel, C., Nikolić, D. & Singer, W. (2008). The role of oscillations and synchrony in cortical networks and their putative relevance for the pathophysiology of schizophrenia. *Schizophrenia bulletin*, **34**, 927–43. [37](#), [55](#), [58](#)
- Umbricht, D., Vyssotky, D., Latanov, A., Nitsch, R., Brambilla, R., D’Adamo, P. & Lipp, H.P. (2004). Midlatency auditory event-related potentials in mice: comparison to midlatency auditory ERPs in humans. *Brain research*, **1019**, 189–200. [31](#), [33](#), [83](#)
- Wan, L., Friedman, B.H., Boutros, N.N. & Crawford, H.J. (2008). P50 sensory gating and attentional performance. *International journal of psychophysiology: official journal of the International Organization of Psychophysiology*, **67**, 91–100. [82](#)
- Wehr, M. & Zador, A.M. (2005). Synaptic mechanisms of forward suppression in rat auditory cortex. *Neuron*, **47**, 437–45. [6](#)
- Weinberger, N.M. (2007). Associative representational plasticity in the auditory cortex: a synthesis of two disciplines. *Learning & memory (Cold Spring Harbor, N.Y.)*, **14**, 1–16. [7](#)

- Weisser, R., Weisbrod, M., Roehrig, M., Rupp, A., Schroeder, J. & Scherg, M. (2001). Is frontal lobe involved in the generation of auditory evoked P50? *Neuroreport*, **12**, 3303–7. [6](#)
- Wetzel, W., Wagner, T., Ohl, F.W. & Scheich, H. (1998). Categorical discrimination of direction in frequency-modulated tones by Mongolian gerbils. *Behavioural brain research*, **91**, 29–39. [63](#)
- White, P. & Yee, C. (1997). Effects of attentional and stressor manipulations on the P50 gating response. *Psychophysiology*. [14](#), [63](#), [83](#)
- Witten, I.B., Lin, S.C., Brodsky, M., Prakash, R., Diester, I., Anikeeva, P., Gradinaru, V., Ramakrishnan, C. & Deisseroth, K. (2010). Cholinergic interneurons control local circuit activity and cocaine conditioning. *Science (New York, N.Y.)*, **330**, 1677–81. [87](#)
- Woldeit, M.L., Schulz, A.L. & Ohl, F.W. (2012). Phase de-synchronization effects auditory gating in the ventral striatum but not auditory cortex. *Neuroscience*, **216**, 70–81. [90](#)
- Xiong, Y., Zhang, Y. & Yan, J. (2009). The neurobiology of sound-specific auditory plasticity: a core neural circuit. *Neuroscience & Biobehavioral Reviews*, **33**, 1178–1184. [2](#), [64](#)
- Yadon, C., Bugg, J., Kisley, M. & Davalos, D. (2009). P50 sensory gating is related to performance on select tasks of cognitive inhibition. *Cognitive, affective & behavioral neuroscience*, **9**, 448–458. [82](#)
- Yee, C. & White, P. (2001). Experimental modification of P50 suppression. *Psychophysiology*, 531–539. [14](#), [63](#)
- Zhou, D., Ma, Y., Liu, N., Chen, L., He, M. & Miao, Y. (2008). Influence of physical parameters of sound on the sensory gating effects of N40 in rats. *Neuroscience letters*, **432**, 100–4. [4](#)
- Znamenskiy, P. & Zador, A.M. (2013). Corticostriatal neurons in auditory cortex drive decisions during auditory discrimination. *Nature*. [66](#)

Zouridakis, G. & Boutros, N.N. (1992). Stimulus parameter effects on the P50 evoked response. *Biological psychiatry*, **32**, 839–41. [8](#), [33](#)

# Lebenslauf

## PERSÖNLICHE DATEN

---

<b>Name:</b>	<b>Woldeit</b>
<b>Vorname:</b>	<b>Marie</b>
<b>Akademischer Grad:</b>	Diplom-Biologin
<b>Nationalität:</b>	deutsch
<b>Geburtsdatum und -ort:</b>	29.08.1981 in Berlin
<b>Wohnsitz und Anschrift:</b>	Annastr. 10, 39108 Magdeburg
<b>Familienstand:</b>	verheiratet, 1 Kind (17 Monate)
<b>Geschlecht:</b>	weiblich

## AUSBILDUNG

---

<b>Jun. 2008 – heute</b>	<b>Doktorandin Neurobiologie,</b> Leibniz-Institut für Neurobiologie, Magdeburg
<b>Okt. 2005 – Jul. 2006</b>	<b>Computermathematik,</b> Otto-von-Guericke Universität, Magdeburg, (zwei Semester)
<b>Okt. 2004 – Jan. 2008</b>	<b>Neurobiologie,</b> Otto-von-Guericke Universität, Magdeburg, Abschlussnote Diplom: 1.2
<b>Okt. 2001 – Sept. 2004</b>	<b>Biologie,</b> Humboldt-Universität, Berlin, Gesamtnote Vordiplom: 1.3
<b>Jul. 1992 – Mai 2001</b>	<b>Gymnasium,</b> Canisius-Kolleg Berlin, Gesamtnote Abitur: 1.5

## BERUFSPRAXIS

---

<b>Jun. 2008 – heute</b>	<b>Wissenschaftliche Mitarbeiterin</b> , Leibniz-Institut für Neurobiologie, Abt. Systemphysiologie des Lernens (Prof. Frank W. Ohl), Magdeburg; Arbeit an der Dissertation: "Auditory gating in the ventral striatum and auditory cortex: the role of stimulus-locking and the influence of discrimination learning"
<b>Feb. 2008 – Mai 2008</b>	<b>Wissenschaftliche Mitarbeiterin</b> , Universität Oslo, Abt. Physiologie (Prof. J. Storm), Oslo, Norwegen
<b>Okt. 2006 – Jan. 2008</b>	<b>Diplomandin</b> Leibniz-Institut für Neurobiologie, Abt. Neurophysiologie (Prof. Julietta Frey/ Dr. Volker Korz), Magdeburg; Diplomarbeit: "Electrophysiological properties of hippocampal dentate gyrus cells and individual behaviour during spatial training in rats"
<b>Jul. 2006 – Aug. 2007</b>	<b>Hilfswissenschaftlerin</b> Leibniz-Institut für Neurobiologie, Abt. Akustik, Lernen, Sprache (Prof. Michael Brosch), Magdeburg

Magdeburg, 25.11.2013

Dipl.-Biol. Marie Woldeit

# List of Publications

- **Woldeit, M. L., Schulz, A. L. and Ohl, F. W.** (2012). Phase de-synchronization effects auditory gating in the ventral striatum but not auditory cortex. *Neuroscience*, **216**, 70–81.
- **Woldeit, M. L. and Korz, V.** (2010). Theta oscillations during holeboard training in rats: different learning strategies entail different context-dependent modulations in the hippocampus. *Neuroscience*, **165(3)**, 642–653.